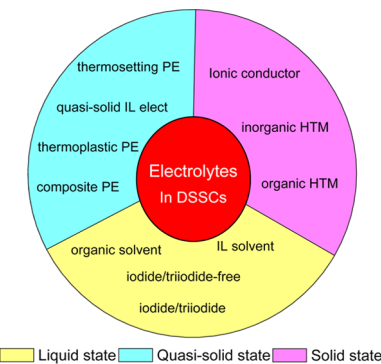


Electrolytes in Dye-Sensitized Solar Cells

Jihuai Wu,* Zhang Lan, Jianming Lin, Miaoliang Huang, Yunfang Huang, Leqing Fan, and Genggeng Luo

Engineering Research Center of Environment-Friendly Functional Materials, Ministry of Education, Institute of Materials Physical Chemistry, Huaqiao University, Quanzhou, Fujian 362021, China



CONTENTS

1. Introduction	2136
1.1. Solar Cells	2136
1.2. Structure and Operational Principle of Dye-Sensitized Solar Cells	2137
1.3. Development of Dye-Sensitized Solar Cells	2139
1.4. Electrolytes in Dye-Sensitized Solar Cells	2140
1.5. Transport Mechanism of Electrolytes in Dye-Sensitized Solar Cells	2140
2. Liquid Electrolytes	2142
2.1. Organic Solvents	2143
2.2. Ionic Liquids	2144
2.3. Iodide/Triiodide Redox Couples	2146
2.4. Iodide/Triiodide-Free Mediator	2147
2.5. Electrical Additives	2148
3. Quasi-Solid-State Electrolytes	2149
3.1. Thermoplastic Polymer Electrolytes	2149
3.2. Thermosetting Polymer Electrolytes	2152
3.3. Composite Polymer Electrolytes	2154
3.4. Quasi-Solid Ionic Liquid Electrolytes	2155
4. Solid-State Transport Materials	2156
4.1. Solid-State Ionic Conductors	2156
4.2. Inorganic Hole-Transport Materials	2158
4.3. Organic Hole-Transport Materials	2159
4.4. Perovskite Solar Cells	2160
5. Summary and Outlook	2163
Author Information	2163
Corresponding Author	2163
Notes	2163
Biographies	2163
Acknowledgments	2164
References	2164

1. INTRODUCTION

1.1. Solar Cells

In 2003, Nobel Laureate Richard E. Smalley outlined humanity's top 10 problems for the next 50 years.¹ The top problem is energy (Figure 1). Human society is facing a global energy problem, which is closely related to three ever-growing issues:^{2–6} the increasing energy demand to support economic growth, the gradual depletion of fossil fuels, and the greenhouse effect caused by fossil fuel combustion. At present, humans consume approximately 15 TW in a typical year (2008).⁷ World energy consumptions will increase 53% from 2010 to 2035, driven not only by the economic growth and increasing population in developing countries but also by emerging economies such as China and India.⁸ Fossil fuels, supplying 80% of total world energy with oil of 34.3%, natural gas of 20.9%, and coal of 25.1% (in 2005),⁹ are facing rapid resource depletion. The resource reserves of fossil fuels throughout the whole world in 2002 were projected to last 40 years for oil, 60 years for natural gas, and 200 years for coal.¹⁰ In order to reduce environmental pollution and adverse climate change as a result of traditional fuel use, the European Union in its Energy Roadmap 2050 plans to reduce greenhouse gas emissions to 80–95% below 1990 levels by 2050.¹¹

Nowadays, renewable sources comprise about 13% of all energy production (2008).⁷ Among all the renewable energy technologies, photovoltaic technology is considered as the most promising one.^{12–15} The sun is a champion among all

Humanity's Top Ten Problems for next 50 years

1. ENERGY
2. WATER
3. FOOD
4. ENVIRONMENT
5. POVERTY
6. TERRORISM & WAR
7. DISEASE
8. EDUCATION
9. DEMOCRACY
10. POPULATION



2003 6.3 Billion People
2050 8-10 Billion People

Figure 1. Humanity's top 10 problems for the next 50 years according to Richard Smalley. Reproduced with permission from ref 1. Copyright 2003 American Chemical Society.

Received: July 14, 2014

Published: January 28, 2015

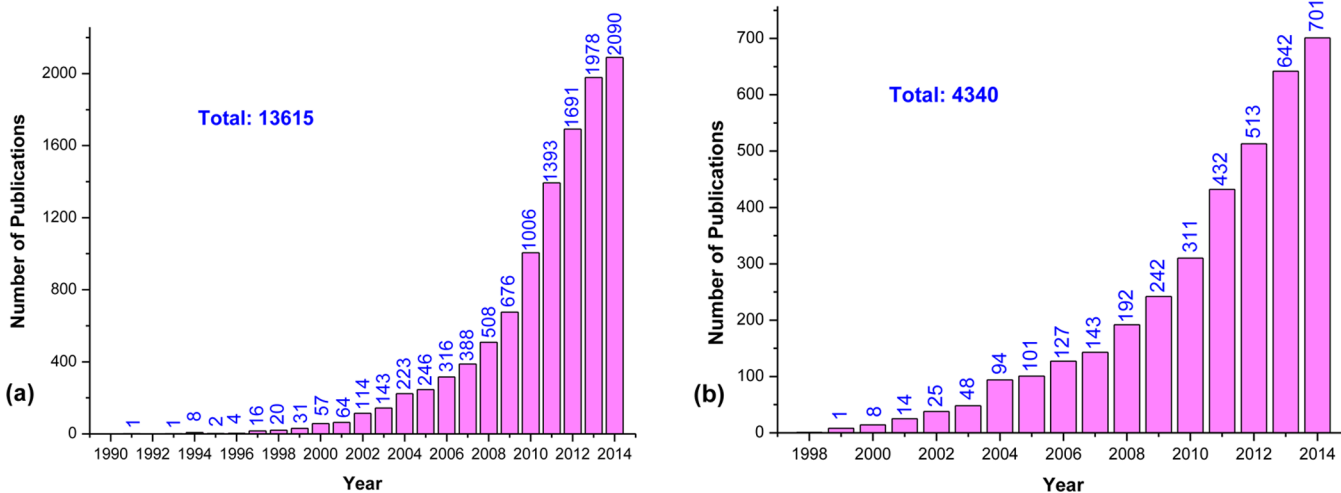


Figure 2. Number of articles published per year obtained from a literature search using the keywords “dye-sensitized solar cell” (a) and “dye-sensitized solar cell” and “electrolyte” (b) (data source ISI Web of Knowledge).

renewable or nonrenewable energy sources and provides the earth with 174 000 TW in a year;¹⁶ in other words, more energy from the sun hits the earth in 1 h than all of the energy consumed on our planet in an entire year. Within the last few decades, photovoltaic production featured an annual growth rate of more than 20%, making it the world’s fastest growing energy technology.^{17,18} However, present photovoltaic cells contribute only 0.04% to the world energy supply, leaving a large room for improvement of existing technologies and the development of new systems.

A solar cell, or photovoltaic cell (PV), is an electrical device that converts the energy of light directly into electricity by the photovoltaic effect. In 1954, Chapin et al. at Bell Lab demonstrated the first crystalline silicon solar cell with 6% efficiency.¹⁹ A few years later, they were already intensively used in space exploration. The first-generation solar cells (element silicon) of monocrystalline and polycrystalline silicon (mc-Si and pc-Si) cells can achieve power conversion efficiency (PCE) up to 25% and have totally dominated the terrestrial PV market so far.²⁰ However, the high production and environmental costs have prevented their widespread applications and prompted the search for environmentally friendly and low-cost solar cell alternatives. The second-generation solar cells are compound films, such as gallium arsenide (GaAs, PCE ≈ 28%), cadmium telluride (CdTe, PCE ≈ 20%), copper indium gallium selenide (CIGS, PCE ≈ 20%), etc.²⁰ These second-generation solar cells enrich the PV technology system and share the same performance as conventional Si devices. However, similar to the first-generation cells, the disadvantages of high production and environment cost still exist. After approximately 20 years of research and development, the third-generation hybrid film solar cells emerged. This new generation of photovoltaic systems include dye-sensitized solar cells (DSSCs, PCE ≈ 13%),^{21,22} organic solar cells (PCE ≈ 11%),²⁰ quantum dots solar cells (PCE ≈ 6–10%),²³ perovskite solar cells (PCE ≈ 19.3%),²⁴ etc. In comparison with the conventional solar devices, the third-generation solar cells have lower processing costs and minor environmental impact and thus short payback time. At the present stage, the third-generation PV technologies are still behind the efficiency values of the conventional Si-based solar cells (~25%); nevertheless, the promise of usage of available environmentally friendly raw materials and low

processing costs subjects them to intensive research and development.

After some preliminary exploration,^{25–28} Gratzel and O’Regan²⁹ put forward a novel solar cell: dye-sensitized titania nanocrystalline solar cell (shortly, dye-sensitized solar cell, DSSC, or Gratzel cell) in 1991. Similar to the photosynthetic process in plants where chlorophyll absorbs photons but does not participate in charge transfer, the photoreceptor and charge carrier are implemented by different components in DSSCs. This is contrary to conventional PV cells where a semiconductor assumes both functions. This separation of functions leads to lower purity demands on raw materials and consequently makes DSSCs a low-cost alternative. Because of the low cost, easy preparation, good performance, and environmental benignity compared with traditional photovoltaic devices,^{29–36} DSSCs have aroused intense interest and been regarded as one of the most prospective solar cells among the third-generation PV technologies. This field is growing fast; it can be seen from Figure 2a that recently more than five articles are being published each day. Although the power conversion efficiencies of the DSSCs are lower than that first- and second-generation PV cells,²⁰ there still is a high potential for improvement in their efficiency.

1.2. Structure and Operational Principle of Dye-Sensitized Solar Cells

A schematic illustration of the structure of DSSC is shown in Figure 3.^{29,30,35,37} A typical DSSC consists of the following: (i) A transparent glass sheet covered with a conductive indium-doped tin oxide (ITO) or fluorine-doped tin oxide (FTO) layer is used as anode substrate which allows light to pass through and electron transport; (ii) a mesoporous oxide layer (typically, TiO₂) deposited on the substrate to transfer electrons; (iii) a monomolecular layer of dye (typically ruthenium complexes) adsorbed on the surface of the mesoporous oxide layer to harvest incident sunlight, i–iii compose the photoanode; (iv) an electrolyte (usually an organic solvent containing a redox mediator, such as iodide/triiodide couple) for the recovery of dye and the regeneration of electrolyte itself during operation; (v) a counter electrode (cathode) made of an ITO or FTO conductive glass sheet coated with a catalyst (typically, platinum) to catalyze the redox couple regeneration reaction and collect electrons from the external circuit.^{29,30,35,37}

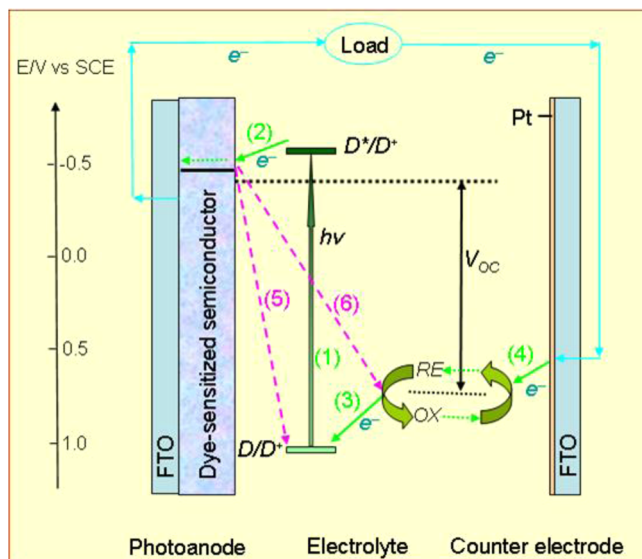
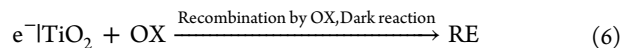
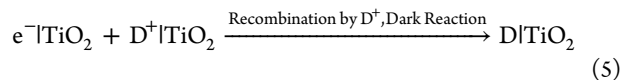
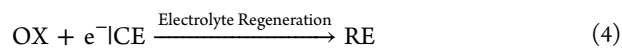
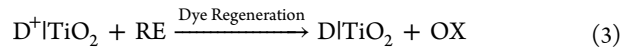
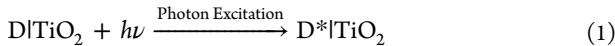


Figure 3. Operating principle of dye-sensitized solar cells. Process 1: light-induced excitation of the dye to produce excitons (D^*). Process 2: separation of the excitons at the dye/ TiO_2 interface and injecting electrons into the conduction band of the TiO_2 semiconductor and leaving holes (D^+) in the dye. Process 3: dye regeneration via accepting electrons from the reduced state of the redox couple (RE) and producing the oxidized state of the redox couple (OX) in electrolyte. Process 4: electrolyte regeneration via OX-accepting electrons from the counter electrode and producing RE. Process 5: injected electrons recombination by donating electrons to D^+ . Process 6: injected electrons recombination by donating electrons to OX.

The role of the dye in DSSC consists in acting as a molecular electron pump. The dye absorbs visible light, pumps an electron into semiconductor, accepts an electron from the reduced state of the redox couple (RE) in solution, and then repeats the cycle.³¹ The dye molecule (D) harvests photons and produces the excited electrons (D^*) from its highest occupied molecular orbital (HOMO) in the ground state to the lowest unoccupied molecular orbital (LUMO) in the excited state (eq 1). The dye injects the excited electrons into the conduction band of mesoporous TiO_2 film to form oxidized dye (D^+), and the electrons transfer through TiO_2 film to anode (eq 2). The oxidized dye (D^+) receives electrons from the reduced component (RE) of the redox couple in electrolyte to regenerate the dye (D), and the reduced component (RE) is oxidized into the oxidized component (OX) of the redox couple (eq 3). The OX migrates to the cathode to compensate for its missing electrons from the cathode, the RE is regenerated by the reduction of OX at the cathode, and the circuit is completed by the immigration of an electron through the external load (eq 4). Meanwhile, there are two competitive reactions in the process. One is that the electrons in TiO_2 film are captured by the oxidized dye (D^+), resulting in the recombination of electrons (eq 5); the other is that the electrons in TiO_2 film are captured by OX of the redox couple, also leading to the recombination of electrons (eq 6). Overall, the device generates electric power from light without suffering from any permanent chemical transformation.^{29,30,35,37}



In “Gratzel cells”, the light-to-electric conversion is a complex process. Reactions 1–4 are a requirement and advantageous reactions for completing the light-to-electric conversion.^{34,35,37,38} Reactions 5 and 6 are dark reactions related to the charge carrier recombination, which are disadvantageous for the efficiency of DSSCs, but they do not play a remarkable negative effect owing to their slower reaction speed compared with that of the forward reactions (green) and the dark reactions (red). The typical time constants for the forward reactions (green) and the dark reactions (red) are shown in Figure 4.^{35,40} Besides the above reactions, the orientated diffusion of electrons in TiO_2 semiconductor film and the orientated diffusions of OX and RE

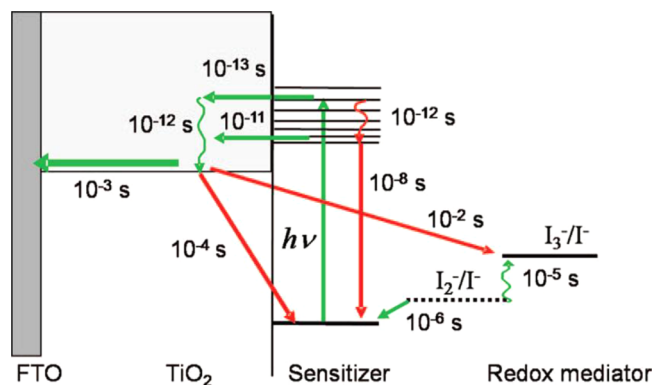


Figure 4. Typical time constants for the forward reactions (green) and dark reactions (red) in a Ru-dye-sensitized solar cell with iodide/triiodide electrolyte under working conditions (1 sun). Reproduced with permission from ref 40. Copyright 2009 American Chemical Society.

species in the electrolyte are also significant for the performance of the DSSCs.

The photovoltage generated under illumination corresponds to the potential difference between the Fermi level of the electron in the TiO_2 and the redox potential of the electrolyte, and the photocurrent depends on the incident sunlight harvest efficiency, charge carrier transportation, and collection efficiencies. The overall sunlight-to-electric power conversion efficiency (η or PCE) of the DSSC is determined by^{34,35}

$$\eta = P_{\max} / P_{\text{in}} = J_{SC} V_{OC} FF / P_{\text{in}} \quad (7)$$

where P_{\max} is the maximum obtainable power, P_{in} is the intensity of the incident light, J_{SC} is the photocurrent density measured at short circuit, V_{OC} is the photovoltage measured at open circuit, and FF is the fill factor of the solar cell. The photovoltaic parameter measurement is often under standard irradiation condition (100 mW·cm⁻², AM 1.5). The standard measurement condition will be omitted in the text later. The FF can assume values between 0 and 1 and reflects the electrical (Ohmic) and electrochemical (overvoltage) losses occurring during operation of the DSSC. Increasing the shunt resistance

and decreasing the series resistance as well as reducing the overvoltage for diffusion and electron transfer will lead to a higher FF value, thus resulting in greater efficiency and pushing the output power of the solar cell closer toward its theoretical maximum.

Similarly, the overall sunlight-to-electric power conversion efficiency can be expressed as the product of the three key terms⁴¹

$$\eta = \eta_{\text{abs}} \eta_{\text{inj}} \eta_{\text{coll}} \quad (8)$$

where η_{abs} is the efficiency of light absorption by the dye, η_{inj} is the efficiency of the charge injection from the excited state of the dye, and η_{coll} is the efficiency of charge collection in the electrodes. Another important parameter is the “external quantum efficiency (EQE)”, normally called “incident photon to current conversion efficiency (IPCE)”, which corresponds to the photocurrent density produced in the external circuit under monochromatic illumination of the cell divided by the photon flux that strikes the cell. The IPCE as a function of wavelength can be expressed as follows

$$\begin{aligned} \text{IPCE} &= \text{LHE}(\lambda) \Phi_{\text{inj}} \eta_{\text{coll}} = 1240 (J_{\text{SC}} / \lambda \phi) \\ &= 1240 (J_{\text{SC}} / \lambda P_{\text{in}}) \end{aligned} \quad (9)$$

Here LHE (λ) is the incident light-harvesting efficiency for photons with wavelength λ (nm), Φ_{inj} is the quantum yield for electron injection from the excited sensitizer in the conduction band of the semiconductor oxide, η_{coll} is the electron collection efficiency, ϕ is the incident light flux, J_{SC} is the photocurrent density produced in the external circuit ($\text{mA} \cdot \text{cm}^{-2}$), and P_{in} is the incident light intensity ($\text{mW} \cdot \text{cm}^{-2}$). IPCE values provide practical information about the monochromatic quantum efficiencies of a solar cell. Another parameter, internal quantum efficiency (IQE, $\text{IQE} = \text{IPCE}/\text{LHE}$), refers to the efficiency of charge carrier injection and collection. The EQE includes the effects of optical losses such as transmission and reflection. The IQE does not include these losses.

1.3. Development of Dye-Sensitized Solar Cells

The development objectives of PV technology should focus on the “Golden Triangle” issues,^{42,43} i.e., increasing light-to-electric energy conversion efficiency, enhancing long-term stability, and decreasing device cost. In order to solve these problems, in the last two decades, scientists have devoted a great deal of effort on DSSCs’ four important components: sensitized dyes, photoanodes, electrolytes, and counter electrodes; some significant processes have been achieved.^{30,34,35}

The improvement of power conversion efficiency of DSSCs hinges on the development of combinations of new dyes, redox couples, and photoanodes, especially in new sensitized dyes.^{44,45} The sensitizer constitutes the heart of DSSC, pumps using sunlight electrons from a lower to a higher energy level, and generates an electric potential difference in this fashion, which can be exploited to produce electric work. In 1991, the sensitizer used in the first successful DSSC was trimeric ruthenium complex $\text{RuL}_2(\mu\text{-CN})\text{Ru}(\text{CN})\text{L}'_2$ ($\text{L} = 2,2'\text{-bipyridine-4, 4'-dicarboxylic acid}$; $\text{L}' = 2,2'\text{-bipyridine}$) with absorption onset at 750 nm,²⁹ and the DSSC obtained an efficiency of 7.12% under full sunlight irradiation. In 1993,⁴⁶ N3 dye [$\text{RuL}_2(\text{NCS})_2 \cdot 2\text{H}_2\text{O}$ ($\text{L} = 2,2'\text{-bipyridyl-4,4'-dicarboxylic acid}$)] was developed, the spectral response of the solar cell was extended to the 800 nm, and the efficiency of the solar cell was enhanced to 10%. In 2006, black dye (N-749)

[$\text{RuL}'(\text{NCS})_3 \cdot 3\text{TBA}$ ($\text{L}' = 2,2',2''\text{-terpyridyl-4,4',4''-tricarboxylic acid}$; TBA = tetrabutyl ammonium)] was introduced in DSSCs. In comparison to the N3 sensitizer, the spectral response of the black dye extends into the near IR, with photocurrent onset around 920 nm. This corresponds to a band gap of 1.4 eV and is close to the optimum threshold absorption for single-junction photovoltaic cells; the DSSC achieved an efficiency of 11.1%.⁴⁷ In 2009, the advent of heteroleptic ruthenium complexes endowed with an antenna function led to striking advances in the performance of the DSSC.^{48–52} Compared with the classical Ru dyes, C101 dye [$\text{RuLL}'(\text{NCS})_2$ ($\text{L} = 2,2'\text{-bipyridyl-4,4'-dicarboxylic acid}$; $\text{L}' = 4,4'\text{-bis(5-hexylthiophen-2-yl)-2,2'-bipyridine}$)] and CYC-B1 dye [$\text{RuL}_2(\text{NCS})_2 \cdot 2\text{H}_2\text{O}$ ($\text{L} = 4,4'\text{-di-2-octyl-5-(thiophen-2-yl)-thiophen-2-yl-2,2'-bipyridine}$)] have thiophene moieties attached to the ancillary bipy ligand, which enhance the light-harvesting capacity by increasing their extinction coefficient and shifting their spectral response to the red, giving an efficiency of 12% for the DSSC.^{34,52}

In 2011, the Gratzel group used a new dye donor–p-bridge–acceptor zinc porphyrin (YD2-o-C8) in combination with a Co-complex-based electrolyte to fabricate DSSC.²¹ The specific molecular design of YD2-o-C8 greatly retards dark reaction and attains a high photovoltage approaching 1 V. Because the YD2-o-C8 porphyrin harvests sunlight across the visible spectrum, large photocurrent is generated, achieving a conversion efficiency of 12.3% for the DSSC. Very recently, Mathew and Gratzel used a panchromatic porphyrin dye SM315 featuring a porphyrin core and a bulky bis(2',4'-bis(hexyloxy)-[1,1'-biphenyl]-4-yl) amine donor in conjugation with a cobalt(II/III) redox shuttle in DSSC, which resulted in an high V_{OC} of 0.91 V, J_{SC} of 18.1 $\text{mA} \cdot \text{cm}^{-2}$, FF of 0.78, and PCE of 13% under full sunlight irradiation (AM 1.5).²² The advent of organometal halide (RNH_3PbX_3 , X = Br, I) with a perovskite structure and high extinction coefficient absorbance, as a light harvester in the initial stage, brings out and triggers a revolution in PV technology field, the efficiencies of the cell increasing from 3.8% in 2009⁵³ to 19.3% now,²⁴ which opens a new and promising field for PV technology.

With regard to the device cost, a platinum counter electrode is the most expensive component in DSSCs. In order to reduce the device cost, the load amount of platinum on the counter electrodes is decreased by using various platinum composite materials.^{54–57} On the other hand, free-platinum conductive and electrocatalytic materials,^{41,58} such as carbonaceous materials,^{59,60} conductive polymers,^{61,62} inorganic transition metal compounds,^{63,64} and metal or alloy,^{65,66} are used to replace expensive platinum. The performance of some free-platinum materials is even superior to that of platinum counter electrodes. Flexible DSSCs can also be fabricated by using large-scale continuous and rapid coating methods,^{67–69} which will decrease the cost of DSSCs. However, the preparation techniques for flexible photoanodes and counter electrodes are not mature and limit the application of flexible DSSCs.

In the case of the long-term stability, for a DSSC cell to be durable for more than 15 years outdoors, the turnover number of sensitizer must be over 10^8 , which may be satisfied by most of the ruthenium complex dyes.^{35,70,71} On the other hand, the long-term stability of DSSCs is strongly related to electrolyte components.^{34,37} Using the liquid electrolytes with interfacial affinity and high ionic conductivity, the solar cells can obtain an efficiency of 13%;²² however, the long-term stability of the device is not so good by virtue of volatilization and leakage of

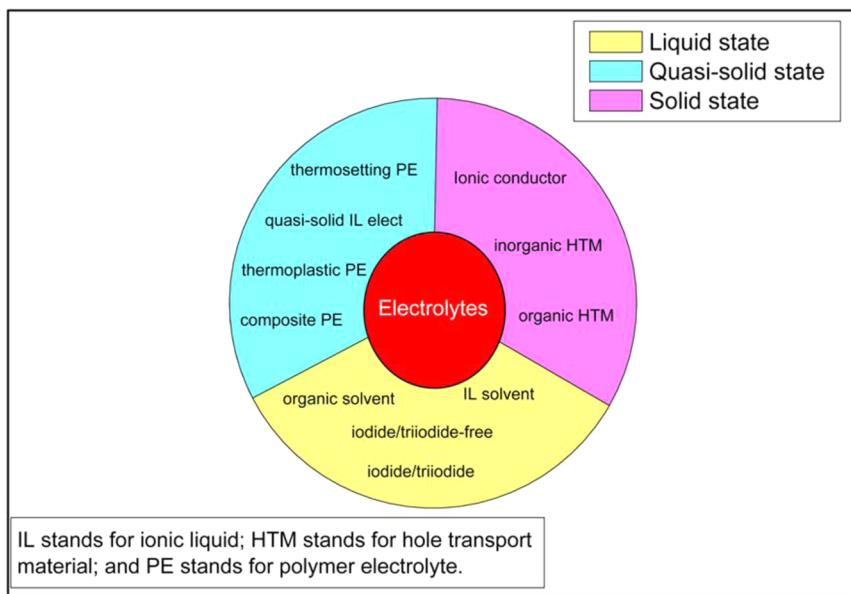


Figure 5. Classification of the electrolytes used in dye-sensitized solar cells.

solvent, instability and corrosion of iodine specimen, and encapsulation difficulty. By using the solid-state electrolytes, the DSSCs show good long-term stability, but the efficiency of this kind of DSSCs is lower (before perovskite solar cells) as a result of low conductivity and poor interfacial electrolyte/electrode contacts. The design and synthesis of novel electrolytes with high effective charge carrier transportation and fine long-term stability is still on the way.

1.4. Electrolytes in Dye-Sensitized Solar Cells

The electrolyte is one of the most crucial components in DSSCs;³⁶ it is responsible for the inner charge carrier transport between electrodes and continuously regenerates the dye and itself during DSSC operation. The electrolyte has great influence on the light-to-electric conversion efficiency and long-term stability of the devices. The efficiency of a DSSC device is determined by its photocurrent density (J_{SC}), photovoltage (V_{OC}), and fill factor (FF).³⁴ All of the three parameters will be significantly affected by the electrolyte in DSSCs and by the interaction of the electrolyte with the electrode interfaces. For instance, J_{SC} can be affected by the transport of the redox couple components in the electrolyte. The FF can be affected by the diffusion of charge carrier in electrolyte and the charge transfer resistance on the electrolyte/electrode interface. The V_{OC} can be significantly affected by the redox potential of the electrolyte. In order to improve the performance of the DSSCs, many scientists have been devoting their research to the electrolytes. It can be illustrated by Figure 2b that about two articles on electrolytes in dye-sensitized solar cells are being published each day, and among all dye-sensitized solar cells articles, approximately one-third is associated with the electrolytes according to Figure 2.

Electrolyte is a material that provides pure ionic conductivity between the positive and the negative electrodes in an electrochemical device.⁷² Electrolytes are ubiquitous and indispensable in most electrochemical devices. The role of electrolytes in capacitors, supercapacitors, electrolytic cells, fuel cells, or batteries would remain the same: to serve as the medium for the transportation of charge carriers, which are in

the form of ions, between a pair of electrodes.⁷³ Several aspects are essential for the electrolytes used in DSSCs.^{37,39,74}

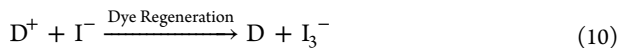
- (i) The electrolytes must be able to transport the charge carriers between photoanode and counter electrode. After the dye injects electrons into the conduction band of TiO_2 , the oxidized dye must be rapidly reduced to its ground state. Thus, the choice of the electrolyte should take into account redox potential and regeneration of dye and itself.
- (ii) The electrolytes must guarantee fast diffusion of charge carriers (higher conductivity) and produce good interfacial contact with the mesoporous semiconductor layer and the counter electrode. For liquid electrolytes, the solvent should have smaller leakage and/or evaporation to prevent loss of the liquid electrolyte.
- (iii) The electrolytes must have long-term stabilities, including chemical, thermal, optical, electrochemical, and interfacial stability, and not cause desorption and degradation of the sensitized dye.
- (iv) The electrolytes should not exhibit a significant absorption in the range of visible light. Since the iodide/triiodide redox couple in the electrolyte shows color and reduces visible light absorption, triiodide ions can react with the injected electrons and increase the dark current. The concentration of iodide/triiodide must be optimized.

According to physical states, compositions, and formation mechanisms, the electrolytes used in DSSCs can be broadly classified into 3 categories (liquid electrolytes,^{75,76} quasi-solid electrolytes,^{37,77} and solid-state conductors^{10,78}) and 11 kinds, as shown in Figure 5.

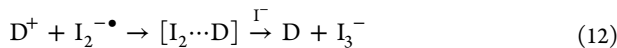
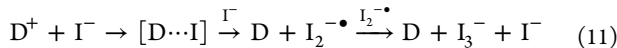
1.5. Transport Mechanism of Electrolytes in Dye-Sensitized Solar Cells

In the electrochemical circuit of DSSCs, the electrons transport through TiO_2 crystalline film and the holes transport through the electrolytes or hole conductors. In this sense, electrolytes or hole conductors are hole-transport mediators. The basic function of electrolytes or hole conductors is the regeneration

of dye and itself in DSSCs. For typical I^-/I_3^- redox electrolytes, the regeneration of dye can be expressed as follows



In fact, the reaction contains a series of successive reactions on the TiO_2 interface.^{40,79–82}



The regenerative cycle of electrolytes is completed by the conversion of I_3^- to I^- ions on the counter electrode. The counter electrode must have catalytic activity to ensure rapid reaction and low overpotential,^{35,40} and in this sense, Pt is a suitable counter electrode material. The charge transfer reaction at the counter electrode leads to a charge transfer resistance (R_{CT}) in the DSSC. The overpotential (ζ) is needed to drive the reaction at a certain current density (J). At small overpotentials, $R_{CT} = \zeta/J$. Ideally, R_{CT} should be $\leq 1 \Omega\cdot cm^2$ to avoid significant losses. A poor counter electrode will decrease the performance of the DSSC by lowering the fill factor. The reduction of I_3^- may be expressed as a successive and rapid one-electron reaction on counter electrode.^{40,83}



The implementation of the above reactions depends on the transport of the redox mediator between the photoanode and the cathode in DSSCs. Conductivity and diffusivity of electrolyte are two important parameters reflecting the transport ability. The conductivity of an electrolyte can be expressed as⁸⁴

$$\sigma = \sum \mu_i n_i q_i \quad (14)$$

Here, σ , μ_i , n_i , and q_i are conductivity, mobility, carrier concentration, and charge of i ionic specimen, respectively. It is noted that electrons or holes do not contribute to the summation in eq 14. Owing to the temperature effect on mobility of the specimen, the temperature dependence of conductivity ($\ln \sigma \approx 1/T$) shows linear plots in homogeneous electrolytes or nonlinear plots in heterogeneous systems, which are expressed by Arrhenius⁸⁵ and Vogel–Tamman–Fulcher (VTF)^{86–88} equations, respectively

$$\sigma = \sigma_0 \exp(-E_A/k_B T) \quad (15)$$

$$\sigma = \sigma_0 \exp[-B/(k_B(T - T_0))] \quad (16)$$

Here, σ_0 is a constant that depends on the properties of the material, k_B is Boltzmann's constant, E_A is the activation energy, B is the pseudo activation energy, T is temperature, and T_0 is the equilibrium temperature related with the glass-transition temperature (T_g). The Arrhenius formula describes the conductive behavior that mobile ions hop through energy favorable sites of the framework lattice (sublattice),⁸⁴ and VTF formula interprets the conductive phenomena that carrier transports through free volume and assisted by segmental motion.⁸⁴ Both Arrhenius and VTF equations also are used to explain the temperature behavior of different physical magnitudes, including viscosity, diffusion constant, etc.

The charge carrier transportation between the two electrodes in DSSCs is actualized by diffusion. We conclude the diffusions between the two electrodes in DSSCs as four models: (i)

general ion diffusion through hopping in the lattice of framework (D_{gen}), where the $T-\sigma$ behavior can be explained by the Arrhenius equation (eq 15); (ii) ion diffusion is realized through free volume and assisted by segmental motion (D_{fv}), in which the $T-\sigma$ phenomena can be interpreted by the VTF formula (eq 16); (iii) ion diffusion via an electron exchange Grotthus-like mechanism (D_{ex}), and (iv) hole diffusion via hole conductors (D_{hole}). The total charge carrier diffusion between the two electrodes can be expressed as follows

$$D_{\text{Tot}} = D_{\text{gen}} + D_{\text{fv}} + D_{\text{ex}} + D_{\text{hole}} \quad (17)$$

In homogeneous solid electrolytes, general ion diffusion is achieved through mobile ions hopping in empty, interstitial, and lattice sites in host materials. In even liquid electrolytes, the diffusion is due either to ion hopping or to liquid-like diffusion of one ionic sublattice.⁸⁴ The host backbone for the above cases is fixed and provides the activation energy to the mobile ions. The general ion diffusion apparently associates with characteristics of solution and solute. The general diffusion coefficient can be represented by the Einstein–Stokes equation^{89,90}

$$D_{\text{gen}} \propto \mu k_B T / \mu R_{\text{ion}} \quad (18)$$

Here, μ is the viscosity of the solvent and R_{ion} is the spherical radius of diffusion species; thus, a large solute ion radius and high fluidity ($1/\mu$) are expected to cause high ion mobility.

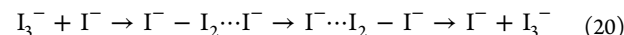
For heterogeneous electrolytes, such as polymer electrolytes above the glass transition temperature, amorphous phase, and multiphase system, the ions diffuse through the free volume promoted by polymer segmental motion. During the diffusion process, the host polymer chain segment is movable. Owing to the promotion, the ion diffusion coefficients in the amorphous polymer electrolytes are obviously higher than those in the crystalline polymer electrolytes.^{91–94} The free volume is defined as the unoccupied space between the polymer chains.⁹⁵ Cohen and Turnbull developed an equation to describe the free volume dependence of the diffusivity^{96,97}

$$D_{\text{fv}} = D_0 \exp[B(1 - 1/f)] \quad (19)$$

Here, f is the free volume fraction of the total volume, D_0 is the reference diffusivity, and B is related to the critical voids for transportation. Thus, fast ion diffusion in a system with large free volume fractions can be expected.^{98,99}

In high iodide concentration system, owing to the formation of polyiodides (I_3^- , I_5^- , I_7^- , I_9^- , etc.),^{100,101} carrier transportation through an electron exchange mechanism (Grotthus-like mechanism) was proposed.^{101,102} Although the length of the polyiodide chain has not been clearly determined, some polyiodides have been observed by IR and Raman spectral measurements,^{102–107} implying the intermediate state of electron exchanges through these polyiodides.

In the model of Grotthus-like diffusion, the electrons transport among iodide anion species, I^- , I_3^- , and polyiodides, through chemical bond exchanges as protons do in the water system;^{89,101} charge transportation corresponds to formation and cleavage of chemical bonds



The Grotthus-like mechanism reasonably explains the unexpected high photocurrent density independent of the viscosity of electrolyte in DSSCs.^{101,108–110} For an electron exchange Grotthus-type mechanism, the relationship between temperature (T) and conductivity (σ) obeys the Arrhenius

Table 1. Physical Parameters of Some Frequently Used Organic Solvents for Electrolytes in DSSCs*

Name (abbr)	Formula	Melting point/°C	Boiling point/°C	Viscosity/cp	Dielectric constant	Donor number
Water	H ₂ O	0	100	0.89	78	18.0
Ethanol	CH ₃ CH ₂ OH	-114	78	1.08	25	29
Dimethyl carbonate (DMC)	(CH ₃ O) ₂ CO	4.6	91	0.59(20°C)	3.107	
Diethyl carbonate (DEC)	(CH ₃ CH ₂ O) ₂ CO	-74.3	126	0.75	2.805	
Acetonitrile (AN)	CH ₃ CN	-44	82	0.33(30°C)	36	14.1
Propionitrile(PPN)	CH ₃ CH ₂ CN	-93	97	0.39(30°C)	27(20°C)	16.1
Butyronitrile(BN)	CH ₃ (CH ₂) ₂ CN	-112	118			
Valeronitrile (VN)	CH ₃ (CH ₂) ₃ CN	-96	139	0.78(19°C)	21	
Glutaronitrile (GN)	NC(CH ₂) ₃ CN	-29	287	5.3	37	
3-Methoxy-propionitrile(MPN)	CH ₃ O(CH ₂) ₂ CN	-63	164	2.5	36	16.1
Ethylene carbonate (EC)		36	238	90	90	16.4
Propylene carbonate (PC)		-49	241	2.5	64	15.1
γ-Butyrolactone (GBL)		-44	204	1.7	42	18.0
N-Methyl-oxazolidinone(NMO)		15	270	2.5	78	
N-methylpyrrolidone (NMP)		-24	203	1.65	32.2	27.3

* All data at 25 °C and 760 mmHg unless otherwise indicated.

formula (eq 15). According to the model of the electron exchange diffusion by Dahms–Ruff,^{111,112} the electron exchange diffusion coefficient can be described as

$$D_{\text{ex}} \propto k_{\text{ex}} \delta^2 C \quad (21)$$

where k_{ex} is the rate constant of exchange-reaction, δ is the center-to-center distance in the exchange reaction, and C is the total concentration of the iodide species.

For solid-state DSSCs using hole-transport materials (HTMs), the charge carrier transportation and dye recombination are different from those in liquid-state DSSCs; the charge carriers transport via hole hopping in HTMs rather than ionic conduction in electrolytes. Using transient absorption laser spectroscopy in 1999, Bach et al. first reported the photoinduced interfacial charge separation in solid-state DSSCs.¹¹³ They found that the hole transported from dye to HTM primarily on a 10⁻⁹ s scale with multiphase kinetics, which is much faster than the recombination reaction of the holes with the electrons injected in the TiO₂ (10⁻⁶–10⁻³ s)^{114,115} and faster than the dye regeneration (>10⁻⁸ s) in traditional liquid electrolytes.⁴⁶ These results demonstrate that the charge separation and dye regeneration are not the major bottlenecks for the low performance of solid-state DSSCs.¹¹⁶

In 2003, Haque et al. found that the yield of hole transport was controlled not by kinetic competition between the rate of the hole-transportation process and the rate of the hole recombination process¹¹⁷ but rather by the thermodynamic driving force, $\Delta G_{\text{dye-HTM}}$, which is defined as $\Delta G_{\text{dye-HTM}} =$

$E_{\text{HTM}} - E_{\text{dye}}$. In 2006, Gratzel et al. found that the best device performance corresponded to HTMs with the best penetration rather than the highest hole mobility,^{118,119} indicating that hole mobility is not a major determining factor for device performance. Hole diffusion in HTMs is not a mass-transportation process, and the transportation obeys the Arrhenius relationship (eq 15).¹²⁰

Besides aforementioned diffusion models, several factors strongly affect the diffusion process:⁷⁵ (i) the size of the redox species, (ii) the viscosity of the solvent, (iii) the concentration of the redox mediator, (iv) the distance between the electrodes.¹²¹ For instance, Han et al. achieved a diffusion resistance of 0.7 Ω·cm² by minimizing the distance between the working and the counter electrodes, while the distance of 20 μm led to the resistance of 2 Ω·cm².¹²²

2. LIQUID ELECTROLYTES

In 1991, using a very rudimentary liquid electrolyte consisting of an organic solvent and a dissolved iodide/triiodide redox couple without extra additives, O'Regan and Gratzel pioneered an efficient DSSC with an efficiency of 7.1–7.9%.²⁹ The liquid electrolytes possess some important features,^{37,75} such as easy preparation, high conductivity, low viscosity, and good interfacial wetting between electrolytes and electrodes and thus high conversion efficiency for the DSSCs. Today, liquid electrolytes are still the most widely utilized transport medium for DSSCs and have produced the highest efficiency of 13% for traditional DSSCs.²²

In DSSCs, liquid electrolytes should be chemically and physically stable, low viscous to minimize charge carrier transport resistance, and a good solvent for redox couple components and various additives; meanwhile, they do not cause significant dissociation of the adsorbed dye, electrode, and sealing materials.⁷⁵ In general, a liquid electrolyte consists of three main components: solvent, ionic conductor, and additives.

2.1. Organic Solvents

The organic solvent is a basic component in liquid electrolyte, and it gives an environment for the dissolution and diffusion of ionic conductor. The following general requirements should be fulfilled for the solvents in DSSCs:⁷⁵ (i) Melting point below -20°C and boiling point above 100°C , so that the electrolyte prepared with these solvents will not evaporate under cell operating conditions, especially in an outdoor environment; (ii) sufficient chemical stability in the dark and under illumination. The solvent should have a wide electrochemical window, so that electrolyte degradation would not occur within the range of the working potentials of both the cathode and the anode;³³ (iii) high dielectric constants, so that electrolyte salts are sufficiently soluble and exist in a fully dissociated state. Good solubility for the redox mediators, for instance, highlighted by the unwanted precipitation of a solid iodide–triodide compound from electrolytes containing a popular additive, 1-methyl-benzimidazole;¹²³ (iv) low viscosity, so that redox mediators possess high diffusion coefficients and the liquid electrolytes have high conductivity; (v) low light absorption; (vi) inertness with respect to the surface-attached dye, including the dye–metal–oxide (or other semiconductor) bond; (vii) poor solubility to the sealant materials; (viii) low toxicity and low cost.

Hundreds of chemical compounds have been experimented, and those that meet most requirements above are the two types of solvents: polar organic solvents and ionic liquids. The physical parameters of some frequently used organic solvents for the electrolytes in DSSCs are listed in Table 1.^{35,73,75}

It is notable that no single solvent can simultaneously fulfill all the requirements aforementioned; those requirements for one solvent often are in several respects contradictory. Therefore, when one wishes to obtain optimal DSSC performances, the mixed solvents are often used. For example, a mixed solvent of acetonitrile and valeronitrile is popularly used, and the mixed volume ratio is either 50:50¹²⁴ or 85:15.¹²⁵ The choice of solvents depends on the particular use of the DSSC under consideration.⁷⁵

Water is a common solvent. In the initial phase of DSSC research,^{126–131} water was used as solvent in liquid electrolytes. Research by O'Regan et al. indicated that for a Ru-based DSSC,¹³² an addition of up to 20% of water into a nonaqueous electrolyte slightly enhanced the conversion efficiency from 5.5% to 5.7% without deterioration of the long-term stability. The efficiency decreased upon further water addition, so that for pure water electrolytes the efficiency of the DSSC was 2.4%. To date, this is the highest conversion efficiency obtained for a pure aqueous solvent. An alternative explanation for the long-term instability of DSSCs in the presence of water is the oxidation of iodide to iodate (IO_3^-) instead of triiodide,¹³³ which cannot be reduced at the counter electrode, resulting in a progressive I_3^- depletion and decrease in cell performance. More generally,^{35,75} many organometallic sensitizing dyes are sensitive toward hydrolysis, and water and other alcohols are

lower in chemical stability; thus, they are not optimal choices as electrolyte solvent.

Acetonitrile (AN) is considered as the best electrolyte for fundamental studies due to its low viscosity, good solubility, and excellent chemical stability (electrochemical window $> 4\text{ V}$).³² For example, Hauch et al. determined the diffusion constant of triiodide in different solvents and cations and found that the best diffusion constant was achieved in AN with Li^+ .¹³⁴ However, low boiling point (82°C) and the relatively high toxicity limit its utilization in industrial solar cells. Thus, the mixtures of nitriles are often used aiming at higher boiling points in order to minimize evaporation and cell sealing problems. Nevertheless, AN is a preferred solvent for laboratory investigations on new sensitizers, particularly when one wishes to maximize cell efficiency, since the photochemical processes occur without mass-transport limitations in this solvent. Using AN as the main solvent, the traditional DSSC achieved a highest conversion efficiency record of 13%.²²

Another class of nitriles containing methoxy groups with low toxicity and high boiling point, such as methoxyacetonitrile (MAN) and 3-methoxypropionitrile (MPN), has been extensively used as DSSC electrolytes.³⁵ MPN possesses a melting point of -63°C , a boiling point of 164°C , and a viscosity of 2.5 cP and nowadays is one of the most common electrolyte solvents in applications. MPN has good chemical stability to bear long-term DSSC stability tests for a retaining over 98% of its initial performance (efficiency $\geq 8\%$) after 1000 h of accelerated tests subjected to thermal stress at 80°C in dark. The performance degradation was negligible following 1000 h of visible light soaking at 60°C .¹³⁵

Esters and lactones compounds, such as ethylene carbonate (EC), propylene carbonate (PC), γ -butyrolactone (GBL), and *N*-methyloxazolidinone (NMO), have been widely used in DSSC research. Usually, these compounds have a high boiling point and melting point. The melting points of EC and NMO are 36 and 15°C , respectively, so the addition of a solvent with a lower melting point (PC, -49°C ; AN, -44°C) may be necessary.^{29,35,46} The electrolyte for the first efficient DSSC device based on Ru-trimer dye contained an EC–AN mixture as solvent (80%:20% vol).²⁹ In the first DSSC device with a standard Ru-based red dye (N3) and an efficiency of 10% the solvent employed was an AN–NMO mixture (90%:10% vol).⁴⁶ In electrochemical research, PC is known to have a high electrochemical window (above 4 V).⁷⁵ Another frequently used solvent in DSSCs, for long-term outdoor tests in particular, is GBL, with a favorable melting point, boiling point, and viscosity (-44°C , 204°C , and 1.7 cP, respectively). For instance, Kato et al. determined the DSSC module stability data; using GBL solvent electrolyte, the DSSC works under the outdoor condition for almost 2.5 years.¹³⁶ They believed that this data was the longest stability for the DSSC module using liquid electrolytes. In addition, using a solvent-free ionic liquid (imidazolium salts) electrolyte,¹³⁷ the lifetime of the DSSC for outdoor use was estimated at over 15 years.

The acid–base (or donor–acceptor) interaction between solvents and other components is an important factor affecting the photovoltaic performance of DSSCs. The Gutmann donor number (DN) of solvent is a characteristic parameter indicating the solvent donating electron capacity.¹³⁸ The donor number of a mixed solvent can be estimated as the mole-fraction-weighted average of the component donor numbers:¹³⁹ $D_{\text{mix}} = (D_X \times X \text{ vol } \%) + (D_Y \times Y \text{ vol } %)$. Higher DN means stronger donating electron capacity or stronger basicity.

Kebede et al. investigated the donor–acceptor interaction between nonaqueous solvents and iodide species and could predict the extent of transformation from iodide to triiodide ions according to the DN of the solvent.¹⁴⁰ Fukui et al. reported that the V_{OC} increased and J_{SC} decreased with the increase of the DN of solvent in DSSCs.¹⁴¹ Similar phenomena of the solvent DN on the photovoltaic performance of DSSCs were also found by other groups.^{139,142,143} Wu's group investigated the influence of the DN of the mixed solvent of GBL and NMP on the photovoltaic performance of DSSCs (Figure 6).^{37,144,145} The results showed that V_{OC} increased and J_{SC} decreased with the increase of the DN of the mixed solvent.

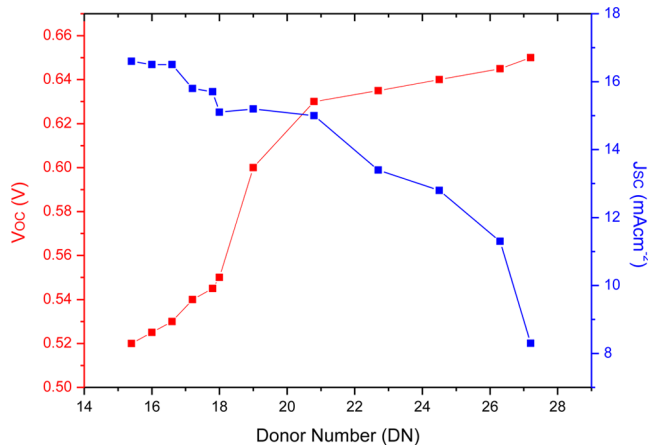


Figure 6. V_{OC} and J_{SC} of the DSSCs function as the donor numbers of the mixed organic solvents. (The donor number of the mixed solvent is controlled by adjusting the ratio of GBL, NMP and PC solvents.) Data extracted from ref 37.

The effect of solvent basicity can be rationalized by considering the state of the TiO_2 electrode surfaces. It has been argued that an electron-donating (basic) solvent will decrease the amount of surface-bound protons, leading to a more negatively charged TiO_2 surface and elevation of the flatband potential (V_{fb}) of the TiO_2 surface.¹⁴⁶ The driving force for electron transfer from the dye excited state to the TiO_2 decreases, resulting in a lower J_{SC} ; the potential difference between the V_{fb} and the redox potential of the electrolyte increases, resulting in a higher V_{OC} . The above effects of basicity could also be explained by the Gratzel proposition,⁴⁶ according to which an electron-donating solvent will be bound more strongly to electron-accepting TiO_2 sites and will in this way passivate them. This will cause hindering of both electron injection from the dye to the TiO_2 and electron recombination from the TiO_2 surface to the oxidized components of the redox mediator, giving lower J_{SC} and higher V_{OC} . Apart from the effects above, the interactions of solvents with particular redox mediators should be considered. For example, electron-donating solvent molecules incline to bond with I_3^- or I_2 ,^{140,144,147} resulting in a decrease of their effective (available) concentration and an increase in V_{OC} .

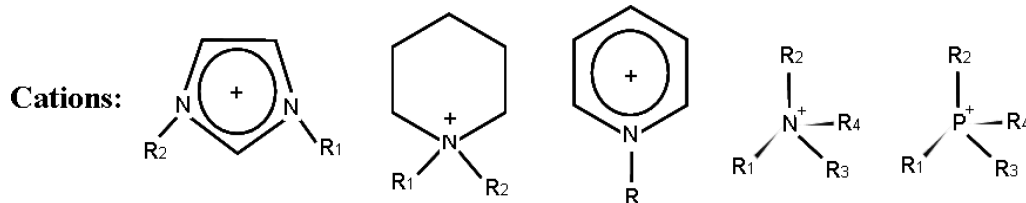
2.2. Ionic Liquids

Ionic liquid (IL) is a salt in liquid state; ionic liquids or molten salts are generally defined as liquid electrolytes composed entirely of ions.^{148–151} More detailed, the melting point criterion was proposed to distinguish between the molten salts with high melting point, high viscosity and the ionic liquids with low melting point below 100 °C and relatively low viscosity. The latter are free-flowing liquids at room temperature; thus, they often are called room-temperature ionic liquids (RTILs). Ionic liquids have been widely used in the electrolytes in DSSCs, which is due to their unique features, such as good

Table 2. Photovoltaic Performances^a of the DSSCs Based on Liquid Electrolytes Using Ionic Liquid as Solvents

composition of electrolyte	$D(\text{I}_3^-)(\text{cm}^2\cdot\text{s}^{-1})$	$J_{SC}(\text{mA}\cdot\text{cm}^{-2})$	V_{OC} (V)	FF	η (%)	dye	ref
0.2 M I_2 , 0.5 M NMBI in PMImI/EMImTCM (vol ratio 1/1)	6.3×10^{-7}	12.8	0.752	0.764	7.4	Z907Na	71
5 mM I_2 , 10% HMImI, 90% EMImTFSI	3.4×10^{-7}	11.8	0.57	0.72		N3	101
0.2 M I_2 , 0.14 M GuanSCN, 0.5 M TBP in PMImI/EMImSCN (vol ratio 13/7)	2.95×10^{-7}	13.3	0.746	0.72	7.0	Z907	155
0.1 M I_2 , 0.1 M LiI, 0.45 M NMBI in PMImI/EMImDCN (vol ratio 13/7)	4.4×10^{-7}	12.8	0.707	0.727	6.6	Z907	156
0.2 M I_2 , 0.5 M NMBI, 0.1 M GuanSCN in PMImI/EMImB(CN) ₄ (vol ratio 13/7)	3.42×10^{-7}	13.55	0.736	0.698	7.0	Z907Na	157
0.8 M PMImI, 0.15 M I_2 , 0.1 M GuanSCN, 0.5 M NMBI in MPN		15.1	0.747	0.699	8.0	K19	158
0.5 M I_2 , 0.1 M Cul in HMImI		13.6	0.538	0.62	4.54	N3	159
0.2 M I_2 , 0.5 M NMBI, 0.1 M GuanSCN in REImI/REImTFSI (vol ratio 13/7)		13.54	0.70	0.717	6.8	K60	160
0.2 M I_2 in PMImI/EMImTFSI/EMImTf (vol ratio 2/2/1)	2.48×10^{-7}	16.13	0.612	0.676	6.67	D149	161
0.2 M I_2 , 0.5 M NMBI in PMImI	1.9×10^{-7}	13.07	0.678	0.71	6.27	K19	162
0.2 M I_2 , 0.5 M NMBI, 0.12 M GuanSCN in PMImI/EMImSCN (vol ratio 13/7)	3.0×10^{-7}	13.99	0.707	0.71	7.05	K19	163
0.12 M I_2 , 0.5 M KI, 0.9 M BMIMI in GBL		17.65	0.602	0.58	6.16	N3	164
0.05 M $[\text{Co}((\text{MeIm-Bpy})\text{PF}_6)_3]^{2+}$, 0.02 M NOBF ₄ , 0.14 M GuNCS, 0.5 M TBP in PMII/EMINCS (vol ratio 13/7)		15.1	0.706	0.691	7.37	N719	164
1 M PMII, 0.1 M I_2 , 0.2 M LiTFSI, 0.5 M NBB in MPN		15.3	0.661	0.669	6.8	D205	165
1 M PMII, 0.1 M 4-OH-TEMPO, 0.01 M NOBF ₄ , 0.2 M LiTFSI, 0.5 M NBB in MPN		17.4	0.710	0.580	7.2	D205	165
1 M PMII, 0.1 M [MeIm-TEMPO][TFSI], 0.01 M NOBF ₄ , 0.2 M LiTFSI, 0.5 M NBB in MPN		18.4	0.729	0.608	8.2	D205	165
0.1 M I_2 , 0.1 M LiI, 0.1 M ILBOBs in PMII/EmimBOB (vol ratio 3/1)		13.91	0.539	0.65	5.38	N719	166
1 M DMII, 0.15 M I_2 , 0.5 M NBB, 0.1 M GNCS in MPN		17.51	0.771	0.709	9.6	C103	167
1 M DMII, 0.15 M I_2 , 0.5 M NBB, 0.1 M GuNCS, 50 mM NaI in BN	4.6×10^{-5}	17.9	0.733	0.76	10	C106	168

^aPhotovoltaic performances of all DSSCs were measured under simulated solar light irradiation with an intensity of 100 mW·cm⁻², AM 1.5.



Anions: Cl^- , Br^- , I^- , CN^- , SCN^- , $[\text{N}(\text{CN})_2]^-$, PF_6^- , BF_4^- , CF_3COO^- , CF_3SO_3^- , etc

Figure 7. Examples of the cationic and anionic parts of ionic liquids.

chemical and thermal stability, tunable viscosity, relative nonflammability, high ionic conductivity and broad electrochemical potential window, and more importantly, extremely low vapor pressure making less evaporation and leakage.^{76,152–154} Ionic liquids have two applications in electrolytes in DSSCs. One is acting as solvents in liquid electrolytes, and another is functioning as organic salts in quasi-solid-state electrolytes. The latter will be discussed in the next section. Table 2 shows some examples for using ionic liquids as solvents in electrolytes for DSSCs.⁷⁶

Ionic liquids are composed of anions and cations. The cations are generally bulky, ammonium or phosphonium salts or heteroaromatics, with low symmetry, weak intermolecular interactions, and low charge densities.¹⁶⁹ The anions can crudely be divided into two types:^{76,169} the halide/pseudohalide anions and the complex anions, such as the various borates, triflate derivatives, etc. Some cations and anions frequently used in ionic liquids are shown in Figure 7.

In 1996, Papageorgiou et al. first demonstrated a long-term stable DSSC by using ionic liquids as solvent in electrolyte.¹⁰¹ Using methyl-hexyl-imidazolium iodide (MHImI) as an involatile electrolyte, the DSSC showed outstanding stability with an estimated sensitizer redox turnover number in excess of 50 million. Since that, imidazolium salts and other ionic liquid have been widely used as solvents in electrolytes for DSSCs.

Wang et al. reported a solvent-free ionic liquid electrolyte-based $\text{SeCN}^-/(\text{SeCN})_3^-$ redox couple.¹⁷⁰ The viscosity and conductivity of this ionic liquid, 1-ethyl-3-methylimidazolium selenocyanate (EMImSeCN), were 25 cP and $14.1 \text{ mS}\cdot\text{cm}^{-1}$, respectively. Thus, the DSSC achieved an unprecedented conversion efficiency of 7.5–8.3%. The low viscosity, higher conductivity, and visible-light absorbency of this ionic liquid electrolyte ensured the high photovoltaic performance of the DSSC. However, the long-term stability of this system was not good. Thus, an amphiphilic heteroleptic ruthenium complex Z907Na as a sensitizer in conjunction with a solvent-free ternary eutectic melt ionic liquid electrolyte to low melting points and reduce mass-transport limitation significantly improved the long-term stability of the DSSC, achieving an efficiency over 8%.^{171,172}

Imidazolium-based ionic liquids are the most commonly used and efficient electrolytes in electrochemical applications,¹⁰⁸ also in DSSCs. Other ionic liquids with cations such as sulfonium, guanidinium, ammonium, pyridinium, or phosphonium have also been explored as solvent-free electrolytes.^{173–178} However, they show low efficiencies and photocurrents due to high viscosity and mass-transport limitations. Xi et al. reported a remarkable enhancement of device efficiency by employing a high-fluidity tetrahydrothiophenium melt, demonstrating that nonimidazolium ionic liquids can also be used for high-

efficiency DSSCs.¹⁷⁹ Using a binary melt of *S*-ethyltetrahydrothiophenium iodide and *S*-ethyltetrahydrothiophenium tricyanomethide or dicyanamide in DSSCs, they obtained high power conversion efficiencies of 6.9% and 7.2%, respectively.

The photoelectrochemical properties of the ionic liquids are dependent on the nature of the cation and the anion.¹⁸⁰ In terms of Lewis acid–base behavior,⁷⁵ the cations in ionic liquids are typically weak Lewis acids, thus potentially coordinating electron-rich species in the ionic liquid solutions. The halides/pseudohalides are well-known Lewis bases; they can interact with organometallic sensitizers causing ligand exchange, whereas the other types most commonly used are quite weak Lewis bases. Using a series of substituted imidazolium iodides as electrolytes, Son et al. found that small cation substitutes gave higher diffusion coefficients of triiodide and thus higher photocurrents, whereas larger substitutes displayed an increase in photovoltage.¹⁸¹ The choice of cation and anion and the combination of both will have a significant impact on DSSC performance.

The relatively high viscosity and low ion mobility of pure ionic liquids limit the transportation of iodide/triiodide and the restoration of oxidized dye because the diffusion coefficients of the triiodide in ionic liquid are about 1–2 orders of magnitude lower than those in volatile organic solvents, especially at high illumination intensities.⁷⁶ In rather low-viscosity imidazolium dicyanamide ionic liquids, triiodide diffusion is a limiting factor at low temperature, whereas recombination reactions limit the performance at high temperatures.¹⁸² In order to reduce the mass-transport limitations of ionic liquids, one frequently used way is diluting the ionic liquid with organic solvents, such as AN, in spite of the high volatility of organic solvents.⁷⁶ The decrease of viscosity is not the only factor. It was also found that a high concentration of imidazolium iodides caused an effective reduction of the dye molecules, and the reduced dye did not effectively inject electrons into the TiO_2 semiconductor.⁷¹ According to calculations, about 25% of the dye Z907Na undergoes a reductive quenching in the presence of pure 1-propyl-3-methylimidazolium iodide (PMIImI). Sauvage et al. mixed organic solvent of butyronitrile (BN) with ionic liquid 1,3-dimethylimidazolium iodide (DMII) and *N*-butylbenzimidazole (NBB), which effectively enhanced the triiodide diffusion coefficient.¹⁶⁸ The DSSC based on this BN electrolyte in conjunction with C106 sensitizer achieved a champion efficiency of 10%. Another effective way to solve the mass-transport limitation of pure ionic liquids is mixing imidazolium iodides with low-viscosity ionic liquids.¹⁸³ For example, an ionic liquid electrolyte composed of EMImSCN and PMIImI had a triiodide diffusion coefficient of $2.95 \times 10^{-7} \text{ cm}^2\cdot\text{s}^{-1}$, which was 1.6 times higher than that in the pure PMIImI electrolyte.¹⁵⁵

The cell using this electrolyte together with Z907 dye achieved an efficiency of 7%. Another way to enhance the conductivity of ionic liquid electrolyte is introducing solid components.¹⁸⁴ Neo et al. decreased the viscosity of PMIImI from 1380 to 400 cP (25 °C) by adding 0.10 wt % carboxylic group-functionalized multiwalled carbon nanotubes (oMWCNTs).¹⁸⁵ The addition of oMWCNTs did not affect the thermal stability of PMII and significantly improved the conversion efficiency of DSSCs.

Owing to the high viscosity for ionic liquids, the transportation and diffusion of ions are limited in the electrolytes. On the basis of the measurements of diffusion coefficients of I₃⁻ in pure HMIImI, the Grotthus electron exchange mechanism was proposed.¹⁰¹ Later, it was confirmed that triiodide might be transferred to the counter electrode not only by diffusion but also by a nondiffusional Grotthus-like hopping mechanism,¹⁸⁶ which compensated for mass-transport limitation in the rather viscous ionic liquids.^{76,108}

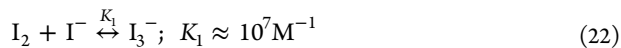
Ionic liquid is a promising alternative to organic solvents as the electrolyte solvent for DSSCs.⁷⁶ Their potential advantage remains to be explored, and the main drawbacks of high viscosity and low ion mobility have to be overcome.

2.3. Iodide/Triiodide Redox Couples

The redox couple is a key component of the DSSCs. In the photoelectrochemical cycle of the DSSCs, the reduced state (RE, iodide) of the couple regenerates the photo-oxidized dye (D⁺) and the oxidized state (OX, triiodide) of the couple diffuses to the counter electrode, where it is reduced. With regard to the reaction kinetics, the redox couple should have "asymmetric behavior",¹⁸ the electron donation from RE to D⁺ should be sufficiently fast to ensure efficient dye regeneration (eq 3), while the electron acceptance from the TiO₂ film to OX should be slow enough to decrease electron recombination (eq 6) losses.⁷⁵ Besides, the reduction of OX to form RE (eq 4) on the counter electrode in a minimal overpotential should be fast to provide enough couple sources and complete the electrochemical cycle.¹²¹ In terms of energy level, to increase the photovoltage of the DSSCs it is critical to use a redox electrolyte that has energy as close as possible to the D⁺/D energy level but with sufficient driving force to regenerate the dye quantitatively.⁴⁰

The iodide/triiodide couple has a suitable redox potential and provides rapid dye regeneration and slow electron recombination; meanwhile, the couple has good solubility, high conductivity, and less light absorption, in addition to favorable penetration ability into the mesoporous semiconductor film and being proven to have long-term stability. Owing to these unique features, the iodide/triiodide couple has been the preferred redox couple since the beginning of DSSC development.⁴⁰

In solution, iodine will bind with iodide to form triiodide in an equilibrium reaction¹⁸⁷



If the iodine concentration is high, polyiodide species like I₇⁻, I₉⁻, and I₁₁⁻ may also be formed. In fact, only triiodide seems important in DSSC electrolytes because K₁ is high in organic solvents. For example, an electrolyte made from 0.7 M I⁻ and 0.05 M I₂ should contain an equilibrium concentration of 8 × 10⁻⁹ M of I₂; the rest of the I₂ is converted to I₃⁻. In the DSSC, a two-electron reaction (eq 23) occurs at the counter electrode, and in fact, it contains successive and rapid one-electron

reactions (eq 13). According to eq 23, the redox potential of the electrolyte (E_{redox}) is given by the Nernst equation (eq 24)⁴⁰



$$E_{\text{redox}} = E^\circ + \frac{RT}{2F} \ln \frac{[I_3^-]}{[I^-]^3} \quad (24)$$

Here, E° is the formal potential, R is the gas constant, T is the absolute temperature, and F is the Faraday constant. For the standard sensitizer N3 or N719, $E^\circ(D^+/D)$ is 1.10 V vs NHE.⁴⁶ The potential difference between $E^\circ(D^+/D)$ and $E^\circ(I_3^-/I^-)$ is about 0.75 V. This potential is used to drive the forward reactions in the DSSC. On the basis of the reaction scheme for dye regeneration (eqs 11 and 12), the driving force for the dye regeneration reaction is given by the difference between $E^\circ(I_2^-/I^-)$ and $E^\circ(D^+/D)$. This corresponds to a potential loss of several hundred millivolts [$E^\circ(I_2^-/I^-) - E^\circ(I_3^-/I^-)$] in the DSSC.

A series of recombination reactions compete with the forward reactions in the DSSC. Radiative and nonradiative decay of the excited dye (D*) is competing with electron injection. It is found that the electron injection efficiency is approaching 100% for sensitizers with energetic match to the TiO₂ conduction band.⁴⁰ After injection, the electrons can recombine with oxidized dye molecule D⁺ (eq 5). Although this process is slow under low light intensity, it is accelerated dramatically under high electron concentration, for example, at high light intensity or at the maximum power point, leading to competition with dye regeneration.¹⁸⁸

Though a definitive mechanism for the recombination of electrons in mesoporous TiO₂ with triiodide (eq 6), including what the acceptor and intermediate species are, remains elusive,^{39,121} it has been clear that the recombination occurs both at the interface between the TiO₂ and the electrolyte and at the part of the conducting substrate that is exposed to the electrolyte. The latter is usually less important in the case of I⁻/I₃⁻ and can be suppressed by using a compact blocking layer of metal oxide.¹⁸⁹ The recombination is strongly temperature dependent and an activation-controlled process.¹⁹⁰ It can be suppressed by additives in the electrolyte, such as 4-*tert*-butylpyridine^{46,191,192} and guanidium thiocyanate.¹⁹³ Both additives give a decreased recombination rate. The most probable mechanism is that these additives adsorb at the TiO₂ surface, blocking active reduction sites or preventing approach of I₃⁻ to the surface. Dyes adsorbed at the mesoporous TiO₂ electrode affect the reduction of I₃⁻. The dyes with additional hydrophobic chains can reduce the recombination rate by a blocking effect, as demonstrated for the Z907 dye in comparison with N719.¹⁹⁴ Certain dyes adsorbed on TiO₂ increase the recombination rate,^{195–198} which may be attributed to a locally increased concentration of triiodide near the dye¹⁹⁷ or binding of the dye with iodine.¹⁹⁸

For rapid regeneration of the oxidized dye, iodide should have a high concentration and diffusion rate. In nonviscous solvents such as acetonitrile, an iodide concentration of 0.3 M is sufficient, while in viscous ionic liquids a higher iodide concentration may be necessary.⁷¹ Transport of triiodide to the counter electrode can be a rate-limiting step in the DSSC if the concentration of triiodide is low or if the solvent is viscous.¹⁹⁹ Under high triiodide concentration, the apparent diffusion coefficient may increase by the Grotthus mechanism.²⁰⁰

The cations, combined with the I^-/I_3^- anions in electrolyte, have some influence on the properties of liquid electrolyte and the photovoltaic performances of DSSCs. The influences include three aspects at least. (i) As a band bending and depletion layer,^{30,33,35} the position of the TiO_2 conduction band edge depends on the type and concentration of cations in the electrolyte. Pelet et al. found that adsorption of cations onto the TiO_2 surface affects the local iodide concentration; with the increase of cations concentration, the conduction band of TiO_2 film shifts to lower energy.²⁰¹ (ii) The cations in electrolyte significantly affect the electron transport in the TiO_2 film. The diffusion of electrons in the conduction band of TiO_2 is considered as an ambipolar diffusion mechanism, namely, electron transport is strongly correlated with ion diffusion to ensure the electrical neutrality of TiO_2 film.^{202–206} For example, when LiI was added into liquid electrolyte, the small-radius Li^+ cations can deeply penetrate deep into the mesoporous TiO_2 film and combine with the electrons in the conduction band of TiO_2 to form an ambipolar $Li^+ - e^-$, which increases the transport speed of electrons and enhances the J_{SC} of DSSCs.^{131,207–210} (iii) The negative influence of the small cations in the TiO_2 film is that the cations easily combine with triiodide, which leads to the recombination loss and the decrease of V_{OC} of the DSSCs.^{207,211} Liu et al. found that with the increase of the cation radius in the order $Li^+ < Na^+ < K^+ < Rb^+ < Cs^+$; the potential of the conduction band shifts negatively, leading to an increase in V_{OC} and a decrease in J_{SC} .¹³¹ In a study of the effects of monovalent to trivalent main group iodides on solar cell performance, it was found that the cations with higher charge density had a larger effect on the photovoltaic properties of DSSCs, which was caused by the expected energy band shifts and recombination losses.²¹² In order to overcome this negative influence, an imidazole cation with larger ionic radius was used in liquid electrolyte to form a Helmholtz layer on the surface of TiO_2 film and block direct contact of triiodide with ambipolar $Li^+ - e^-$, resulting in a suppressing combination between ambipolar $Li^+ - e^-$ and triiodide and thus enhancing the V_{OC} of DSSCs.^{208,211}

Though the I^-/I_3^- redox couple shows remarkable performance in DSSCs, there are several negative features limiting its further application: (i) iodine is extremely corrosive to many sealing materials, especially metals, causing difficult assembling and sealing for a large-area DSSC and poor long-term stability for DSSC;²¹³ (ii) iodine has a relatively high vapor pressure, which makes it challenging for device encapsulation; (iii) the I_3^- ion and other possible polyiodides (such as I_5^- , I_7^- , and I_9^-) absorb part of the visible light, lowering the photocurrent and hence the conversion efficiency of the devices;¹⁸ (iv) the mismatch (about 0.8 V) between the redox potential of a typical sensitizer ($E_{redox} \approx 1.1$ V vs NHE) and that of I^-/I_3^- ($E_{redox} \approx 0.3$ V vs NHE) causes a loss in V_{OC} for the device. According to Marcus theory,²¹⁴ a driving force of 0.2–0.3 eV should be sufficient for outer-sphere single-electron-transfer reactions to ascertain a fast dye regeneration rate, opening up the opportunity to increase the V_{OC} . This beneficial effect has indeed been observed when the I^-/I_3^- redox couple was replaced by new cobalt complexes^{21,22} or solid-state hole conductors,^{121,215} yielding higher V_{OC} values.

2.4. Iodide/Triiodide-Free Mediator

Before 2010, studies on the electrolyte mainly focused on the traditional iodide/triiodide electrolyte. The development of new redox mediators falls far behind that of the sensitizing dyes

and other materials for the DSSC components. However, the field has received renewed attention recently. The number of articles on new redox shuttles in 2010 and 2011 was more than the sum of all those published earlier.^{215–217} In 2011, by using a new Co-complex-based electrolyte in combination with new sensitized dye YD2-o-C8, the Gratzel group reported a DSSC with an efficiency of 12.3%.²¹

The bromide/tribromide couple has a more positive redox potential (about 1.1 V vs NHE) in comparison to the iodide/triiodide couple (about 0.35 V vs NHE).⁴⁰ Thus, electrolytes containing the Br^-/Br_3^- redox system can improve greatly the photovoltage of the DSSCs if used together with well-designed dyes. The research results approved that the DSSCs with Br^-/Br_3^- electrolyte had higher V_{OC} values than that of the DSSCs with I^-/I_3^- electrolyte for appointed dyes but lower J_{SC} values.^{218–221} For example, Teng et al. compared the photovoltaic properties of the DSSC with TC306 dye based on Br^-/Br_3^- and I^-/I_3^- acetonitrile-based electrolyte.²¹⁹ The DSSC with Br^-/Br_3^- electrolyte obtained a V_{OC} of 0.94 V and an efficiency of 5.2%, whereas the DSSC with I^-/I_3^- electrolyte obtained a V_{OC} of 0.62 V and an efficiency of 4.1% under similar conditions. From an energy level point of view, the development bottleneck for Br^-/Br_3^- -based electrolyte is less suitable dyes.

Interhalogen redox systems, such as I^-/IBr_2^- and I^-/I_2Br^- , have been studied in various electrolytes used in the DSSCs in combination with ruthenium-based sensitizing dyes. Conversion efficiencies up to 6.4% were achieved.²²² However, complex equilibrium between various interhalogen anions limits the couple's full characterization.

Two pseudohalogen redox couples, $SCN^-/(SCN)_3^-$ and $SeCN^-/(SeCN)_3^-$, have been studied as redox mediators for DSSCs.^{170,223,224} The redox potentials of the two redox couples are 0.19 and 0.43 V more positive than that of the I^-/I_3^- redox couple, respectively. In 2004, Wang et al. reported an ionic liquid-based electrolyte containing the $SeCN^-$ -based redox couple.¹⁷⁰ A conversion efficiency of 7.5% was achieved for a DSSC in combination with the dye N3. Although pseudohalogen redox can reach a high efficiency, the poor stability limits the development of the redox couple.¹⁷¹

Organic redox disulfide/thiolate (T^-/T_2) was successfully used as a redox couple in DSSCs.²²⁵ Here, T^- represents the 1-methyl-1-*H*-tetrazole-5-thiolate anion, and T_2 is its dimer. Using a ruthenium-based Z907-Na as sensitized dye and T^-/T_2 (0.4 M/0.4 M) based electrolyte containing 0.5 M TBP and 0.05 M $LiClO_4$, the DSSC obtained a J_{SC} of $16.18\text{ mA}\cdot\text{cm}^{-2}$, a V_{OC} of 681 mV, a FF of 0.58, and an efficiency of 6.44%.²²⁵ Recently, an unprecedented power conversion efficiency of 7.9% was achieved for the DSSC based on the T^-/T_2 redox couple together with PEDOT counter electrode,²²⁶ which represents the highest efficiency for the DSSCs with an organic redox couple so far. It is notable that despite promising results obtained for new sulfide-based redox couples, the long-term stability of these cells still needs to be improved. The T^-/T_2 redox couple is a member of a larger family of similar organosulfur compounds based on disulfide, polysulfides, thiourea, cysteine, etc.,^{227–229} which were also tested in DSSCs, but the T^-/T_2 is a generic redox shuttle exhibiting better performance in various systems. Since the redox potential of T^-/T_2 is close to that of I^-/I_3^- , one cannot expect further improvement in DSSC voltage.

In 2001, Nusbaumer et al. first reported the charge-transfer dynamics of a Co-complex redox system ($Co(dbip)_2^{2+/3+}$) in

DSSCs.²³⁰ With this one-electron redox couple and a ruthenium dye (Z316), the DSSC achieved a power conversion efficiency of 2.2%. The lower efficiency is due to the fast recombination of TiO_2 conduction band electrons with Co(III). The advantages of this kind of one-electron outer-sphere transition metal complex are that redox couples are nonvolatile, noncorrosive, light-colored, and tunable potential (0.3–0.9 V) through modification of the ligands. However, owing to the large size of the cobalt complex and the higher viscosity of the electrolyte, Co-complex redox couple electrolytes are subjected to mass-transport limitation and recombination loss. In order to overcome these disadvantages, many investigations have been implemented.^{18,231–241} For example, Nelson et al. reported that the diffusion of Co^{3+} (4,40-di-*tert*-butyl-2,20-bipyridine) was 1 order of magnitude slower than the diffusion of I_3^- in bulk solution for TiO_2 mesoporous film.²³¹ Thus, the mesoporous TiO_2 films with larger porosity would be advantageous for cobalt complex-based electrolytes. Hamann et al. determined the recombination kinetics (photo-electron lifetimes) in different cobalt redox electrolytes and found that the lifetime at a given electrode was in the order $[\text{Co}(\text{dtb-bpy})_3]^{2+/3+} > [\text{Co}(\text{dm-bpy})_3]^{2+/3+} > [\text{Co}(\text{bpy})_3]^{2+/3+}$, and the recombination rate constants decreased in the reverse order.²³² These results showed that the structure of the Co complexes is fairly important to the performance of DSSCs. It is very significant that in 2011 Yella et al. boosted the efficiency of DSSC to 12.3% by using a Co(II/III)(bipyridine)₃-based redox electrolyte in conjunction with a donor–p-bridge–acceptor zinc porphyrin (YD2-o-C8) as a sensitizer.²¹ Rather recently, Mathew and Gratzel used a panchromatic porphyrin dye SM315 featuring a porphyrin core and a bulky bis(2',4'-bis(hexyloxy)-[1,1'-biphenyl]-4-yl)amine donor in conjugation with a cobalt(II/III) redox shuttle in DSSC, which resulted in a high V_{OC} of 0.91 V, J_{SC} of 18.1 $\text{mA}\cdot\text{cm}^{-2}$, FF of 0.78, and efficiency of 13% at an AM 1.5 full sunlight irradiation.²² This is so far the highest efficiency record for the classical DSSCs. This system generated a strikingly high photovoltage close to 1 V and had an impressive photocurrent density of 18.1 $\text{mA}\cdot\text{cm}^{-2}$. Right now, Co-complex mediators are the most efficient redox couples for DSSCs. By tuning the redox potentials of the Co-complex systems and the energy level of the sensitizing dyes it is possible to see a DSSC with a higher conversion efficiency in the near future.

Apart from cobalt-based redox couples, other metal complexes and clusters, such as Ni(III)/Ni(IV), Cu(I)/Cu(II), and ferrocene/ferrocenium (Fc/Fc^+), have also been investigated.^{242–246} Using a Cu(I)/Cu(II)-based electrolyte in combination with an organic dye C218, Bai et al. assembled a DSSC with a conversion efficiency of 7%.²⁴² The Fc/Fc^+ redox potential (0.62 V) is more positive than that of the I^-/I_3^- (0.35 V vs NHE) redox couple, which is expected to be higher V_{OC} than that of DSSC with I^-/I_3^- electrolyte. The best result for the DSSC with Fc^+/Fc -based electrolyte was reported by Daeneke et al.²⁴⁶ using chenodeoxycholic acid as coabsorbent dye. This DSSC gave photovoltaic data: $J_{\text{SC}} = 12.2 \text{ mA}\cdot\text{cm}^{-2}$, $V_{\text{OC}} = 842 \text{ mV}$, FF = 0.73, and $\eta = 7.5\%$. In this study the electrolyte and device fabrication were performed in a glovebox under nitrogen atmosphere to avoid the influence of oxygen on the redox electrolyte.

2.5. Electrical Additives

Electrical additive is another substantial component in liquid electrolytes for optimizing the photovoltaic performance of

DSSCs. The redox couple potential, semiconductor surface state, shift of the conduction band edge, recombination kinetics, as well as the photovoltaic parameters of DSSCs can be improved by adding a small amount of additives.^{247,248}

In 1993, 4-*tert*-butylpyridine (TBP) was first used as an additive in electrolyte by Gratzel et al. resulting in a significant improvement of the V_{OC} of DSSC.⁴⁶ Thus, nitrogen-containing heterocyclic compounds, such as analogues and derivatives of pyridine, alkylaminopyridine, alkylpyridine, benzimidazole, pyrazole, quinoline, etc., have been studied as additives in liquid electrolytes. These nitrogen-containing heterocyclic compounds exhibited similar effects to TBP; therefore, they have become the most frequently used additives in electrolytes to improve the V_{OC} .^{76,167,171,249–252}

Huang et al. found that the addition of TBP and pyridine derivatives may reduce the electron recombination rate by 1–2 orders of magnitude.²⁵³ On the basis of intensity-modulated photovoltage spectroscopy (IMVS) measurements, Schlichthorl et al. indicated that the dramatic increase of V_{OC} was mainly ascribed to the negative shift of the conduction band edge of TiO_2 film.²⁵⁴ Boschloo et al. found that the increase of the V_{OC} could be attributed to a combined effect of the conduction band edge shift of TiO_2 toward higher energy levels and longer electron lifetimes in the conduction band.²⁵⁵ An *in situ* Raman spectroscopic measurement showed that TBP bound to the TiO_2 surface and likely also to iodine or the dye molecules,²⁵⁶ which was further supported by the surface analysis.^{257,258} The additives have a similar effect and mechanism as the aforementioned solvent donor number since the nitrogen-containing heterocyclic additive is a kind of base.^{250–252} The difference is that the function of additive for optimizing the photovoltaic performance of DSSCs is more efficient than that of the donor number of solvent. It is notable that the superfluous additive will cause a poor photovoltaic performance of DSSCs. The negative effects of additives were also found in Wu's research.^{144,289}

Another class of frequently used additives contains specific cations, such as lithium ions (Li^+) or guanidinium [$\text{C}(\text{NH}_2)_3^+$, abbreviated G^+] ions. These cation additives can also improve the photovoltaic performances of DSSCs. However, the mechanisms are different from that of the nitrogen-containing heterocyclic compounds. The studies on the effect of Li^+ cations in liquid electrolytes indicated that Li^+ additives caused the conduction band edge shift of TiO_2 film toward lower energies due to the adsorption of Li^+ ions on the TiO_2 surface,^{131,260–264} resulting in an increase of the electron injection from the D^* to the conduction band of TiO_2 , and the higher electron injection enhanced the photocurrent of DSSCs. Kopidakis et al. found that Li^+ ions could irreversibly intercalate into the TiO_2 films, which strongly affected the electron recombination and electron transportation of DSSCs.²⁶⁵

The G^+ cation also is used to improve the photovoltaic performance of DSSCs. Zhang et al. observed a significant enhancement of J_{SC} of DSSCs when G^+ ions were added into the electrolyte, which was due to an increase of the electron injection yield.²⁶⁶ It was reported that G^+ cations along with the N3 dye were adsorbed on the surface of TiO_2 film to form a self-assembly compact dye monolayer, thus reducing the dark current, remarkably enhancing the photovoltage and achieving a recorded conversion efficiency of 11% for the DSSC.²⁶⁷ The research by Kopidakis et al. indicated that the collective effect of a slower electron recombination by a factor of 20 and a downward shift of conduction band edge TiO_2 by G^+ cation

Table 3. Some Commonly Used Polymer Matrixes for TPPEs in DSSCs

polymer name	polymer framework	repeat unit	glass transition temp/°C	melting point/°C
PEO or PEG	poly(ethylene oxide)	$-\{\text{CH}_2\text{CH}_2\text{O}\}_n-$	-64	65
PPO	poly(propylene oxide)	$-\{\text{CH}(-\text{CH}_3)\text{CH}_2\text{O}\}_n-$	-60	
PAN	poly(acrylonitrile)	$-\{\text{CH}_2-\text{CH}(-\text{CN})\}_n-$	125	317
PS	polystyrene	$-\{\text{CH}_2-\text{CH}(-\text{C}_6\text{H}_5)\}_n-$	90	240
PVP	poly(vinyl pyrrolidinone)	$-\{\text{CH}_2-\text{CH}(-\text{NC}_4\text{H}_9\text{O})\}_n-$	110	180
PMMA	poly(methyl methacrylate)	$-\{\text{CH}_2\text{C}(-\text{CH}_3)(-\text{COOCH}_3)\}_n-$	-105	
PVC	poly(vinyl chloride)	$-\{\text{CH}_2\text{CHCl}\}_n-$	85	
PVDF	poly(vinylidene fluoride)	$-\{\text{CH}_2\text{CF}_2\}_n-$	-40	171
PVdF-HFP	poly(vinylidene fluoride-hexafluoropropylene)	$-(\text{CH}_2\text{CF}_2)_x\{\text{CF}_2\text{CF}(\text{CF}_3)\}_y-$	-90	135

gave a net improvement in V_{OC} of about 20 mV for the DSSCs.¹⁹³

Although the nitrogen-containing heterocyclic compound additives and cations additives in electrolytes have opposite function with respect to the TiO_2 energy level, these two kinds of additives are often simultaneously used in the electrolytes.^{15,167,171} It is expected that both benefits can be simultaneously obtained, i.e., the conduction band is shifted to higher energy level and the surface of semiconductor is blocked to reduce recombination losses. The Durrant group revealed that the electrolyte containing both Li^+ ions and TBP gave the highest device photovoltaic performance, better than two other electrolytes containing only one additive.^{261,262} Yu et al. investigated the effects of the additives GSCN and *N*-methylbenzimidazole (MBI) on the photovoltaic performance of DSSCs.²⁶⁸ A synergistic effect was observed when GSCN and MBI were used jointly in an ionic liquid-based electrolyte, resulting in an optimal photovoltaic performance.

The special feature of the liquid electrolyte equips it with the highest efficiency, and it is the most extensively used in traditional DSSCs. The performance of the electrolytes depends on the individual properties of the constituents of the electrolyte (solvent, ionic conductor, and additives), their own interactions, as well as the interactions among electrolytes, electrodes, and sensitized dyes. Enhancement of liquid electrolyte performance involves understanding and controlling the properties of each component, in addition to knowing their effect on the related energy conversion processes.

3. QUASI-SOLID-STATE ELECTROLYTES

Using liquid electrolytes as charge carrier transporters, the DSSC achieves great development. However, the use of liquid electrolytes causes some practical problems, such as leakage and volatilization of solvent, photodegradation and desorption of dye, corrosion of counter electrode, and ineffective sealing of the cells for long-term applications. One of the methods to solve these problems is using quasi-solid-state electrolytes. Although the efficiencies of the DSSCs with quasi-solid-state electrolytes are often lower than those of the DSSCs with liquid electrolytes, the quasi-solid electrolytes may become viable alternatives to the liquid electrolytes owing to improved stability and better sealing ability.^{35,37,74,77}

Quasi-solid state or semisolid state is a special state of a substance between solid and liquid states. Quasi-solid-state electrolyte is a macromolecular or supramolecular nanoaggregate system characterized by a remarkable ionic conductivity, usually higher than $10^{-7} \text{ S}\cdot\text{cm}^{-1}$,^{269,270} for DSSCs, usually higher than $10^{-3} \text{ S}\cdot\text{cm}^{-1}$.²⁷¹ Quasi-solid-state electrolytes always possess, simultaneously, both the cohesive property of solid and the diffusive property of liquid,^{82,272–277}

namely, quasi-solid-state electrolytes show better long-term stability than liquid electrolytes and have the merits of liquid electrolytes including high ionic conductivity and excellent interfacial contact property. Due to their excellent characteristics, quasi-solid electrolytes are widely used in DSSCs²⁷¹ and other electronic or electrochemical devices, such as secondary batteries,²⁷⁸ fuel cells,²⁷⁹ sensors and actuators,²⁸⁰ supercapacitors,²⁸¹ and electrochromic displays.

There are three methods often used for preparing quasi-solid electrolyte: (i) liquid electrolytes are solidified by organic polymer gelators to form thermoplastic polymer electrolytes or thermosetting polymer electrolytes; (ii) liquid electrolytes are solidified by inorganic gelators, such as SiO_2 , nanoclay powder, to form composite polymer electrolytes; (iii) ionic liquid electrolytes are solidified by organic polymer or inorganic gelators to form quasi-solid ionic liquid electrolytes.^{76,108} According to the features, formation mechanisms, and physical states of the electrolytes, we divide quasi-solid-state electrolytes into four main kinds: thermoplastic polymer electrolytes,²⁸² thermosetting polymer electrolytes,²⁸³ composite polymer electrolytes,²⁷⁰ and ionic liquid electrolytes.⁷⁶

3.1. Thermoplastic Polymer Electrolytes

In general, polymer gel electrolyte consists of polymer or oligomer, organic solvent, inorganic salt, and inorganic salts as well as sometimes containing additives. The main functions of polymer or oligomer is acting as matrix or framework to gel, solidify, absorb, swell, hold, and interact with liquid electrolyte (containing solvents and salts); the polymer often is called a gelator or adsorber.^{37,74} The solvent, often termed plasticizer, provides the room and surroundings for ionic salt migration; it reduces the crystallization and glass temperature of electrolyte, because it exists between the adjacent polymer chains, decreases the polymer–polymer chain interaction, and increases the free volume and segmental mobility of the system. When mixing the polymer matrix with liquid electrolyte, the system converts gradually from a dilute heterogeneous system to a viscous homogeneous system or from a sol state to gel state. In this gelation process, owing to weak interaction between the polymer matrix (gelator) and the solvents (plasticizer), a polymer gel electrolyte is obtained by the gelation, adsorption, inflation, and “entanglement network” of the polymer in liquid electrolyte.^{37,74} The weak interaction included in hydrogen bonds, van der Waals, electrostatic interaction, etc., is a “physical cross-linking”,^{37,74} it depends on the temperature. Therefore, the state of this kind of electrolyte can be reversibly changed from the sol state to the gel state by controlling temperature. According to this feature, we name this kind of electrolyte “thermoplastic polymer electrolyte” (TPPE),²⁸² borrowing a word from the polymer elastomer field. Because a fair amount of solvent remained, the TPPE

shows the liquid electrolyte feature with high ionic conductivity and good interfacial wetting and filling; moreover, owing to the solvent trapped to some extent, the TPPE has some solid electrolyte merit in stability with low liquid fluidity, reducing the vaporization and leakage of liquid.³⁷ In TPPEs, the charge carriers are transported in the ion diffusion and free volume model as well as the electron exchange model.

TPPEs contain a key component, polymer gelator. The linear polymers are often used as gelators, including poly(ethylene oxide) (PEO or PEG), poly(acrylonitrile) (PAN), poly(vinyl pyrrolidinone) (PVP), polystyrene (PS), poly(vinyl chloride) (PVC), poly(vinylidene ester) (PVE), poly(vinylidene fluoride) (PVDF), poly(methyl methacrylate) (PMMA), etc.^{74,284} Table 3 displays the properties of some commonly used polymer matrixes for TPPE in DSSCs.²⁸⁵

In 1995, Cao et al. was a pioneer in using TPPE in a quasi-solid-state DSSC (QS-DSSC). The TPPE was obtained by incorporating a liquid electrolyte containing EC, PC, AN, NaI, and I₂ in PAN polymer, and the QS-DSSC exhibited photovoltaic property and stability comparable with liquid electrolyte cells.²⁸⁶ Since then, the TPPE has been studied and applied in QS-DSSCs.

Our group has been focusing research on the TPPEs for DSSCs, including (polymer host/solvent/ionic conductor) PEG/PC/KI + I₂, P(AC-ST)/PC + EC/C₅H₅-N⁺-CH₃I⁻ + I₂, PEG/PVP/KI + I₂, PMMA/EC + PC + DMC/NaI + I₂, P(AC-ST)/PC + EC/NaI + I₂ + TBP, MPN + AN/AlI₃ + I₂, PAS/PC + DMC + GBL/C₉H₇-N⁺-CH₃I⁻ + I₂, etc.^{275,282,287-295}

As a typical example of TPPEs, the PEG/PC/KI + I₂ system is introduced.²⁸² Using PEG (40 wt %) as polymer host, PC (60 wt %) as organic solvent, and KI (0.65 M) and I₂ (0.065 M) as ionic conductors, a TPPE with a conductivity of 2.61 mS·cm⁻² was prepared by simply mixing the components above. The QS-DSSC based on this TPPE exhibited almost the same conversion efficiency (7.22%) as the DSSC based on liquid electrolyte (7.60%). Moreover, the long-term stability of the QS-DSSC was greatly improved. The viscosity, conductivity, and phase state of the TPPE could be adjusted by tuning the temperature and compositions of electrolyte. The TPPE showed a sol state (Figure 8) with a viscosity of 0.76 Pa·s at temperatures higher than 50 °C, which benefited a deep penetration into the mesoporous TiO₂ film²⁹⁶ and formed a sufficient electrolyte/electrode interfacial contact, while at temperature below 20 °C, the TPPE existed in a gel state with a viscosity of 2.17 Pa·s. The reversible thermoplastic

behavior of the TPPE is highly beneficial for the fabrication and long-term stability of QS-DSSCs.

The PEO and its copolymer are the most widely used gelators for preparing TPPEs.^{74,77,284} The first DSSC assembled with PEO-based electrolyte was reported by De Paoli et al. in 1999, although the efficiency of this cell was lower.²⁹⁷ The use of PEO copolymers as gelator was also initiated by the De Paoli group.²⁹⁸ They systematically investigated the ionic conductivity and thermal properties of the copolymers of ethylene oxide (EO) and epichlorohydrin (EPI).²⁹⁹⁻³⁰¹ PEG (PEO) contains many ether groups in the main chain and polyhydric groups in the side chain; these two kinds of groups can interact with the alkali metal cations; therefore, the iodide anions can be separated from alkali cations and freely migrate, which favors an enhancement in ionic conductivity.^{74,302} On the other hand, the ether groups and polyhydric side groups on PEG can interact (hydrogen bond) with solvents, such as PC, hanging the solvent molecules on the polymer chain to form an “entanglement network”, and results in the formation of a stable thermoreversible polymer gel electrolyte. It is notable that the molecular weight of PEO segments is important for the ionic conductivity and thus for the efficiency of DSSCs.¹⁰ Shi et al. used a high molecular weight PEO ($M_w = 2 \times 10^6$ g·mol⁻¹) as polymer host to gelate liquid electrolyte and form a polymer gel electrolyte; the QS-DSSC with the polymer electrolyte (PEO 10 wt %) showed a conversion efficiency of 6.12% and 10.11% under 100 and 30 mW·cm⁻² illumination, respectively.²⁰⁹

PAN offers a homogeneous hybrid electrolyte where the salts and plastics are molecularly dispersed.²⁹⁶ PAN host structure is inactive in ionic conduction but provides a matrix for structural stability. Ileperuma group prepared a PAN-based polymer gel electrolyte with a conductivity of 4.33 mS·cm⁻¹.³⁰³ Using this TPPE, a DSSC achieved a high efficiency of 7.23%. The lower efficiency compared to the DSSCs based on liquid electrolyte can be attributed to incomplete wetting of pores and mass-transfer limitations of redox species through a more viscous medium.

PVDF and its copolymer poly(vinylidenefluoride-co-hexa-fluoropropylene) (PVDF-HFP) have been used as host in many polymer gel electrolytes.³⁰⁴ For example, by using PVDF-HFP (5 wt %) as polymer host to gel MPN-based liquid electrolyte, Wang et al. prepared a quasi-solid-state electrolyte; the QS-DSSC using an amphiphilic ruthenium sensitizer in conjunction with this polymer gel electrolyte achieved an efficiency > 6%.^{269,305} The cell sustained heating for 1000 h at 80 °C, maintaining 94% of its initial performance, and showed excellent stability under light irradiation.

Besides simply mixing polymer gelator with liquid electrolytes, there are some useful methods for preparing TPPEs. Lee et al. reported an interesting method for preparing polymer gel electrolytes.³⁰⁶ The polystyrene (PS) nanobeads were coated on the surface of the Pt counter electrode. When a liquid electrolyte was filled into the assembled DSSC, the PS as gelator was dissolved and transferred liquid electrolyte into gel electrolyte, by which the pore-filling problem in DSSCs could be diminished. The QS-DSSC based on the gel electrolyte showed almost the same conversion efficiency (7.59%) as the DSSC based on liquid electrolyte (7.54%). Moreover, the long-term stability of the QS-DSSC was greatly improved. Seo et al. positioned brominated poly(2,6-dimethyl-1,4-phenylene oxide) (BPPO) nanofiber mats on the surface of photoanode; the BPPO as gelator was dissolved by the liquid electrolyte and



Figure 8. Digital images of thermoplastic polymer electrolyte (TPPE) PEG/PC/KI + I₂ (a) at 50 and (b) at 20 °C. Reproduced with permission from ref 282. Copyright 2007 John Wiley and Sons.

then formed a gel electrolyte.³⁰⁷ The efficiency of the QS-DSSC was comparable to the DSSC with conventional liquid electrolyte. Furthermore, the QS-DSSCs exhibited good long-term stability.

Another frequent method to prepare TPPE is using organic molecules as gelators. These organic molecules are required for strong interacting or bonding ability with solvents, which makes liquid electrolyte transforming into gel electrolyte. For example, 1,3:2,4-di-O-benzylidene-D-sorbitol (DBS) and its derivatives had strong interaction with MPN, and DBS (1 wt %) could transfer MPN-based liquid electrolyte to gel state; the conductivity of the gel polymer electrolyte was $10 \text{ mS}\cdot\text{cm}^{-1}$, which was comparable with the liquid electrolyte.²⁷⁴ Using this thermoreversible electrolyte, the QS-DSSC obtained a conversion efficiency of 6.1%. Huo et al. used tetradodecylammonium bromide as a low molecular weight gelator to gel MPN-based liquid electrolyte, and the QS-DSSC obtained an efficiency of 5.35%.³⁰⁸ On the basis of the hydrogen bond interaction between amphiphatic amide derivatives and MPN, Yu et al. incorporated a low molecular weight gelator of cyclohexanecarboxylic acid-[4-(3-octadecylureido)phenyl] amide (3 wt %) to MPN-based liquid electrolyte to form a gel electrolyte.³⁰⁹ The QS-DSSC based on this gel electrolyte in combination with C105 dye boasted a conversion efficiency of 9.1%, which was comparable with the DSSC with liquid electrolytes. The QS-DSSC also retained excellent thermal and light-soaking stability during 1000 h accelerated aging tests. It was believed to be the best efficiency ever reported for a QS-DSSC based on low molecular weight organic gelator, so far.

The Wu group reported a special gel electrolyte containing only mixed organic solvents of 3-methoxy-propionitrile and aniline (MPN + ANI) and iodide salt ($\text{AlI}_3 + \text{I}_2$), as shown in Figure 9.^{288,289} On the basis of a Lewis acid–base interaction

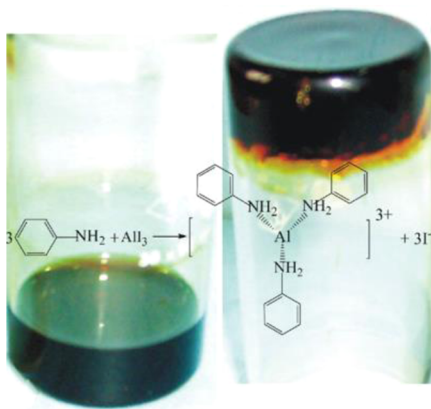


Figure 9. Digital photos of the AlI_3 –MPN liquid and AlI_3 –MPN–ANI gel electrolytes and the related chemical equations between the Lewis acid AlI_3 and the Lewis base ANI. Reproduced with permission from ref 288. Copyright 2011 Elsevier.

between the ionic conductor AlI_3 and the organic solvent ANI, a gel electrolyte was obtained. FTIR analysis verified formation of an AlI_3 –ANI complex. The photovoltaic performance of the QS-DSSC with AlI_3 –MPN–ANI gel electrolyte was better than the DSSC with AlI_3 –MPN liquid electrolyte.

The TPPE without gelator was also reported by Yang et al.;³¹⁰ they synthesized 1-alkyl-3-carboxypyridinium iodide molten salts, $[\text{ACP}][\text{I}]$, and these $[\text{ACP}][\text{I}]$ salts could transfer AN–MPN liquid electrolytes into gel electrolytes via the

interaction with Li^+ ions in liquid electrolyte. The peculiarity of this gel electrolyte lies in its formation by complexation between organic iodide and inorganic ions, without addition of any nanoparticles, small molecules, oligomers, or polymer matrix.

The conductivity and diffusibility of the polymer gel electrolytes depend on the structure and concentration of solvent, polymer host, ionic conductor, additives, as well as temperature. For highly viscous polymer gel electrolytes, sample ion hopping is unlikely and the conductivity–temperature variation ($\ln \sigma \approx 1/T$) in general shows curvature.^{77,271} The ion transport in these electrolytes is dominated by the mobility of solvent molecules, and the temperature dependence of ionic conductivity is described by the empirical VTF relationship (eq 16).^{304,311}

Generally, the ionic conductivity of polymer gel electrolyte decreases with an increase of the polymer host concentration,^{209,271,282} which is due to the fact that (i) the polymer host hinders ionic movement and (ii) the polymer cages trap liquid electrolyte and results in smaller electrolytes in the liquid. Decreasing the polymer concentration, the electrolyte has high conductivity; however, the sealing problems with the electrolytes still remain; increasing the polymer content, on the other hand, causes a decrease in the ionic conductivity, and this is the dilemma faced by researchers endeavoring in this area.

The conductivity of polymer gel electrolyte increases initially with an increase in the concentration of ionic salt and then decreases after reaching the maximum conductivity. The conductivity increase in the initial stage is easily comprehensible, and the conductivity decrease in the subsequent stage can be explained by the pair ions model (Figure 10) and the phase

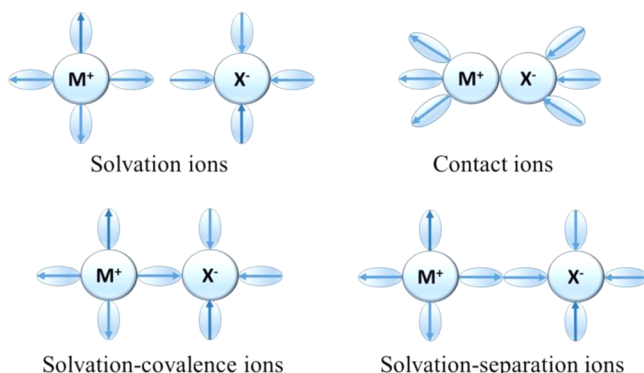


Figure 10. State of ions in solvent according to the ion-pair model.

disengagement,^{271,275,292,312} namely, high salt concentration leads to the state change of most ions from solvated ions to contact ions, and the contact ions have less contribution to the conductivity. On the other hand, the high salt concentration causes the shrinkage of the polymer chains and phase disengagement, which hinder ion transportation. In addition, the high salt concentration limits the segmental motion of the polymer chains, which also decreases ionic conductivity.³¹³

With the increase of ion radius of the cation in polymer gel electrolyte, the photovoltage of the QS-DSSC increases. Compared to the liquid electrolytes this trend is more apparent,¹³¹ such as PEO-based gel electrolytes, which is attributed to the rise of electron Fermi level (E_F) of TiO_2 caused by a decrease in I_3^- diffusion with the increase of ion radius of the cation.³¹⁴ With an increase in the chain length of

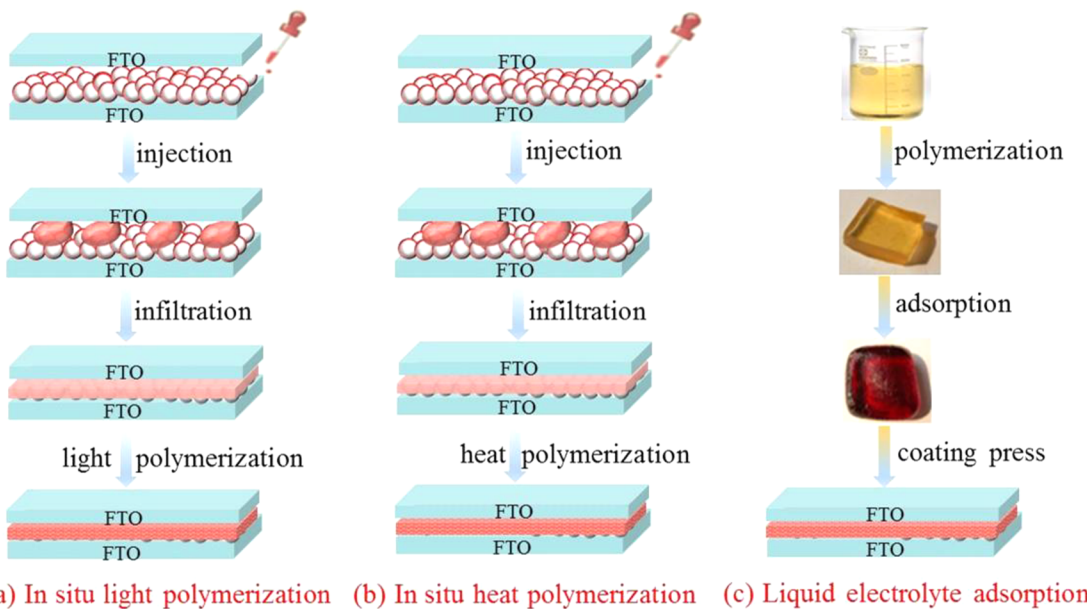


Figure 11. Preparation of thermosetting polymer electrolytes and fabrication of quasi-solid dye-sensitized solar cells.

the alkyl group of organic iodide salts, the conversion efficiencies of QS-DSSCs decrease, on account of the fact that the longer lengths of the alkyl groups result in higher viscosity, lower diffusion coefficients, and lower ionic conductivity, such as PVDF-HFP-based electrolyte containing imidazolinium when the side carbon chain lengths increased from C3 to C10.³¹⁵

3.2. Thermosetting Polymer Electrolytes

Another kind of polymer gel electrolyte is thermosetting polymer electrolyte, in which the electrolyte is obtained by organic molecule chemical or covalent cross-linking, leading to the formation of a three-dimensional polymer network and hence wrapping liquid electrolytes inside.^{10,27,74} Since the states of this kind of polymer gel electrolytes cannot reversibly change with temperature, we name this kind of electrolyte “thermosetting polymer electrolyte” (TSPE).²⁸³ In appearance, the thermosetting polymer electrolytes are the same as the solid-state electrolytes. However, because some liquid electrolytes still remain in the system, we classify them as quasi-solid-state electrolytes. The main difference between TPPE and TSPE lies in that the former is physical cross-linking and the latter is chemical cross-linking. Although the TSPEs have lower ionic conductivity than liquid electrolyte and TPPEs, the physical, chemical, and thermal stabilities of TSPEs are better than both electrolytes; so, TSPE is also an optional electrolyte for high photovoltaic performance and good long-term stability for DSSCs.^{283,316,317}

There are three frequently used methods to prepare thermosetting polymer electrolytes (shown in Figure 11). The first is a light-induced in situ polymerization method,^{318–325} i.e., the uncross-linked monomer or oligomer is dissolved in liquid electrolyte, and latent cross-linker is contained in the liquid electrolyte or directly on the electrodes of DSSCs. After the device is assembled, the cross-linking reaction is in situ initiated by light irradiation, which results in the formation of chemical cross-linking electrolyte in the device. The second is a heat-induced in situ polymerization method,^{326–328} which is similar to the first method; the difference rests on that the polymerization reaction is initiated

by heating. The third is the liquid electrolyte adsorption method,^{279,283,317,329–337} i.e., using the chemical cross-linked macromolecular polymer as host to absorb liquid electrolytes or swell in liquid electrolytes.

The in situ polymerization can promote electrolytes filling and wetting with mesoporous photoanode and counter electrode. Otherwise, some empty left in photoanode or counter electrode, electron–hole recombination, and parasitic current can occur. This is the reason why the preparation of quasi-solid electrolytes is evolving toward the in situ polymerization by chemical, thermal, or photochemical processes.³²⁴

Several conditions are necessary for in situ preparing chemical cross-linking electrolytes.³¹⁸ (i) Polymerization must occur in the presence of iodine. (ii) Polymerization must occur at a temperature below dye decomposition. (iii) Polymerization has to be completed without generating byproducts that could decrease the photovoltaic performance. (iv) Polymerization can proceed without an initiator because the byproducts of the initiator may decrease the photovoltaic performance.

In situ photopolymerization reaction (including in photo-induced polymerization, UV curing, and photopolymerization) is used in the preparation of TSPEs.^{326–328,339–348} In 2001, Matsumoto et al. first used a thermosetting polymer electrolyte by photoinduced in situ polymerization of α -methacryloyl- ω -methoxyocta (oxyethylene) at porous TiO₂ film and absorbing liquid electrolyte.³²⁶ The DSSC based on this TSPE with a conductivity of 2.67 mS·cm^{−1} achieved a conversion efficiency of 2.62%, which was 86.4% of the device efficiency using liquid electrolytes. After that, the Hayase group systematically investigated the chemically cross-linked electrolytes, i.e., TSPEs, by photoinduced in situ polymerization used in QS-DSSCs.^{318,319,349–353}

Parvez et al. injected PEG and bifunctional PEGDA [poly(ethylene glycol) diacrylate] monomer electrolyte solution into the TiO₂ porous film of DSSC.³²⁸ PEGDA is a typical difunctional oligomer, which can induce the formation of cross-linked networks by irradiation. Under ultraviolet (UV) light irradiation of 100 mW·cm^{−2} for up to 20 min, the conversion efficiency of the DSSC increased from 2.58% to

4.18% by virtue of the formation of a cross-linked structure by PEG and bifunctional PEGDA upon UV light illumination. The DSSCs with the cross-linkable PEG/PEGDA-based polymer electrolytes exhibited a better long-term stability in comparison to those with electrolytes containing only PEG.

The *in situ* light-induced polymerization is a controllable process, which occurs in a pretty short time at room temperature in free solvents and does not damage the device components.³⁵⁴ Unfortunately, *in situ* photopolymerization of monomers in the presence of I₂ is an enormous problem because I₂ is a well-known free-radical inhibitor,³⁵⁵ even at extremely low concentrations of I₂.³⁵⁶ Therefore, the design of light sources and the choice of components are crucial for the photopolymerization. In order to overcome the inhibitory effect of I₂, Winther-Jensen et al. proposed an alternative strategy by combining photocatalysis and photoinduced polymerization in 2010.³⁵⁷ They used TiO₂ nanoparticles as photoinitiator in a charge-transfer photopolymerization reaction between 2-hydroxyethyl methacrylate (HEMA) and tetra(ethylene glycol) diacrylate (TEGDA) in an ionic liquid electrolyte containing I₂. The DSSC based on this electrolyte showed a conversion efficiency of 5.0% under 0.39 sun illumination.

A typical heat cross-linking electrolyte example was reported by Komiya et al.³²⁰ They used poly(ethylene oxide-*co*-propylene oxide) trimethacrylate (oligomer) with three polymerizable reactive groups as gel electrolyte precursor and injected it into the assembled cells. After being heated at 90 °C for 90 min, a three-dimensional polymer network was formed in the device. The QS-DSSC with this TSPE showed higher V_{OC} than that of the DSSC with liquid electrolytes, which may be attributed to suppression of the back current. The QS-DSSC with this electrolyte realized a high efficiency of 8.1%. Wang et al. prepared a necklace-like polymer gel electrolyte containing latent and chemically cross-linked gel electrolyte precursors and injected it into an already set DSSC.³²⁴ The gelation was carried out in the cell by heating at 80 °C, which triggered an *in situ* quaternation reaction and the formation of a three-dimensional covalent polymer network to form TSPE in the cell. These cells exhibited current densities of 13–17 mA·cm⁻² and an efficiency of 7.72%.

Our group has synthesized a series of TSPEs by liquid electrolyte adsorption method, including systems of (polymer host/solvent/ionic conductor) PAA–PEG/NMP+GBL/NaI + I₂, PAA–PEG/TBP + GBL/NaI + I₂, PAA–PEG/NMP + GBL/NaI + I₂, PAA–PEG/GBL + NMP/NaI + I₂ + PY, PAA–PEG-PPy/GBL + NMP/NaI + I₂ + PY, PAA–PEG/GBL + NMP/Acac-Py + I₂, (PAA-*g*-CTAB)PANI/NMP + AC/TRAI + MI + I₂, PAA-Gel-PANI/NMP + AC/TRAI + MI + I₂, PAC-PGE/PC + EC/KI + I₂, PEG-TEOS/KI + I₂, PGA-PPy/NMP + AC/TRAI + MI + I₂, P(MMA-*co*-AN)/EC + PC + DMC/KI + LiI + I₂ + TBP, P(MMA-*co*-MAA)/PEG/KI + I₂, etc.^{145,259,283,317,329–338}

As a typical example of TSPEs,^{283,317} the PAA–PEG/NMP + GBL/NaI + I₂ system is introduced. It is known that poly(acrylic acid) (PAA) is a superabsorbent polymer; it can absorb a large amount of liquid to form a stable elastomer due to the formation of three-dimensional networks structure in the elastomer.^{358,359} However, pure PAA is not a good absorbent for organic solvents. By modifying with amphiphilic PEG, the PAA–PEG polymer showed a high absorbent ability for organic solvents. Soaking PAA–PEG in a liquid electrolyte, a polymer electrolyte was obtained. It showed a yellow color before soaking and brown color after soaking (shown in Figure 12),

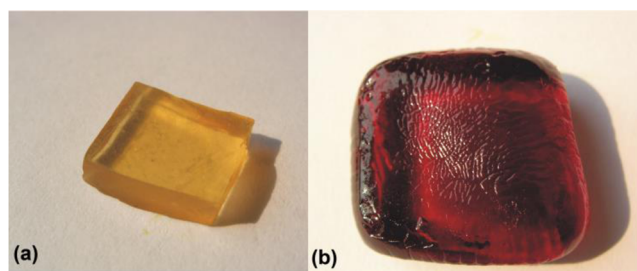


Figure 12. Digital images of thermosetting polymer electrolyte (TSPE) PAA – PEG/NMP + GBL/NaI + I₂ before (a) and after (b) soaking in iodide/triiodide liquid electrolyte. Reproduced with permission from ref 283. Copyright 2007 John Wiley and Sons.

indicating that iodide electrolyte had been absorbed. Since the state of elastomer cannot reversibly change with temperature, we named the electrolyte “thermosetting polymer electrolyte (TSPE)”. The prepared PAA–PEG could absorb 8–10 times liquid electrolyte of own weight, and the TSPE showed high conductivity and excellent long-term stability owing to a large quantity of liquid electrolyte adsorbed in the PAA–PEG networks. The DSSC based on this TSPE with a conductivity of 6.12 mS·cm⁻¹ achieved a conversion efficiency of 6.10% and showed a better long-term stability than the DSSC based on liquid electrolytes. Further, the third component of PPY was introduced in the PAA–PEG to form a PAA–PEG–PPY polymer host; the efficiency of the DSSC with this electrolyte reached 7.0%.^{283,317}

Ileperuma and his colleague *in situ* synthesized ultrathin porous poly(vinylidene fluoride-*co*-hexafluoropropylene) (PVDF-HFP) membranes (thickness 150 nm) by a phase inversion method on TiO₂ electrode.³⁶⁰ The membrane was then soaked in the organic liquid electrolyte to form the *in situ* ultrathin porous PVDF-HFP membrane electrolyte. The QS-DSSC with the membrane electrolyte yielded a conversion efficiency of 8.35%, while the efficiency was 7.90% for the cell with liquid electrolyte. The higher V_{OC} was due to the suppression of charge recombination at the electrolyte/electrode interface.

Recently, the Ho group used a multiple functional copolymer with poly(oxyethylene) segments, amido-acid linkers, amine termini, and amide cross-linker to form 3D interconnected nanochannels and absorb a liquid electrolyte.³⁶¹ The QS-DSSC with this TSPE achieved a conversion efficiency of 9.48%, which was superior to that of the DSSC with the liquid electrolyte (8.84%); the high efficiency was mainly attributed to the suppression of the back electron transfer through the TSPE.

Wang et al. prepared a porous copolymer of polyvinyl-(acetate-*co*-methyl methacrylate) [P(VA-*co*-MMA)];³⁶² by soaking this porous copolymer in a liquid electrolyte containing I⁻/I₃⁻ (AN or MPN as solvent), a quasi-solid electrolyte with high ionic conductivity was prepared. The QS-DSSC based on this electrolyte achieved a high conversion efficiency of 9.10%, nearly the same as that of the DSSC based on the liquid electrolyte. Introduction of TiO₂ nanoparticles into the electrolyte further enhanced conductivity and the conversion efficiency to 9.40%. Subsequent results revealed that the QS-DSSC had a better stability so that it could maintain 96.7% of its initial efficiency after 1000 h under sunlight soaking.

Park et al. developed a new *in situ* surface-induced polymerization method.³⁶³ They demonstrated that nanocrystalline TiO₂ surface-induced cross-linking polymerization

resulted in the formation of the encapsulation of the TiO_2 particles. The encapsulation improved the stability and increased the photovoltaic performance of DSSC. This kind of QS-DSSC yielded a high power conversion efficiency ($7.6 \rightarrow 8.1\%$) and excellent stability during heating at 65°C over 30 days.³⁶⁴ These performance characteristics were superior to those obtained from a conventional DSSC ($7.5 \rightarrow 3.5\%$) prepared in a similar condition. Recently, Park et al. synthesized nanoporous network polymer via the surface-induced cross-linking polymerization of methyl methacrylate (MMA) and 1,6-hexanediol diacrylate (HDDA) on the surfaces of nanocrystalline TiO_2 particles.³⁶⁵ The nanopore selectively transports iodide ions, remarkably suppressing the dark current, and achieving a high conversion efficiency of 10.6% for the QS-DSSC, with a 20% increase compared to the DSSC with liquid electrolyte.

Generally,^{35,270,316} compared to the DSSCs based on liquid electrolytes, the DSSCs based on polymer gel electrolytes have lower J_{SC} and higher V_{OC} ; the former is due to the lower conductivity coming from the lower mobility of redox couple components, and the latter is due to the suppression of dark current by polymer chains covering the surface of TiO_2 electrode.

3.3. Composite Polymer Electrolytes

Inorganic materials, such as TiO_2 , SiO_2 , ZnO , Al_2O_3 , carbon, etc., as gelators are introduced into liquid polymer electrolytes to form quasi-solid electrolytes. These quasi-solid electrolytes are labeled composite polymer electrolytes.^{10,270} In DSSCs, the main objective for incorporating inorganic nanoparticles aims to the enhancement of long-term stability and ionic conductivity,^{109,110,366–372} since the inorganic nanoparticles can solidify liquid electrolyte and convert the electrolyte from liquid state to quasi-solid state and thus enhance the long-term stability of electrolyte. Meanwhile, an organic and/or organic-inorganic network is constructed by incorporation of inorganic nanoparticles in the electrolyte, and I^-/I_3^- ions are able to align and transport on the inorganic particles network, leading to an acceleration of the charge-transport dynamics.^{373–378}

As is well known, many polymer electrolytes exhibit low ambient ionic conductivity because of the severe crystallization of polymers. To hinder the crystallization, liquid plasticizers are added, but this reduces the mechanical properties of the electrolytes. In 1998, Scrosati and Croce et al. first proposed the addition of inorganic nanoparticles into polymer electrolytes to change the physical state and conductivity of electrolytes.^{379–381} They found that the conductivities of unfilled PEO- LiClO_4 electrolytes were $10^{-4}\text{--}10^{-8}\text{ S}\cdot\text{cm}^{-1}$ in the temperature range of $80\text{--}30^\circ\text{C}$; when adding TiO_2 and Al_2O_3 nanopowders with particle sizes of 5.8–13 nm in the electrolytes, the conductivities reached $10^{-4}\text{ S}\cdot\text{cm}^{-1}$ at 50°C and $10^{-5}\text{ S}\cdot\text{cm}^{-1}$ at 30°C . The increase in conductivity was attributed to the enlargement of the amorphous phase in the electrolytes. Since then, addition of TiO_2 and other inorganic nanoparticles has been extensively applied to change the states and ionic conductivities of polymer electrolytes.

The most frequently used approach for preparing composite polymer electrolytes is the addition of TiO_2 nanoparticles to polymer electrolytes.^{292,316,377,382–386} Falaras et al. investigated the addition of TiO_2 nanoparticles (P25) to the polymer electrolyte containing PEO, LiI, and I_2 .^{382,383} The polymer chains separated by the TiO_2 particles were arranged in a stable three-dimensional network that created free space and voids

inside which I^-/I_3^- anions could migrate easily.³⁸² The QS-DSSC with this composite polymer electrolyte exhibited an efficiency of 4.2% ($65.6\text{ mW}\cdot\text{cm}^{-2}$).³⁸³

Huo et al. investigated the TiO_2 nanoparticles gelling PVDF-HFP electrolytes for QS-DSSCs.³⁷⁷ The apparent diffusion coefficient of I_3^- increased six times from 0.76×10^{-10} to $4.42 \times 10^{-10}\text{ m}^2\cdot\text{s}^{-1}$ and thus reached the level of liquid electrolytes ($4.04 \times 10^{-10}\text{ m}^2\cdot\text{s}^{-1}$). The light-to-electric conversion efficiency of the DSSC based on the nano- TiO_2 polymer electrolyte reached 7.18% in comparison with 7.01% for liquid-electrolyte-based DSSCs. The electrical impedance spectrum revealed that the addition of TiO_2 nanoparticles could reduce the charge recombination at dyed TiO_2 electrode/electrolyte interface. The nano- TiO_2 polymer electrolyte-based device could maintain 90% of its photovoltaic performance after heating at 60°C for 1000 h.

In 2003, Wang et al. used fumed silica (SiO_2) nanoparticles (12 nm, 5 wt %) as gelator to solidify ionic liquid-based electrolytes.³⁸⁷ The ionic liquid-based QS-DSSC yielded an efficiency of 7%. After that, SiO_2 as gelator was widely investigated.^{109,367,388–390} For example, the Meng group investigated environmentally friendly composite polymer electrolytes and found that when adding SiO_2 nanoparticles (14 nm, 5 wt %) in $\text{LiI}-\text{C}_2\text{H}_5\text{OH}$ liquid electrolyte, the state of the electrolyte changed from sol state to quasi-solid state.^{391–393} The DSSC based on $\text{Li}(\text{C}_2\text{H}_5\text{OH})_4\text{I}/\text{SiO}_2$ composite polymer electrolyte achieved an efficiency of 6.1%. Yoon et al. found that the SiO_2 nanorods have a better effect than that of SiO_2 nanoparticles.³⁹⁰ Kim et al. used hydrophilic silica nanoparticles as gelators to prepare $\text{PEO}_{13}\text{BIm-I}/\text{MPN}$ -based thixotropic electrolytes.³⁸⁹ The QS-DSSC with this thixotropic electrolyte achieved an efficiency of 5.25%. Thixotropic gels can be converted into sols by applying a suitable mechanical stress,^{277,389} i.e., by shaking, and then the sols returned to gels again when the stress is removed. The advantage of thixotropic gel electrolytes lies in that the electrolytes (sol state) penetrate easily into the mesoporous TiO_2 layer by shearing and thereby provides good electrode/electrolyte interfacial contact.

Al_2O_3 ^{394,395} and ZnO ³⁹⁶ are introduced in liquid electrolytes to improve the properties of the electrolytes. Chi et al. utilized a hybrid consisting of MPII and MPII-modified Al_2O_3 nanoparticles as an I_2 -free electrolyte for QS-DSSCs.³⁹⁴ The viscosity of the electrolyte continuously increased with the increase of IL- Al_2O_3 content, and the fluidity almost disappeared when the mass ratio of MPII:IL- Al_2O_3 was 95:5 or 90:10. The efficiencies of DSSCs with IL- Al_2O_3 were always greater than those with pristine Al_2O_3 , which was due to the favorable interactions and good miscibility between MPII and IL- Al_2O_3 and the formation of an interconnected channel pathway for ion transport. When utilizing the MPII/IL- Al_2O_3 hybrid electrolyte in a double-layer structure with a top layer of mesoporous TiO_2 beaded on a nanocrystalline TiO_2 bottom layer, the conversion efficiency of the QS-DSSC reached 7.6%. Zhang et al. dispersed PEG-grafted ZnO nanoparticles in liquid electrolyte to form a composite polymer electrolyte ($\text{ZnO-PEG:PEG:KI:I}_2 = 19.3:73.3:6.7:0.67$ in mass ratio),³⁹⁶ thus obtaining a QS-DSSC with an efficiency of 3.1%. With addition of TBP into the electrolyte, the efficiency of the cell was increased to 5.0%. Xia et al. modified ZnO nanoparticle with amphiphilic β -diketone PMOP and used it as a framework to form quasi-solid electrolyte.³⁹⁷ Since a long alkyl-chain superstructure of PMOP-capped ZnO nanoparticle interacted

Table 4. Photovoltaic Performance of QS-DSSC Based on Quasi-Solid Ionic Liquid Electrolytes^a

compositions of the electrolyte	σ (mS·cm ⁻¹)	J_{SC} (mA·cm ⁻²)	V_{OC} (V)	FF	η (%)	dye	ref
0.12 M I ₂ , 0.5 M KI, 0.9 M BMIMI, in GBL, 35 wt % of PVP	2.3	15.72	0.626	0.55	5.41	N3	163
DMII/EMIImI/EMIImB(CN) ₄ /I ₂ /NBB/GNCS (mol ratio 12/12/16/1.67/3.33/0.67)		15.93	0.710	0.747	8.5	C103	167
PVDF-HFP (5 wt %), 0.6 M DMPImI, 0.1 M I ₂ , 0.5 M NMBI in MPN		12.5	0.67	0.730	6.1	Z907	272
0.3 M I ₂ , PVP(2 wt %), HOOC(CH ₂) ₁₄ COOH(4 wt %), H ₂ O(5 wt %) in PMImI		13.43	0.60	0.55	4.4	N3	322
CH ₃ CO ₂ H, TMOS, 0.5MPMImI, 0.04 mMNMBI, 20 mM I ₂ in PC/Triton (mol ratio 4/1)	0.36	12.9	0.65	0.66	5.4	N3	373
40 g/L of gelator, I ₂ (8.7 wt %) in HMImI		11.8	0.635	0.669	5.01	N719	374
0.5 M I ₂ , 0.45MNMBI, SiO ₂ (5 wt %) in PMImI		12.75	0.672	0.709	6.1	Z907	387
Gelator (2%), 0.2 M I ₂ , 0.12 M GuanSCN, 0.5 M NMBI in PMImI/EMIImSCN (vol ratio 13/7)		12.7	0.706	0.70	6.3	K19	420
PVDF-HFP (10 wt %), I ₂ /NMBI in MPII		11.29	0.665	0.712	5.3	Z907	421
0.5 M I ₂ , 0.45MNMBI, SiO ₂ (5 wt %) in PMImI/MPN (vol ratio 13/7)		11.56	0.603	0.753	5.3	N3	422
0.1MII, 0.5 M NBB, 0.1 M GNCS, EMII/PMII/EMISCN (vol ratio 6/6/7) in poly[BVIIm][HIm][TFSI] (25 wt %)	5.83	12.92	0.676	0.678	5.92	N3	423
I ₂ , TBAI, EMIImI, EC/PC (vol ratio 4/1), PEG		20.0	0.69	0.52	7.13	N719	424
PMAPII (16 wt %) 0.05 M I ₂ , 0.05 M TBP in GBL	4.9	14.7	0.79	0.70	8.12	TBA	425
0.1 M LiI, 0.45 M NMBI, 0.4 M DMPII, PEO/PVDF-HFP (2:3 wt %) 20 wt % in MeCN	21.18	14.12	0.68	0.72	6.97	N719	426
0.1 M LiI, 0.9 M EMII/SN, 0.1 M I ₂ , 0.5 M TBP in ACN/MPN (vol ratio 1/4)	1.272	14.8	0.674	0.75	7.46	N719	427
0.5 M LiI, 0.05 M I ₂ , 0.5 M NMBI, 10 wt % P(MOEMImCl) in HMIImI/EMIImBF ₄ (vol ratio 2/1)	0.4	15.50	0.618	0.64	6.1	N719	428
poly(1-ethyl-3-(acryloyloxy)hexylimidazolium iodide) (PEAI)	0.363	9.75	0.838	0.65	5.29	N3	429
poly((1-(4-ethenylphenyl)methyl)-3-butyl-imidazolium iodide) (PEBII) in AN (10 wt %)	0.2	18.1	0.643	0.51	5.93	N719	430

^aPhotovoltaic performances of all DSSCs were measured under simulated solar light irradiation with intensity of 100 mW·cm⁻², AM 1.5.

with solvent and offered a channel for free transportation of I⁻/I₃⁻, the QS-DSSC showed a higher stability and overall efficiency of 6.8%.

Mesoporous particles (MCM-41) with unique structure and ordered nanochannels are served as a new kind of gelator for quasi-solid electrolytes.³⁹⁸ The DSSC with MCM-41 electrolyte achieved a conversion efficiency of 4.65% (30 mW·cm⁻²). Owing to unique pore structure and high specific BET surface area, mesoporous silica MCM-41 was expected to afford conducting nanochannels for redox couple diffusion.

Nanoclay minerals as gelators have been used in liquid electrolyte to form a quasi-solid-state composite polymer electrolyte for DSSCs^{399–405} by virtue of its multifunction and features, such as high chemical stability, unique swelling capability, ion exchange capacity, light scattering property, and rheological property. Quite recently, the Mhaisalkar and Uchida groups prepared a quasi-solid-state composite polymer electrolyte by solidifying liquid electrolytes with synthetic nitrate–hydrotalcite nanoclay.^{404,405} The conversion efficiency of the QS-DSSC with the clay-based electrolyte reached 10.1% under 0.25 sun and 9.6% under full sun, which was increased by 10% compared to that of DSSCs with liquid electrolyte. This study demonstrated that nitrate–hydrotalcite nanoclay not only solidified the liquid electrolyte to prevent solvent leakage but also facilitated the efficiency improvement for the device.

Incorporation with carbon nanomaterials can produce quasi-solid electrolytes through networking with liquid electrolyte.⁴⁰⁶ The physical state of these electrolytes is tunable through varying concentrations and types of the carbon nanomaterials.⁵⁹ Moreover, the performance of DSSCs can be improved by introducing carbon materials owing to their good conductivity and extended electron-transfer surface, which provides a catalytic effect for the reduction of the I₃⁻ ions.^{369,407} In 1999, Bach et al. dispersed carbon materials including

multiwalled carbon nanotubes (MWCNTs), single-walled carbon nanotubes (SWCNTs), carbon black (CB), and carbon fibers (CFs) in ionic liquid electrolytes and obtained composite electrolytes by grinding them.^{113,408} The DSSCs based on the carbon composite electrolytes showed superior performance compared to those with pure ionic liquid electrolytes. Henceforward, carbon materials have been widely investigated as gelators used in composite polymer electrolytes.^{59,109,294,369,406–419} For instance, a POME-modified MWCNT was utilized in networking with the (PVDF-HFP)/LiI electrolyte to form quasi-solid electrolyte, the QS-DSSC based on this composite polymer electrolyte containing 0.25 wt % MWCNT/POEM showed an efficiency of 6.86%, while the DSSC with unmodified electrolyte had the efficiency of 4.63%, indicating the role of MWCNT for homogenizing the amorphous PVDF-HFP and facilitating the diffusion of I⁻/I₃⁻ in this electrolyte.⁴¹⁵ Guo et al. used graphene oxide as gelator to gel AN-based liquid electrolytes.⁴¹⁷ The conversion efficiencies for the DSSCs without GO and with GO (1%) quasi-solid electrolytes were 6.9% and 7.5%, respectively. Recently, Mohan et al. prepared a PAN/LiI/activated carbon composite polymer electrolyte by a hot pressing method.⁴¹⁸ The TiO₂ photoelectrode film with 20 μm thickness was prepared by the hand spray technique. The quasi-solid electrolyte showed a conductivity of 8.67 mS·cm⁻¹. The QS-DSSC based on this electrolyte exhibited a high conversion efficiency of 8.42%.

3.4. Quasi-Solid Ionic Liquid Electrolytes

Ionic liquid has multifunctions: it can not only be used as solvent for preparing liquid electrolytes but also be used as ionic conductor, providing iodide salts in quasi-solid-state electrolytes and even solid-state electrolytes. In the former, it is commonly named ionic liquid electrolyte; in the latter, it can be named quasi-solid ionic liquid electrolytes⁷⁶ or solid ionic liquid

electrolytes. Compared with ionic liquid electrolyte, the quasi-solid ionic liquid electrolyte generally shows lower conductivity and better long-term stability. Table 4 exemplifies quasi-solid ionic liquid electrolytes used in QS-DSSCs.

In 2002, Wang et al. prepared a quasi-solid ionic liquid electrolyte by simply mixing PVDF-HFP (10 wt %) with ionic liquid electrolyte containing iodine and *N*-methylbenzimidazole (NMBI) in 1-methyl-3-propylimidazolium iodide (MPII).⁴²¹ Resultant QS-DSSC achieved an efficiency of 5.3%. Almost identical results obtained from the cells with corresponding blank liquid electrolyte (without PVDF-HFP) indicate that the presence of polymer has no adverse effect on the conversion efficiency, which may be attributed to the contribution by Grotthus-type electron exchange mechanism in viscous polymer electrolytes. This research by Wang et al. may be the first example for using polymer as gelator to prepare quasi-solid ionic liquid electrolyte in DSSC.⁴²¹

Besides the thermoplastic-type quasi-solid ionic liquid electrolytes as the above example, as an example of thermosetting ionic liquid electrolytes by adsorption, Li et al. designed an ionic liquid-imbibed polymer gel electrolyte using 1-butyl-3-methylimidazolium chloride (BMICl) as solvent, MPII as iodine source, and poly(hydroxyethyl methacrylate/glycerol) [P(HEMA/GR)] as a gelator.^{431–433} By virtue of the amphiphilic P(HEMA/GR) extraordinary absorption ability, the ionic liquid electrolyte can be imbibed into and interacted with P(HEMA/GR) framework. Resultant quasi-solid ionic liquid electrolyte is honored with a high ionic conductivity of 14.29×10^{-3} S·cm⁻¹ and good retention. The QS-DSSC with this electrolyte achieved a conversion efficiency of 7.15%.⁴³¹

Kato et al. prepared thermosetting quasi-solid ionic liquid electrolytes by in situ thermal polymerization method and using PVP and HOOC(CH₂)_nCOOH (*n* = 4, 7, 10, 14) as the latent chemically cross-linked gelators.³²² When the assembled cell was heated at 90 °C, the gelation was caused by the reaction between PVP and dicarboxylic acid and PMIMI ionic liquid was solidified. The efficiency of the QS-DSSC based on the quasi-solid electrolyte in combination with N3 dye was 5.2% before gelation. After gelation for the PVP reactions with HOOC(CH₂)₁₀COOH and HOOC(CH₂)₁₄COOH, the efficiency was decreased to 3.4% and 4.4%, respectively. This decrease was associated with a decrease in the diffusion coefficient of I₃⁻ in the quasi-solid electrolytes, 10–20% lower than that in the corresponding ionic liquid electrolyte.⁷⁶

Kato et al. compared polymer cross-linkers (above)³²² with nanoparticle cross-linkers³¹⁹ for preparing thermosetting ionic liquid electrolytes. In the latter, they used inorganic nanoparticles (SiO₂, TiO₂) and HOOC(CH₂)_nCOOH (*n* = 4, 10, 14) as latent chemically cross-linked gelators. The viscosity of the precursor was low at room temperature. However, when the precursor was baked at 80 °C, it solidified immediately. Photovoltaic performance of the QS-DSSC was maintained after solidification. The efficiency of the QS-DSSC with this thermosetting ionic liquid electrolyte containing MePrImI was 5.03% before gelation. After gelation with HOOC(CH₂)₁₄COOH and hydrophilic SiO₂ particles (7 nm, 5 wt %), the efficiency was increased to 6.8%. This increase was associated with enhanced electron exchange between I₂ and I⁻ on the surface of nanoparticles¹⁰⁹ and interfacial resistance decrease in TiO₂ layers,³⁵² indicating that the phase separation of gelators by nanoparticles is more effective than by PVP polymers and insoluble nanoparticle may support the phase separation of alkyl chains.

The structure of ionic liquid has an important effect on the properties of electrolytes. For example, Kubo et al. made a systematic study on quasi-solid ionic liquid electrolytes based on 1-alkyl-3-methylimidazolium iodides (alkyl C3–C9).^{374,375} They found that when the alkyl chain was lengthened from C3 to C9, the viscosity increased from 865 to 2099 mPa s and the conductivity decreased from 8×10^{-3} to 8×10^{-5} S·cm⁻¹, resulting in a lower I₃⁻ transport ability and a longer electron recombination lifetime. With a balance between the charge transport and the charge recombination, C6 realized the highest efficiency. A QS-DSSC based on the electrolyte containing 1-hexyl-3-methylimidazolium iodide, iodine, and low molecular weight gelator *N*-benzyloxycarbonyl-L-valyl-L-valine yielded an efficiency of 5% on top of good high-temperature stability.⁴³⁴

Shi et al. used a solvent-free eutectic melt-based electrolyte DMII/EMIImI/EMIImB (CN)₄/I₂/NBB/GNCS (mol ratio 12/12/16/1.67/3.33/0.67) to fabricate a QS-DSSC with C103 dye, yielding a record efficiency of 8.5%.¹⁶⁷ Moreover, the device sustained more than 90% of its initial performance when subjected to accelerate testing for 1000 h at 60 °C under full sunlight soaking.

The application of quasi-solid-state electrolyte improves the long-term stability of DSSCs; however, the efficiencies of general QS-DSSCs are lower than that of DSSCs with liquid electrolytes, as a result of the inferior mass-transfer rates of the redox couples in the highly viscous medium and high electron-transfer resistance at the electrolyte/electrode interfaces owing to imperfect wetting of electrode pores with the electrolyte. Various quasi-solid electrolytes, including thermoplastic polymer electrolytes, thermosetting polymer electrolytes, composites polymer electrolytes, and ionic liquid electrolytes, have different features. By optimizing and designing some QS-DSSCs based on the quasi-solid electrolytes, besides better long-term stability, also can obtain high photovoltaic performances. Accordingly, quasi-solid-state electrolyte is a prospective candidate in highly efficient and stable DSSCs.

4. SOLID-STATE TRANSPORT MATERIALS

For quasi-solid-state electrolytes, the main problem is still stability, since the electrolytes still contain solvents and are generally thermodynamically unstable. Under long storage or exposure in air, solvent exudation is unavoidable. In this regard, all-solid-state transport materials possess more advantages over liquid and quasi-solid-state electrolytes, especially in large-scale actual application for DSSCs. Several materials have been developed for replacing liquid electrolytes or quasi-solid electrolytes by solid-state transport materials, including ionic conductors,^{392,435–437} inorganic hole-transport materials,^{10,438–440} and organic hole-transport materials.^{78,441–443}

4.1. Solid-State Ionic Conductors

On the grounds of easy solidification and higher conductivity compared with hole-transport materials, polymer electrolytes were taken into account for assembling all-solid-state DSSCs (SS-DSSCs), particularly in the early research stage, when the efficiencies of the SS-DSSCs utilizing hole-transport materials were unsatisfactory compared with those using liquid electrolytes and ionic liquid electrolytes.^{10,37,75–78} In fact, many thermosetting polymer electrolytes, quasi-solid ionic liquid electrolytes, and composite polymer electrolytes (discussed above) possess similar structure, mechanism, and functions as solid-state polymer electrolytes and can be used in SS-DSSCs. Here, we mainly discuss the polyelectrolytes used as solid-state

electrolytes in SS-DSSCs. In polyelectrolytes, charged cationic or anionic groups are chemically bonded to a macromolecular backbone chain,^{76,270} while their counterions are free to move and undertake charge carrier transportation. Polyelectrolytes are single-ion conductors.²⁷⁰

In 2000, Nogueira et al. prepared an elastomeric polymer electrolyte based on the copolymer poly(ethylene oxide-co-epichlorohydrin) P(EO-EPI)^{84,16} complexes with sodium or lithium iodide salts.^{74,436,444} Unsealed prototype cells showed an efficiency of 1.6–2.6%, thus demonstrating that polymer electrolyte was an alternative as solid-state electrolytes for SS-DSSCs. Falaras and co-workers prepared a solid polymer electrolyte consisting of PEO/TiO₂, LiI, and I₂. TiO₂ nanoparticles as fillers decreased PEO crystallinity and thus increased the ionic conductivity (10^{-5} S·cm⁻¹).^{382,383} The cell exhibited an efficiency of 4.2% (65.6 mW·cm⁻²).³⁸³

Wu et al. synthesized a polyelectrolyte used as solid-state ionic conductor in SS-DSSCs.⁴³⁷ Owing to the weak interaction between the larger backbone cation poly(*N*-alkyl-4-vinylpyridine) (PNR4VP) and smaller anion I⁻ (Figure 13), the

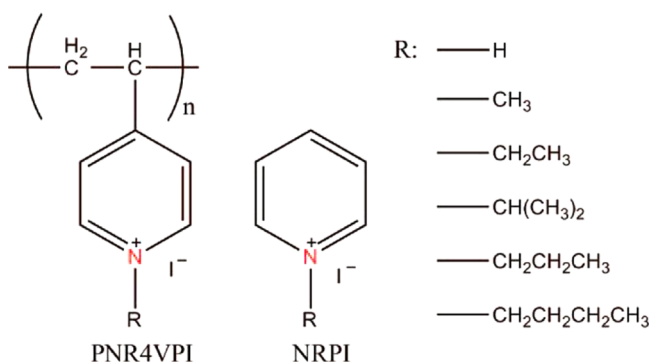


Figure 13. Chemical structure of poly(*N*-alkyl-4-vinylpyridine) iodine (PNR4VPI) and *N*-alkyl-4-vinylpyridine iodine (NR'PI). Reproduced with permission from ref 437. Copyright 2008 American Chemical Society.

polyelectrolyte (PNR4VPI) showed a low conductivity. The conductivity was improved to be 6.41 mS·cm⁻¹ by adding I₂ and *N*-alkylpyridine iodide (NR'PI), and the efficiency of the SS-DSSC based on this polyelectrolyte together with KI layer on TiO₂ anode reached 5.64%.

Similar to the N substituted in the pyridine cycle in this case,⁴³⁷ the N substituted in imidazolium, piperidinium, and carbazole cycles can be realized and thus obtained high conductive solid-state polyelectrolytes. As an example, poly(1-alkyl-3-(acryloyloxy)hexylimidazolium iodide) was used as single-ion transport electrolytes for SS-DSSCs.⁴⁴⁵ In these polyelectrolytes, imidazolium cations are tethered on the polymer main chain and only iodide species are mobile. Poly(1-ethyl-3-(acryloyloxy)hexylimidazolium iodide) (PEI) exhibited the high ionic conductivity of 3.63×10^{-4} S·cm⁻¹. The SS-DSSC based on the PEI electrolyte yielded an efficiency of 5.29%. Midya et al. synthesized a class of solid-state ionic conductors with carbazole-imidazole iodide structure.⁴⁴⁶ The combination between the solid-state ionic conductors and the iodine electrolytes provides dual channels for hole/triiodide transportation. The SS-DSSC with SD2 electrolyte achieved an efficiency of 2.85%. Wang et al. designed and synthesized ester-functionalized imidazolium conductors.⁴⁴⁷ Because of the formation of ionic channels and the interaction of Li⁺ with

the oxygen in the ester group, a conductivity of 5.76 mS·cm⁻¹ was obtained for the conductor mixed with I₂ and LiI, which resulted in fast charge transfer along the polyiodide chain. The SS-DSSC based on this polyelectrolyte exhibited an efficiency of 6.63%. The efficiency remained at 100% of the initial value after continuous light soaking for 1000 h. Recently, Wang et al. attached propargyl group to an imidazolium ring, and the conductivity was enhanced by about 4×10^4 -fold compared to the alkyl-substituted imidazolium iodide.⁴⁴⁸ The SS-DSSC with 1-propargyl-3-methylimidazolium iodide as single-component solid-state electrolyte achieved a conversion efficiency of 6.3%, which also exhibited excellent long-term stability under continuous 1 sun soaking for 1500 h. Li et al. investigated the effect of substitute in the imidazolium ring on the ionic conductivity and the performance of SS-DSSCs.⁴⁴⁹ Compared to the methyl–ethyl-substituted imidazolium iodide, replacement of the alkyl group (methyl group) with an ester group increased the ionic conductivity and the cell performance, and replacement of another alkyl group (ethyl group) with a hydroxyethyl group further increased the ionic conductivity and cell performance significantly. The SS-DSSC based on hydroxyethyl- and ester-cofunctionalized imidazolium iodide solid-state electrolyte and a metal-free organic dye sensitizer achieved a conversion efficiency of 7.45%.

Polyelectrolytes also are used in layer-by-layer (LbL) preparing photoanode for SS-DSSCs.^{438,450–454} Kim et al. deposited ionic polymers of poly(allylamine hydrochloride) (PAH) and poly(sodium 4-styrenesulfonate) (PSS) on the FTO substrate by the LbL technique.⁴⁵³ The ultrathin (PAH/PSS)_n as an interfacial layer created excellent adhesion of the TiO₂ layer on the FTO substrate, leading to an efficient electronic transport from TiO₂ to FTO and blocking the back-transport reaction from FTO to I₃⁻. Consequently, the fill factor of the SS-DSSC was remarkably increased from 0.709 to 0.783 together with an increase in V_{OC} from 760 to 803 mV and an increase in J_{SC} from 8.078 to 8.768 mA·cm⁻², leading to the improvement of efficiency from 4.41% to 5.52%. With optimization of the TiO₂ electrode structure, the efficiency of the SS-DSSC was enhanced to 7.14%. He et al. used amphoteric TiO₂ colloidal particles and polyelectrolytes to assemble polyion/TiO₂ nanomultilayered film by the electrostatic layer-by-layer deposition technique.⁴⁵⁰ The nanoporous polyion/TiO₂ films were sintered and used as working electrodes for DSSC. An efficiency of 7.2% was obtained for the solar cell made from PDAC/TiO₂ (200 bilayers) precursor film.

Besides polyelectrolytes, plastic crystals such as succinonitrile,^{455,456} owing to their plasticity and intrinsic ionic conductivity, have been functioning as solid-state ion conductors. The addition of a small amount of other component, such as I⁻/I₃⁻,^{455,457–459} can produce orders of magnitude increases in conductivity.^{460–464} Zhang et al. reported a thermostable and highly conductive succinonitrile-based electrolyte;⁴⁶⁰ the DSSCs with this electrolyte obtained conversion efficiencies of 5.0–5.3% over a wide temperature range (20–80 °C). Armel et al. demonstrated that molecular plastic crystal (succinonitrile) based solid-state electrolytes can perform very well in SS-DSSCs with a porphyrin sensitizer.⁴⁶¹ Addition of nanoparticulate SiO₂ to the electrolyte produced the highest device efficiency of 5.3% (at 15% sun). Wang et al. prepared a highly conductive iodide/triiodide solid conductor by doping a molecular plastic crystal succinonitrile with *N*-

methyl-*N*-butylpyrrolidinium iodide salt and iodine. The SS-DSSC with this electrolyte achieved an efficiency of 6.7%.⁴⁶⁴

On the basis of the reactions of LiI and small organic molecules (HPN, methanol, ethanol, etc.), the Meng group developed a kind of solid-state composite electrolyte.^{368,392,465} The solid-state electrolytes can increase charge carrier mobility and pore filling into TiO₂ mesoporous film, thus provoking higher photovoltaic performance. A solid-state electrolyte based on LiI₆H₁₀N₂O₂ [LiI(HPN)₂] single crystal and I[−]/I₃[−] was prepared. The I···H–O hydrogen bonding, ionic clusters [Li⁺_kI₃[−]] ($k \neq 1$), as well as their association with the HPN molecules at high salt concentration constructed a 3D framework. This spatial configuration was beneficial to I[−]/I₃[−] transportation in the electrolyte. The SS-DSSC with the electrolyte LiI(HPN)₄/SiO₂ (15 nm, 15 wt %) obtained an efficiency of 5.48%. One month later, the efficiency (without sealing) maintained 70% of the initial value, indicating that the long-term stability of this solid-state electrolyte was superior to the liquid electrolytes.

Rutkowska et al. prepared an inorganic solid electrolyte based on nickel(II) hexacyanoferrate (II, III) (NiHCF, the mixture of K₄Ni^{II}[Fe^{II}(CN)₆] and K₃Ni^{II}[Fe^{III}(CN)₆], mol ratio 1:1) redox mediator using this electrolyte in combination with N3 dye; the SS-DSSC achieved a conversion efficiency of 4%.⁴⁶⁶

4.2. Inorganic Hole-Transport Materials

According to the principle of DSSC,^{30,31,35} the mesoporous TiO₂ layer and the I[−]/I₃[−] redox couple can be regarded as electron-transporting layer and hole-transporting layer, respectively, and thus the I[−]/I₃[−] redox electrolyte can be replaced by a p-type semiconductor material as a hole-transporting material (HTM).^{467,468} According to the definition,⁷² the HTM is not an electrolyte but a semiconductor since the charge carrier transportation is by electrons or holes not by ions. In HTMs,^{10,35} charge carrier transports takes place through hole hopping between neighboring molecules or moieties, which are a typical electronic transport, as opposed to electrolytes where charge carrier transport is due to movement of ions, a typical ionic transport. In SS-DSSCs, the HTMs are allowed to contain some salts and ionic conductivity, which is significant for local charge compensation.³⁵

An appropriate HTM for fabricating SS-DSSCs must satisfy several requirements. (i) It must be able to transfer holes from the sensitizing dye after the dye injects electrons into the TiO₂, and the upper edge of the valence band of the p-type semiconductors must be located above the ground state level of the dye.⁴⁴² (ii) It must be able to be deposited within the mesoporous TiO₂ films in amorphous state because the crystallization of HTM will inhibit efficient pore filling of mesoporous TiO₂ film, which is regarded as a major limiting factor for device performance.^{118,119} (iii) The hole mobility of HTM should be sufficiently high, as low hole mobility is believed to be another limiting factor for device performance.^{78,392} (iv) It should be transparent in the visible range and cannot dissolve or degrade the sensitized dye during the depositing process.^{10,468}

Known to date are only a very limited number of inorganic p-type materials, coincidentally in accordant with the above requirements and suitable for their application in SS-DSSCs.⁴⁶⁹ Familiar inorganic wide-band HTMs such as SiC and GaN are not suitable to be used in DSSCs since the high-temperature deposition process for these materials will certainly degrade the

sensitized dyes on the TiO₂ electrode.¹⁰ After extensive experimentation, a type of inorganic p-type semiconductor based on copper compounds such as CuI, CuBr, or CuSCN was found.^{470–473} These copper-based materials can be cast from solution or vacuum deposition to form a complete hole-transporting layer, and CuI has good hole conductivity in excess of 10^{−2} S·cm^{−1},⁴⁶⁸ which facilitates their hole conducting ability.

In 1995, Tennakone et al. first demonstrated an SS-DSSC based on CuI HTM.⁴⁷⁰ By substituting cyanidin with a Ru-bipyridyl complex, Tennakone et al. reported an efficiency of 2.4% for the SS-DSSCs with CuI.^{474,475} One reason for lower efficiency compared to other DSSCs is the too fast crystallization CuI rate,³⁹² which results in incomplete filling into TiO₂ mesopores. Tennakone et al. found that the addition of a small amount (~10^{−3} M) of 1-methyl-3-ethylimidazolium thiocyanate (MEISCN) or triethylamine hydrothiocyanate (THT) in the coating solution could inhibit the growth of CuI and improve the contact between CuI and dyed TiO₂ anode.^{476,477} Meng et al. improved the pore filling of the mesoporous dyed TiO₂ layer utilizing MEISCN as growth inhibitors, enhanced the electrical contact using ZnO, and obtained a conversion efficiency of 3.8% for SS-DSSC with CuI HTM.⁴³⁹

The photovoltaic performance of the CuI-based SS-DSSC is unstable and undergoes rapid decay.^{478–480} Sirimanne et al. found that the CuI-based SS-DSSCs deteriorated very rapidly, even much faster than that of liquid-state DSSCs.⁴⁸¹ One of the reasons is the stoichiometric excess of iodine molecules adsorbed at the CuI surface, acting as hole trapping sites and forming a trace amount of Cu₂O and/or CuO for the degradation of the cell.⁴⁸⁰ Taguchi et al. and Kumara et al. fabricated SS-DSSCs with a thin MgO “blocking” layer prior to dye sensitization, showing an improved stability and conversion efficiency of 4.7%.^{482,483} The improvement is attributed to the suppression of the photooxidation capability of TiO₂ by blocking the transfer of photogenerated holes to the CuI layer.⁴⁸³ Another reason for low efficiency for SS-DSSC with CuI seems to be the imperfect contact between the p-type semiconductor and the dye molecules. Tennakone et al. used *cis*-dithiocyanate-bis(2,2'-bipyridyl-4,4'-dicarboxylate) ruthenium(II) as sensitized dye; as a consequence of interaction of NCS ligands bound to the CuI surface (thiocyanate dyes are strongly absorbed by CuI films), the photovoltaic performance of the SS-DSSC was improved, and a conversion efficiency of ~6% (irradiation intensity 5 mW·cm^{−2}) was obtained.⁴⁷⁴ The dye molecule interacting with CuI through both NCS groups was confirmed by Mahrov and Karlsson et al.^{484,485} In order to increase the contact among dyes, hole conductor, and counter electrode, Sakamoto et al. modified the CuI hole conductor and the counter electrode with the NCS group (guanidine thiocyanate);^{486,487} the performance of the resultant DSSC with PEDOT:PSS:C counter electrode was improved dramatically, and a conversion efficiency of 7.4% was obtained.

CuSCN is an alternative to replace CuI with a more stable performance due to its unique chemical robustness associated with its polymeric structure.^{471,488–491} CuSCN does not decompose to SCN[−] and does not have excessive SCN[−] adsorbed on the CuSCN surface, acting as hole trapping sites. In 2001, Kumara et al. dissolved CuSCN in *n*-propyl sulfide ([C₂H₅]₂S) deposited on Ru-dye coated TiO₂ film,⁴⁷¹ giving an efficiency of 1.25% for the SS-DSSC. In 2002, O'Regan et al. reported another solid-state DSSC with CuSCN

HTM, and the cells showed an efficiency of ~2% at 1 sun.⁴⁹² The major drawback of CuSCN as p-type semiconductor in SS-DSSCs is its rather poor hole conductivity (10^{-4} S·cm⁻¹) and consequent slower rate of reduction of oxidized dye molecules, thus allowing the recombination of electrons injected to TiO₂ conduction band with the oxidized dye molecules.^{471,473,493,494}

Perera et al. doped the semiconductor with (SCN)₂ to create acceptor levels 2.6 eV below the band gap (3.6 eV) of CuSCN.⁴⁹³ This modification enhanced the efficiency of the solar cell from 0.75% without SCN doping to 2.39% after SCN doping. The low efficiency of the SS-DSSC based on CuSCN HTM probably is faster orders of magnitude than the recombination reactions rate in CuSCN HTM than in liquid electrolytes, leading to poor fill factors and losses of photocurrent.⁴⁹⁵ It is significant to improve the efficiency of this class of DSSCs by reducing the recombination rate via introducing surface passivation layers⁴⁹⁴ or increasing the electron-transport rates in the nanoporous TiO₂.⁴⁹⁵ In 2012, Premalal et al. incorporated triethylamine-coordinated Cu(II) sites in CuSCN structure.⁴⁸⁹ The Hall effect measurements showed an outstanding enhancement of hole concentration from 7.04×10^{15} to 8.22×10^{16} cm⁻³ and hence p-type conductivity from 0.01 to 1.42 S·m⁻¹ for the structurally modified CuSCN compared to ordinary CuSCN. Using this hole conductor, SS-DSSC achieved a conversion efficiency of 3.4%.

Other p-type semiconductors, such as NiO^{496,497} and CuAlO₂,^{498,499} were used as HTMs in SS-DSSCs; however, owing to their own problems, it is difficult to make an efficient solar cell.

Cesium tiniodide, in particular, the orthorhombic perovskite polymorph (B- γ -CsSnI₃, space group *Pnma*) of this trihalide,^{500,501} is gaining rapid interest due to the possibility used in SS-DSSCs,^{441,469,502} Schottky solar cells,⁵⁰³ and optoelectronic devices.^{504–506} These potential applications are on account of the outstanding properties of CsSnI₃, including^{441,469,500–507} (i) high p-type metal-like conductivity (~200 S·cm⁻²), (ii) high hole mobility (~585 cm²·V⁻¹·s⁻¹), (iii) direct band gap of ~1.3 eV, and (iv) strong near-infrared photoluminescent emission at ~950 nm. Recently, Chung et al. used a p-type direct band gap semiconductor CsSnI₃ as HTM for constructing a SS-DSSC in combination with n-type nanoporous TiO₂ and N719 dye.⁴⁴¹ The CsSnI₃ is solution processable and can fill into TiO₂ mesopores at a molecular level to make intimate contacts with dye molecules and TiO₂. With a band gap of 1.3 eV, CsSnI₃ enhances visible light absorption on the red side of the spectrum even outperforming typical DSSCs in this spectral region. The use of pristine CsSnI₃ in SS-DSSCs yielded a conversion efficiency of 3.72%. Doping CsSnI₃ with 5% SnF₂, the efficiency was increased to 6.81%. By pretreating the TiO₂ electrode with fluorine plasma and introducing photonic crystal over the counter electrode, the device yielded an efficiency of 10.2% (8.51% with a mask).⁴⁴¹ The current highest record result has opened up the opportunity to further optimize SS-DSSCs and search for new inorganic HTMs.

Very recently, Lee et al. introduced Cs₂SnI₆ in DSSCs.⁵⁰⁸ Unlike CsSnI₃ and CH₃NH₃SnI₃, which have Sn in the 2+ oxidation state and must be treated in an inert atmosphere when fabricating solar cells, the Sn in Cs₂SnI₆ is in the 4+ oxidation state, making it stable in air and moisture. Using this lead-free compound Cs₂SnI₆ as a hole transporter, a SS-DSSC was fabricated in air. The SS-DSSC with dye Z907 obtained an

efficiency of 4.7%, and the cell with the mixed dyes of N719, YD2-o-C8, and RLC5 achieved an efficiency of near 8%.⁵⁰⁸

4.3. Organic Hole-Transport Materials

Compared with inorganic hole-transport materials, organic hole-transport materials (organic p-type semiconductors) display attractive features, such as plentiful sources, low cost, and easy preparation. Most of the organic HTMs, either polymers or molecules, are soluble or dispersible in organic solvent; simple methods such as spin coating, in situ electrochemical polymerization, or photochemical polymerization methods can be used for fabricating SS-DSSCs with good pore-filling TiO₂ mesoporous films.⁴⁶⁷ Moreover, it can be tailored by chemical methods to fit different purposes and thus used widely in organic solar cells,^{509,510} organic thin film transistors,^{511,512} organic light-emitting diodes,^{513,514} etc. Organic HTMs can be divided into two classes, polymeric HTMs and molecular HTMs.⁴⁶⁷

In 1997, Yanagida's group first used polypyrrole (PPy) as organic HTM in SS-DSSC.⁵¹⁵ In order to improve the connectivity between the HTMs and the mesoporous TiO₂ film, PPy was deposited by in situ photoelectrochemical polymerization method on N3 dye-anchored TiO₂ surface, and the SS-DSSC obtained an efficiency of 0.1% (light intensity 22 mW·cm⁻²).⁵¹⁵ Subsequently, the dye N3 was replaced by dye *cis*-Ru(dcb)₂(pmp)₂ [dcb = 4,4'-dicarboxy-2,2'-bipyridine, pmp = 3-(pyrrole-1-ylmethyl)pyridine],⁵¹⁶ and Pt counter electrode was replaced by carbon-based counter electrode.⁵¹⁷ The conversion efficiency was improved to 0.62% (light intensity 10 mW·cm⁻²). The poor performance of the cell was owing to the visible light absorption by polypyrrole.^{515–517}

Tan et al. first used polyaniline (PANI) as HTM in SS-DSSCs.⁵¹⁸ However, these devices showed extremely low efficiency. Further studies found that PANI with an intermediate conductivity value (3.5 S·cm⁻¹) offered the best device performance.⁵¹⁹ By optimization of the film morphology and the cluster size of PANIs, the SS-DSSC obtained a J_{SC} of 0.77 mA·cm⁻² and an efficiency of 0.10%. Subsequently, using LiI and TBP as additives and 4-dodecylbenzenesulfonic acid-doped polyaniline (PANI-DBSA), the corresponding devices showed an improved efficiency of up to 1.15%.⁵²⁰ The improvement was attributed to the inhibition of interfacial charge recombination and amelioration of wetting on TiO₂ film.

The initial performances of the SS-DSSCs using poly(3-hexylthiophene) (P3HT) and poly(3-octylthiophene) (P3OT) as HTMs were relatively poor ($\eta < 1\%$), which was attributed to inefficient pore filling of polymer HTMs into mesoporous TiO₂ film,^{521–523} resulting in low charge separation and collection efficiencies.^{524,525} By optimization of a series of parameters such as TiO₂ crystalline state (anatase, brookite), density, and film thickness, an efficiency of 1.3% was obtained for the SS-DSSC with TiO₂/N719/P3OT/Au configuration.⁵²⁶ These devices also showed good stability after storage for 3 months with exposure to light and air. By addition of lithium bis(trifluoromethanesulfonyl)imide (LiTFSI) and TBP, the D102-sensitized⁵²⁷ and HRS-1-sensitized⁵²⁸ TiO₂/P3HT devices obtained conversion efficiencies of 2.63% and 2.7%, respectively. Further improvement of conversion efficiencies (3.2%) was achieved by infiltration of P3HT into the vertically aligned TiO₂ nanotubes sensitized with squaraine dye (SQ-1).⁵²⁹ The exploration of high extinction coefficient perovskite as light absorbers provides a new platform for searching new

HTMs. Recently, Giacomo et al. fabricated a FTO/TiO₂/CH₃NH₃PbI_{3-x}Cl_x/P3HT/Au perovskite solar cell⁵³⁰ using P3HT as hole conductor; the cell achieved an efficiency of 9.3%, which is the highest reported efficiency for the solar cell using P3HT as a hole transporter.

The heterojunction of P3HT/PCBM ([6,6]-phenyl-C61-butyric acid methyl ester) plays a crucial role in polymer solar cells. Recently, our group has implemented investigations on replacing traditional electrolyte by the P3HT/PCBM heterojunctions in DSSCs, including TiO₂/N719/PCBM/P3HT/Pt ($\eta = 3.09\%$),⁵³¹ TiO₂/PCBM/P3OT/Pt (no dye, $\eta = 2.61\%$),⁵³² TiO₂/PDDA–CdTe/PCBM/P3HT/C₆₀/Pt (QD cell, $\eta = 3.40\%$),⁵³³ ITO/PEN/TiO₂/N719/PCBM/P3HT/Pt/Pt–ITO/PEN (flexible, $\eta = 1.43\%$),⁵³⁴ TiO₂/PCBM/P3HT/Pt (no dye, $\eta = 2.97\%$),⁵³⁵ ITO/PEN/TiO₂/PCBM/P3HT/Pt/Pt–ITO/PEN (flexible and no dye, $\eta = 1.04\%$),⁵³⁶ and TiO₂/N719/PCBM/P3HT/PEDOT:PSS/carbon ($\eta = 4.11\%$).⁵³⁷ The results show that the P3HT or P3OT heterojunctions can not only replace electrolytes^{531–537} but also substitute for sensitized dyes in DSSCs as well.^{534,536} These new iodide/triiodide-free conductor candidates exhibit some advantages, such as simple device construction and low device cost. More interestingly, using P3HT or P3OT as hole conductor and TiO₂ as an ultraviolet light absorber and electronic conductor, we first reported an ultraviolet responsive inorganic–organic hybrid solar cell FTO/TiO₂/P3HT/Pt with an efficiency of 1.28%,⁵³⁸ and it was also found that the conductivity of the conductor could be increased and the performance of the cell could be improved by LiI doping.⁵³⁸

Distinct from most of the conjugated polymers HTMs absorbing visible light which compromises the light-harvesting efficiency of dye, poly(3,4-ethylenedioxothiophene) (PEDOT) possesses high transparency in the visible range,^{18,467,468} high hole conductivity (up to 550 S·cm⁻¹),⁵³⁹ and remarkable stability at room temperature and is an excellent alternative HTM in SS-DSSCs. In 2004, Yanagida and co-workers used chemically polymerized PEDOT as HTM and obtained an efficiency of 0.53%.⁵⁴⁰ This system later was improved by using the electropolymerization method, hydrophobic sensitizers, and various doping agents.^{541–547} A PEDOT-based SS-DSSC achieved a conversion efficiency of 2.85% by doping lithium bis-trifluoromethanesulfonylimide (LiTFSI).⁵⁴⁷ In 2010, using organic dye (D149) as sensitizer,⁵⁴⁸ Liu et al. assembled a polymer-HTM-based SS-DSSC by in situ polymerization of 2,2'-bis(3,4-ethylenedioxothiophene) (bis-EDOT) in an electrolytic thin layer; the SS-DSSC achieved a high conversion efficiency (6.1%). In 2011, Kim et al. used a high conductivity of PEDOT (10 S·cm⁻¹) and transparent OM-TiO₂ interface; the SS-DSSC yielded an enhanced efficiency up to 6.8%.⁵⁴⁹

A series of polycarbazoles was studied, and their energy levels were modified in comparison with dye and semiconductor levels.⁵⁵⁰ Recently, the combination of quantum dots with HTM has attracted wide attention. Using Sb₂S₃ nanocrystal as a light harvester, a P3HT-based SS-DSSC achieved a conversion efficiency of about 5%.⁵⁵¹ Replacing P3HT with a modified poly(alkylthiophene), poly[2,6-(4,4-bis(2-ethylhexyl)-4H-cyclopenta-[2,1-b;3,4-b']dithiophene)-alt-4,7(2,1,3-benzothiadiazole)] (PCPD(TBT)), the conversion efficiency was further improved to 6.3%.^{552,553} The colloidal PbS quantum dots by simple solution processing can be used as light harvesters and HTMs, which remarkably improves the photovoltaic performance ($J_{SC} > 20 \text{ mA}\cdot\text{cm}^{-2}$) of the DSSCs.⁵⁵⁴ Using PbSe quantum dots as light harvesters and HTMs, the internal

quantum efficiencies of 130% have been witnessed, suggesting the feasibility of multiple exciton generation and their collection as photocurrent.^{555,556}

Other p-type conjugate polymers, such as triarylamine-based polymers,^{118,119,557,558} polythiophene (PT),^{539,559,560} and poly[2-methoxy-5-(2-ethylhexyloxy)-1,4-phenylenevinylene] (PMEHPV),⁵⁶¹ also were attempted as organic HTMs in SS-DSSCs. However, owing to limited pore filling and other reasons,⁵⁶² the conversion efficiencies of these systems seldom exceed 1%. It is significant that some polymeric HTMs such as PAIN,^{330,432,433,563} PPy,^{317,333,564–566} and polythiophene (PTH)^{567,568} as additives in the liquid or quasi-solid electrolytes can obviously improve the carrier transportation ability and enhance the photovoltaic performances of the resulted DSSCs.

Molecular hole-transport material 2,2',7,7'-tetrakis(*N,N*-di-*p*-methoxyphenylamine)-9,9'-spirobifluorene (spiro-MeOTAD) doping with N(PhBr)₃SbCl₆ and Li[(CF₃SO₂)₂N] was first used in an efficient SS-DSSC in combination with N719 as sensitized dye by Gratzel et al. in 1998.⁴⁴² An IPCE value of 33% and an overall efficiency of 0.74% were obtained. The low efficiency was due to the charge recombination across the interface of the TiO₂/spiro-MeOTAD heterojunction. In 2001, Kruger et al. added TBP, lithium bis(trifluoromethanesulfonyl)-imide (LiTFSI), and Li-[CF₃SO₂]₂N in spiro-MeOTAD as additives,⁵⁶⁹ which resulted in a photovoltage of 900 mV, a photocurrent of 5.1 mA, and a conversion efficiency of 2.56%. Snaith et al. compared a series of molecular sensitizers in DSSC with HTM spiro-MeOTAD.⁴⁴³ The charge recombination was reduced, and the longest electron lifetime was obtained by the diblock alkoxy–alkane pendent groups on the dye. By further increasing the optical path length in the active layer, a power conversion efficiency of 5.1% was achieved. On the other hand, in order to increase the light harvest, Kruger et al. mixed silver ions in N719 dye solution;⁵⁷⁰ the DSSC obtained a power conversion efficiency of 3.2%. The dye N719 was replaced with amphiphilic ruthenium dye (Z907),⁵⁷¹ pure organic indoline dye (D102),⁵⁷² organic dyes C104,⁵⁷³ and C220,⁵⁷⁴ respectively, and power conversion efficiencies were further enhanced to about 4%, 4%, 4.6%, and >6%. Although spiro-MeOTAD is considered as a good HTM, it suffers from low conductivity in its pristine form.^{575,576} A remarkable improvement in conversion efficiency (7.2%) was achieved by increasing the hole mobility of spiro-OMeTAD more than 1 order of magnitude through doping with FK102 cobalt(III) complex (0.7%) and using a high absorption coefficient D–π–A sensitizer (Y123).⁵⁷⁷

Solid transport materials have good long-term stability; however, the efficiencies of the traditional DSSCs based on solid transport materials including solid-state electrolytes and hole-transport materials are lower than those of their analogous liquid DSSCs due to the poor interfacial contact. Recently, using solid hole conductor spiro-OMeTAD together with organolead halide perovskite, the all-solid-state solar cell achieved a highest conversion efficiency close to 20%,²⁴ which will be the most important development direction in the near future.

4.4. Perovskite Solar Cells

Though prospective results, the efficiencies of SS-DSSCs still cannot compete with that of its analogous liquid DSSCs. The relatively low efficiency of the SS-DSSC version is attributed to the low hole mobility in spiro-OMeTAD, causing interfacial

recombination losses 2 orders of magnitude higher than in liquid counterpart DSSCs.⁵⁷⁸ In DSSC, in order to adsorb sufficient dye and turn to absorb most of the incident sunlight, the thickness of 10 μm for TiO_2 mesoporous film is required. This is impractical for SS-DSSCs, where a number of factors collude to limit the thickness less than 2 μm .⁵⁷⁶ Inspired by quantum dot sensitizers and extremely thin absorber (ETA) with high molar extinction coefficient, in 2009, Miyasaka et al. first attempted high absorption coefficient $\text{CH}_3\text{NH}_3\text{PbX}_3$ ($X = \text{Br}, \text{I}$) perovskite nanocrystals as sensitizers in iodide/triiodide liquid electrolyte-based DSSCs and obtained the cell's efficiencies of 3.8% and 3.1% by using $\text{CH}_3\text{NH}_3\text{PbI}_3$ and $\text{CH}_3\text{NH}_3\text{PbBr}_3$, respectively.⁵³ In 2011, Park et al. employed similar structures and spin-coated perovskite precursor solution (equimolar $\text{CH}_3\text{NH}_3\text{I}$ and PbI_2 in γ -butyrolactone solution) on nanocrystalline TiO_2 surface. This $\text{CH}_3\text{NH}_3\text{PbI}_3$ perovskite quantum-dot-sensitized solar cell obtained an efficiency of 6.5%.⁵⁷⁹ Perovskite nanoparticles exhibited better absorption than standard N719 dye sensitizers, but they dissolved in the liquid electrolyte, resulting in a rapid degradation of performance.^{53,579}

This stimulated the replacement of problematic liquid electrolytes by a solid-state HTM.^{580,581} Park, Gratzel et al. introduced a solid-state HTM spiro-MeOTAD to perovskite solar cell.⁵⁸⁰ In the device $\text{CH}_3\text{NH}_3\text{PbI}_3$ nanocrystals were adsorbed in 0.6 μm thick TiO_2 film, the spiro-MeOTAD was dissolved in an organic solvent and then penetrated mesoporous TiO_2 , leaving only solute molecules after solvent evaporation. The solid-state solar cell gave an efficiency of 9.7%. The use of spiro-OMeTAD dramatically improved the device stability, and the device stored in air at room temperature without encapsulation retained its photovoltaic performance for over 500 h.

Almost simultaneously (mid-2012), Snaith et al. also reported the success in spiro-MeOTAD perovskite solar cell.⁵⁸¹ They found that mixed-halide $\text{CH}_3\text{NH}_3\text{PbI}_{3-x}\text{Cl}_x$ exhibited better stability and carrier transport than its pure iodide equivalent.^{581,582} They named them "meso-superstructured solar cell" (MSSC) and had few fundamental energy losses and high photovoltage of 1.1 V. This low-cost, solution-processable solar cell based on perovskite absorber with intense visible-to-near-infrared absorptivity obtained an efficiency of 10.9%.^{581,582} The recorded results trigger a major breakthrough in perovskite solar cell and lead to immense interest and research.

A jump to a reported efficiency of 12.0% came from the Seok and Gratzel group by using a solid perovskite capping layer overlying the scaffolding (nanoporous TiO_2 infiltrated by perovskite).⁵⁸³ Of the HTMs (including spiro-MeOTAD) they investigated, poly(triarylamine) (PTAA) was proved to be the best. Using similar structures and $\text{CH}_3\text{NH}_3\text{PbI}_{3-x}\text{Br}_x$ perovskites, the Seok group further improved the performance of the solar cell and obtained a reported efficiency of 12.3% in 2013.⁵⁸⁴ A low Br content (<10%) gave the best initial efficiency due to a lower band gap, but higher Br contents (>20%) provided a better high-humidity stability.

At the European Materials Research Symposium in May 2013, efficiencies above 15% were reported by the Gratzel group and Snaith group. The Gratzel group⁵⁸⁵ achieved a 15% efficiency (which confirmed an efficiency of 14.1% by an independent accredited test center) using a sequential deposition route for perovskite-sensitized solar cells. The perovskite was prepared by depositing a PbI_2 solution onto a

nanoporous TiO_2 film followed by $\text{CH}_3\text{NH}_3\text{I}$ solution dipping. These sequential depositions provide much better morphology control and TiO_2 pore filling over the perovskite than previously reported routes. The Snaith group⁵⁸⁶ developed a planar cell architecture using a dual-source thermal evaporation method to form a uniform, compact, flat thin $\text{CH}_3\text{NH}_3\text{PbI}_{3-x}\text{Cl}_x$ absorbing layer for the perovskite solar cell, and the efficiency reached 15.4%. At the end of 2013, the Seok group achieved an independently confirmed efficiency of 16.2% by using the mixed-halide $\text{CH}_3\text{NH}_3\text{PbI}_{3-x}\text{Br}_x$ (10–15% Br) and hole-transport material PTAA.⁵⁸⁷ This was increased to a confirmed efficiency of 17.9% by the Seok group in early 2014.⁵⁸⁷

Very recently, Yang group^{24,588} suppressed charge carrier recombination in the absorber, facilitated carrier injection, and maintained good carrier extraction at the electrodes by controlling the formation of the $\text{CH}_3\text{NH}_3\text{PbI}_{3-x}\text{Cl}_x$ perovskite layer and judiciously choosing device materials. The power conversion efficiency of the perovskite solar cell was boosted to 16.6% on average, with the highest efficiency of ~19.3%.

With the research development of perovskite solar cells, the power conversion efficiency keeps increasing, from 3.9% in 2009 to 19.3% now. This fast increment surpasses most people's expectation. Perovskite solar cell was chosen by *Science* as one of the 10 breakthroughs of the year 2013.⁵⁸⁹

Perovskite is the name of a series of materials with the same crystal structure toward CaTiO_3 . It is named after the Russian mineralogist L. A. Perovski. There are hundreds of different materials that adopt this structure, with a multitude of properties, including superconducting, insulating, antiferromagnetic, piezoelectric, thermoelectric, semiconducting, conducting, etc.^{42,590} The chemical structure of perovskite can be described as AMX_3 and is shown in Figure 14. In the classes of

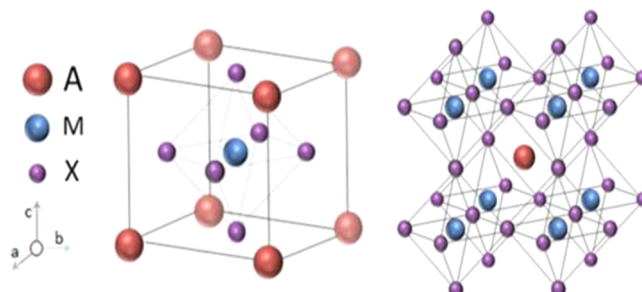


Figure 14. Crystal structure of perovskites.

perovskites being discussed here, the A cations are organic (typically CH_3NH_3^+ , $\text{C}_2\text{H}_5\text{NH}_3^+$, $\text{HC}(\text{NH}_2)_2^+$), the M cations are typically divalent metal ions such as Pb^{2+} , Sn^{2+} , Fe^{2+} , Cu^{2+} , etc., while the X anions are halides (Cl^- , Br^- , I^-). The organolead halide perovskite materials used in mesoscopic perovskite solar cells is due to their excellent properties, such as large absorption coefficient,⁵⁹¹ high charge carrier mobilities,⁵⁹² solution processability, and tunable optical and electronic properties.⁵⁹³ The composition, size, structure, conformation, radius, and charge of the ions dictate the final structure of the material and its properties.

Since the emergence of inorganic–organic perovskite materials, various fabrication methods were developed for high purity and less structural defects. The widely applied and simplest preparation is the spin-coating method. The stoichiometric quantities of $\text{CH}_3\text{NH}_3\text{I}$ and PbI_2 are dissolved

in polar solvents such as GBL or DMF as precursor.^{580,582,594} The mixture is spin coated and annealed to deposit the perovskite within the pores of the mesoporous layers or to form compact perovskite layers for planar solar cells. The preparation is affected by many factors, such as substrate material, film thickness, annealing temperature, solution concentration, spin-coating speed, solvent utilized, etc.

Gratzel et al. first practiced a sequential deposition method in perovskite preparation.⁵⁸⁵ The PbI₂ is spin coated on the TiO₂ film from a solution under appropriate conditions (solution concentration, spin-coating speed) to allow PbI₂ to fully infiltrate within the mesoporous layer. Subsequently, the film is dipped in a CH₃NH₃I solution. During the dipping, CH₃NH₃PbI₃ grew in situ. Sequential deposition improves the pore filling of mesoporous TiO₂, lowering the defects in the device. The cell presented a breakthrough efficiency above 15% for the first time.⁵⁸⁵

The vapor deposition method was first attempted in a planar perovskite solar cell by Snaith et al.⁵⁸⁶ With PbCl₂ and CH₃NH₃I as dual-evaporation sources, by adjusting the vaporizing speed, they obtained CH₃NH₃PbI_{3-x}Cl_x film on the substrate directly and gave an efficiency of 15.4%.⁵⁸⁶ The vapor-deposited films are extremely uniform, with crystalline features on the length scale of hundreds of nanometers. An interesting approach combining solution deposition with vapor transformation was reported by the Yang group.⁵⁹⁵ In the vapor-assisted solution process (VASP), PbI₂ is first deposited from solution onto a compact TiO₂ substrate. Subsequently, the film is exposed to a vapor of CH₃NH₃I at 150 °C in N₂ for 2 h. The slow rate of conversion results in CH₃NH₃PbI₃ films with micrometer-sized grains and a good surface roughness of ~20 nm. The solar cells obtained an efficiency of 12.1%.⁵⁹⁵

As the absorber of solar cells, the spectral response of perovskite has a significant influence on power conversion efficiency. Broad and strong absorption in the visible and near-infrared range is a basic condition for high efficiency. However, though a low-energy band-gap (E_g) material absorbs more light, it has a lower open-circuit voltage. A material with a gap at ca. 1.4–1.6 eV seems to be proper for a solar light absorber.⁵⁹⁶ In perovskite materials, their E_g can be adjusted by element type and ratio. For A ions, with the increment of A ion radius, the lattice expands, producing a reduced band gap and red shift of absorption.^{597,598} For X ions, in the case of CH₃NH₃PbX₃, experiments proved that absorption can be shifted to the blue region by moving from I to Br to Cl.⁵⁷⁸ In the case of CH₃NH₃Pb(I_{1-x}Br_x)₃, Seok et al. obtained a simulated equation to describe the tenability of the band gap: $E_g = 1.57 + 0.39x + 0.33x^2$ (0 ≤ x ≤ 1).⁵⁸⁴ For M ions, insertion of Sn to Pb-based perovskite will effectively extend the absorption to the infrared range.⁵⁹⁹ The stability of the perovskites follows the trend AGeI₃ < ASnI₃ < APbI₃.⁶⁰⁰ However, Pb is a drawback of the perovskite-based solar cells, because it is not only toxic but also sensitive to the water.⁶⁰¹ Therefore, replacing Pb²⁺ with Sn²⁺, Cu²⁺, and Fe²⁺ or developing new perovskite oxide is a promising direction.

The perovskite materials have superior functions not only as light absorbers but also as electron and hole transporters. Etgar et al. fabricated devices with appreciable performance in a configuration without the HTM layer.⁶⁰² Xiao et al. also fabricated some perovskite solar cells without hole-transport materials,^{603,604} indicating that the perovskite material can also work as an absorber and a hole transporter. Lee et al. demonstrated that the perovskite material can also work

effectively as both an absorber and an electron transporter by fabricating solar cells with an insulating Al₂O₃ scaffold instead of the TiO₂ photoanode.⁵⁸¹ Some studies indicated that electron transport through the perovskite layer was much faster than through the n-type TiO₂, meaning that mesoporous TiO₂ is not always necessary.⁵⁸⁶ Utilizing femtosecond transient optical spectroscopy, Xing et al. measured long-range electron–hole diffusion lengths of at least 100 nm in solution-processed CH₃NH₃PbI₃.⁶⁰⁵ Using the same method Stranks et al. determined the electron–hole diffusion length exceeding 1 μm for CH₃NH₃PbI_{3-x}Cl_x.⁵⁸² Both studies clearly show that the electron–hole diffusion lengths in perovskites are much longer than those for most solution-processed materials (typically ~10 nm). A spin-polarized density functional analysis by Giorgi et al. indicated that the effective masses of photogenerated electrons and holes in CH₃NH₃PbI₃ were estimated to be $m_e^* = 0.23 m_0$ and $m_h^* = 0.29 m_0$, respectively.⁶⁰⁶ The calculation provided a theoretical basis for the long-range ambipolar charge transport property and the larger diffusion constant for electrons compared with that for holes in the perovskite.^{582,605} Wehrenfennig et al. determined the charge carrier mobility for CH₃NH₃PbI_{3-x}Cl_x and CH₃NH₃PbI₃ to be 11.6 and ~8 cm²·V⁻¹·s⁻¹, respectively,⁶⁰⁷ which are extremely high for the solution-processed perovskites. Comparatively, these values are >20 times larger than that of mesoporous TiO₂ and several orders larger than those of typical p-conjugated molecular semiconductors.

Perovskite solar cells have achieved an efficiency of ~20%.⁵⁸⁸ The further increment of efficiency depends on the development of new perovskites. Partial substitution of halide anions is an important direction. The reported highest efficiency of the perovskite cell is based on CH₃NH₃PbI_{3-x}Cl_x.⁵⁸⁸ Edri et al. demonstrated a CH₃NH₃PbBr_{3-x}Cl_x solar cell with open-circuit voltages as high as 1.5 V,⁶⁰⁸ and the Seok group showed that partial substitution of I with Br improved the cell stability.⁵⁸⁴ Another key effort is the reduction of the perovskite band gap for increasing spectral response and thus improving cell efficiency. CH₃NH₃PbI₃ does not efficiently harvest photons close to its optical absorption onset (600–780 nm), resulting in photocurrents not approaching the theoretical maximum. The Snaith group developed formamidinium (HC(NH₂)²⁺) lead perovskite with a lower band gap (1.48 eV) and obtained photocurrent as high as 23.3 mA cm⁻² in a planar heterojunction solar cell.⁵⁹⁸ Ferroelectric perovskite may be another important orientation, since the ferroelectric–photovoltaic effect can greatly enhance the open-circuit photovoltage of the device, although the currently used perovskites are probably ferroelectric only at temperatures below 180 K, and a big challenge faced for the ferroelectric photovoltaic devices is the very low photocurrent output.⁶⁰⁹ Very recently, a perovskite-type complex (3-pyrrolinium)(CdCl₃) with room-temperature ferroelectricity was synthesized.⁶¹⁰ The open-circuit photovoltage for the bulky crystal with a thickness of 1 mm reached 32 V. This finding could provide a new approach to develop perovskite solar cells. Pb is another problem (owing its toxic) that has to be solved, especially for large-scale production, although Pb-based halide perovskite currently yields the most efficient solar cells. Sn²⁺ may serve as a replacement to Pb²⁺, but its tendency to be easily oxidized is a drawback.⁶¹¹ In addition, a large variety of possible halide perovskites can be attempted.

Perovskites have evolved as low-cost, low-temperature processable (solution or vapor deposited), versatile, and

mulfifunctional materials capable of performing all of the three basic tasks required in solar cells operation, that is, light absorption, carrier generation, and electron and hole transport. The unique combination of high extinction coefficient absorbance along with their ambipolar nature provides perovskites with a clear advantage over quantum dots and other existing absorber materials in thin-film solar cells.⁵⁸⁰ From 2009 when Miyasaka et al.⁵³ first reported the perovskite as a sensitizer in DSSCs to today it has only been 5 years yet the efficiencies of this new kind of solar cells increases from 3.8%⁵³ to 19.3%.^{24,588} We witnessed an unexpected breakthrough and rapid evolution for the perovskite solar cells. Perovskite solar cells have become the most promising devices in the third-generation PV field by virtue of their low cost, high efficiency, and good stability.

5. SUMMARY AND OUTLOOK

DSSCs efficiently converting solar energy into electricity energy with low cost, easy preparation, and environment benignity are becoming a promising alternative to classical photovoltaic devices. The electrolyte is a crucial component in DSSCs and has great influence on both the photovoltaic performance and the long-term stability of the devices. Using liquid electrolytes, a highest power conversion efficiency of 13% has been achieved for a traditional DSSC. However, the long-term instability caused by the leakage and volatilization of organic solvents limits its practical application; the problems can be partly solved by using ionic liquids as solvents though. The application of quasi-solid-state electrolytes obviously improves the long-term stability of DSSCs. However, owing to the lower mobility of iodide species through the viscous medium and the imperfect wetting of electrode pores with the electrolytes, the power conversion efficiency of QS-DSSC is lower than that of the DSSC based on liquid electrolytes. The highest efficiency of QS-DSSC is higher than 10%. Solid-state conductors can basically meet long-term stability requirements for DSSCs, whereas the efficiencies for traditional SS-DSSCs are lower, which is due to poor electrolyte/electrode interfacial contacts. Using solid hole conductor spiro-OMeTAD with perovskite, the all-solid-state solar cell achieved a power conversion efficiency close to 20%.^{24,588}

Throughout the development of DSSCs, each important breakthrough is achieved by using new concepts, new methods, and new materials. A power conversion efficiency as high as 15% for monolithic DSSC should be expected based on creative work. The key challenges will include further improvement of the overall conversion efficiency, device stability, and scale up of fabrication. The electrolytes, or hole-transport materials, as a key component of DSSCs, play an important role for realizing this significant target. The future studies should be further addressed on the issues of the electrolyte interactions with electrodes and sensitized dyes, of understanding their effect on photoelectrical conversion processes, and of designing alternative charge carrier materials to enhance the charge carrier transport efficiency, to decrease recombination loss, and to improve the long-term stability.

AUTHOR INFORMATION

Corresponding Author

*E-mail: jhwu@hqu.edu.cn.

Notes

The authors declare no competing financial interest.

Biographies



Jihuai Wu is Professor in Chemistry and Materials and the Vice President at Huaqiao University, China. He obtained his Master's degree in Materials in 1988 at Huaqiao University, China, and obtained his Ph.D. degree in Chemistry in 1999 at Fuzhou University, China. He joined the Institute of Materials Physical Chemistry, Huaqiao University, in 1988 and became the director of the institute in 1998. His main research focus on photoelectronic functional materials and devices, superabsorbent polymers, photocatalytic intercalated nanomaterials, especially dye-sensitized solar cell. He has 300 scientific publications and 17 authorized invention patents.



Zhang Lan received his Master's degree and Ph.D. degree in Materials Science from Huaqiao University, China, in 2006 and 2009, respectively. He joined the Institute of Materials Physical Chemistry, Huaqiao University, in 2009 and became an associate professor in 2012. His main interests are on the synthesis and application of nanomaterials in dye/quantum dot-sensitized solar cells and organic-inorganic hybrid solar cells.



Jianming Lin is Professor in Materials and the Dean of the Materials department at Huaqiao University. He received Ph.D. degree in Polymers from Tianjin University, China, in 2002. His main research focus is on photoelectronic functional materials and devices, superabsorbent polymers, and photocatalytic intercalated nanomaterials, especially dye-sensitized solar cells.



Miaoliang Huang is Professor in Materials at Huaqiao University. He received his Ph.D. degree in Physical Chemistry from Fujian Institute of Research on the Structure of Matter, Chinese Academy of Sciences, in 2003. His current research interests focus on the synthesis and application of nanophotocatalytic materials and photoelectronic functional materials.



Yunfang Huang is a professor in Materials Chemistry at Huaqiao University, China. He obtained his Ph.D. degree in Materials Science in 2007 at Huaqiao University, China. He joined the Institute of Materials Physical Chemistry, Huaqiao University, in 1998. His main research interests include photocatalysis, photoelectronic functional materials, dye-sensitized solar cell, and related materials and devices development.



Leqing Fan is an associate professor in Materials Chemistry at Huaqiao University, China. He received his Master's degree in Materials Science from Huaqiao University in 2003 and then his Ph.D. degree in Physical Chemistry from the Chinese Academy of Sciences in 2006. His main research interests include supercapacitors, dye-sensitized solar cells, and inorganic–organic hybrid materials.



Genggeng Luo is an associate professor in Materials Chemistry at Huaqiao University, China. He was born in 1981 in Fujian, China. He earned his Ph.D. degree in 2009 from the College of Chemistry and Chemical Engineering, Xiamen University. After 1 year of research at the University of Rochester under the direction of Professor Richard Eisenberg, he joined the faculty at Huaqiao University in 2010. His current research interests include the development of molecular photochemical devices for solar-energy conversion and investigation of fluorescent molecular systems.

ACKNOWLEDGMENTS

The authors acknowledge the joint financial support by the National High Technology Research and Development Program of China (no. 2009AA03Z217), the National Natural Science Foundation of China (nos. 91422301, U1205112, 90922028, 51472094, 51002053, 50842027), and the specialized research fund for the doctoral program of Higher University, Ministry of Education, China (no. 20123501110001).

REFERENCES

- (1) SmalleyR. E.*Abstracts of Papers*; 226th ACS National Meeting, New York, NY, Sept 7–11, 2003; American Chemical Society: Washington, DC, 2003; U24.
- (2) Hoekstra, A. Y.; Wiedmann, T. O. *Science* **2014**, *344*, 1114.
- (3) Dresselhaus, M. S.; Thomas, I. L. *Nature* **2001**, *414*, 332.
- (4) Witze, A. *Nature* **2007**, *445*, 14.
- (5) Service, R. F. *Science* **2005**, *309*, 548.

- (6) Potocnik, J. *Science* **2007**, *315*, 810.
- (7) World energy consumption, http://en.wikipedia.org/wiki/World_energy_consumption; accessed Oct 2009.
- (8) Conti, J. *International Energy Outlook 2011*; U.S. Energy Administration: Washington, DC, 2011.
- (9) Shafiee, S.; Topal, E. *Energy Policy* **2008**, *36*, 775.
- (10) Li, B.; Wang, L.; Kang, B.; Wang, P.; Qiu, Y. *Sol. Energy Mater. Sol. Cells* **2006**, *90*, 549.
- (11) Oettinger, G. H. Energy roadmap 2050, <http://www.energy.eu/publications/Energy-Roadmap-2050.pdf> (accessed Dec 2011).
- (12) Schiermeier, Q.; Tollefson, J.; Scully, T.; Witze, A.; Morton, O. *Nature* **2008**, *454*, 816.
- (13) Hammond, A. L. *Science* **1972**, *177*, 1088.
- (14) Hammond, A. L. *Science* **1972**, *178*, 732.
- (15) Lewis, N. S. *Science* **2007**, *315*, 798.
- (16) Smil, V. *General Energetics: Energy in the Biosphere and Civilization*; John Wiley: New York, 1991; p 240.
- (17) Hoffmann, W. *Sol. Energy Mater. Sol. Cells* **2006**, *90*, 3285.
- (18) Wang, M.; Gratzel, C.; Zakeeruddin, S. M.; Gratzel, M. *Energy Environ. Sci.* **2012**, *5*, 9394.
- (19) Chapin, D.; Fuller, C.; Pearson, G. *J. Appl. Phys.* **1954**, *25*, 676.
- (20) Green, M.; Emery, K.; Hishikawa, Y.; Warta, W.; Dunlop, E. *Prog. Photovoltaics Res. Appl.* **2014**, *22*, 1.
- (21) Yella, A.; Lee, H.; Tsao, H.; Yi, C.; Chandiran, A.; Nazeeruddin, M.; Diau, E.; Yeh, C.; Zakeeruddin, S.; Gratzel, M. *Science* **2011**, *334*, 629.
- (22) Mathew, S.; Yella, A.; Gao, P.; Humphry-Baker, R.; Curchod, B.; Ashari-Astani, N.; Tavernelli, I.; Rothlisberger, U.; Nazeeruddin, M.; Gratzel, M. *Nat. Chem.* **2014**, *6*, 242.
- (23) Sugaya, T.; Numakami, O.; Oshima, R.; Furue, S.; Komaki, H.; Amano, T.; Matsubara, K.; Okano, Y.; Niki, S. *Energy Environ. Sci.* **2012**, *5*, 6233.
- (24) Service, R. F. *Science* **2014**, *344*, 458.
- (25) Skotheim, T. US Patent 4190950, 1980.
- (26) Desilvestro, J.; Gratzel, M.; Kavan, L.; Moser, J.; Augustynski, J. *J. Am. Chem. Soc.* **1985**, *107*, 2988.
- (27) Liska, P.; Vlachopoulos, N.; Nazeeruddin, M.; Comte, P.; Gratzel, M. *J. Am. Chem. Soc.* **1988**, *110*, 3686.
- (28) Vlachopoulos, N.; Liska, P.; Augustynski, J.; Gratzel, M. *J. Am. Chem. Soc.* **1988**, *110*, 1216.
- (29) O'Regan, B.; Gratzel, M. *Nature* **1991**, *353*, 737.
- (30) Gratzel, M. *Nature* **2001**, *414*, 338.
- (31) Hagfeldt, A.; Gratzel, M. *Chem. Rev.* **1995**, *95*, 49.
- (32) Hagfeldt, A.; Gratzel, M. *Acc. Chem. Res.* **2000**, *33*, 269.
- (33) Gratzel, M. *Inorg. Chem.* **2005**, *44*, 6841.
- (34) Gratzel, M. *Acc. Chem. Res.* **2009**, *42*, 1788.
- (35) Hagfeldt, A.; Boschloo, G.; Sun, L.; Kloo, L.; Pettersson, H. *Chem. Rev.* **2010**, *110*, 6595.
- (36) Goncalves, L.; Bermudez, V.; Ribeiroa, H.; Mendes, A. *Energy Environ. Sci.* **2008**, *1*, 655.
- (37) Wu, J.; Lan, Z.; Hao, S.; Li, P.; Lin, J.; Huang, M.; Fang, L.; Huang, Y. *Pure Appl. Chem.* **2008**, *80*, 2241.
- (38) Kalyanasundaram, K.; Gratzel, M. *Coord. Chem. Rev.* **1998**, *77*, 347.
- (39) Ardo, S.; Meyer, G. *J. Chem. Soc. Rev.* **2009**, *38*, 115.
- (40) Boschloo, G.; Hagfeldt, A. *Acc. Chem. Res.* **2009**, *42*, 1819.
- (41) Thomas, S.; Deepak, T.; Anjusree, G.; Arun, T.; Naira, S.; Nair, A. *J. Mater. Chem. A* **2014**, *2*, 4474.
- (42) Snaith, H. *J. Phys. Chem. Lett.* **2013**, *4*, 3623.
- (43) Baxter, J. B. *J. Vac. Sci. Technol. A* **2012**, *30*, 020801.
- (44) Hiroshi, I.; Tomokazu, U.; Seigo, I. *Acc. Chem. Res.* **2009**, *42*, 1809.
- (45) Clifford, J.; Martinez-Ferrero, E.; Viterisi, A.; Palomares, E. *Chem. Soc. Rev.* **2011**, *40*, 1635.
- (46) Nazeeruddin, K.; Kay, A.; Rodicio, I.; Humphry-Baker, R.; Mueller, E.; Liska, P.; Vlachopoulos, N.; Gratzel, M. *J. Am. Chem. Soc.* **1993**, *115*, 6382.
- (47) Chiba, Y.; Islam, A.; Watanabe, Y.; Komiya, R.; Koide, N.; Han, L. *Jpn. J. Appl. Phys.* **2006**, *45*, 24.
- (48) Chen, C.; Wu, S.; Wu, C.; Chen, J.; Ho, K. *Angew. Chem., Int. Ed.* **2006**, *45*, 5822.
- (49) Chen, C.; Wu, S.; Wu, C.; Chen, J.; Ho, K. *Adv. Mater.* **2007**, *19*, 3888.
- (50) Qin, H.; Wenger, S.; Xu, M.; Gao, F.; Jing, X.; Wang, P.; Zakeeruddin, S.; Gratzel, M. *J. Am. Chem. Soc.* **2008**, *130*, 9202.
- (51) Gao, F.; Wang, Y.; Shi, D.; Zhang, J.; Wang, M.; Jing, X.; Humphry-Baker, R.; Wang, P.; Zakeeruddin, S.; Gratzel, M. *J. Am. Chem. Soc.* **2008**, *130*, 10720.
- (52) Cao, Y.; Bai, Y.; Yu, Q.; Cheng, Y.; Liu, S.; Shi, D.; Gao, F.; Wang, P. *J. Phys. Chem. C* **2009**, *113*, 6290.
- (53) Kojima, A.; Teshima, K.; Shirai, Y.; Miyasaka, T. *J. Am. Chem. Soc.* **2009**, *131*, 6050.
- (54) Li, P.; Wu, J.; Lin, J.; Huang, M.; Huang, Y.; Li, Q. *Sol. Energy* **2009**, *83*, 845.
- (55) Huang, K.; Wang, Y.; Dong, R.; Tsai, W.; Tsai, K.; Wang, C.; Chen, Y.; Vittal, R.; Lin, J.; Ho, K. *J. Mater. Chem.* **2010**, *20*, 4067.
- (56) Wu, M.; Ma, T. *J. Phys. Chem. C* **2014**, *118*, 16727.
- (57) Olsen, E.; Hagen, G.; Lindquist, S. *Sol. Energy Mater. Sol. Cells* **2000**, *63*, 267.
- (58) Hao, F.; Dong, P.; Luo, Q.; Li, J.; Lou, J.; Lin, H. *Energy Environ. Sci.* **2013**, *6*, 2003.
- (59) Brennan, L.; Byrne, M.; Bari, M.; Gunko, Y. *Adv. Energy Mater.* **2011**, *1*, 472.
- (60) Ahmad, S.; Guillen, E.; Kavan, L.; Gratzel, M.; Nazeeruddin, M. *Energy Environ. Sci.* **2013**, *6*, 3439.
- (61) Li, Q.; Wu, J.; Tang, Q.; Lan, Z.; Li, P.; Lin, J.; Fan, L. *Electrochim. Commun.* **2008**, *10*, 1299.
- (62) Wu, J.; Li, Q.; Fan, L.; Lan, Z.; Li, P.; Lin, J.; Hao, S. *J. Power Sources* **2008**, *181*, 172.
- (63) Wang, G.; Wang, D.; Kuang, S.; Zhuo, S. *J. Inorg. Mater.* **2013**, *28*, 907.
- (64) Mulmudi, H.; Batabyal, S.; Rao, M.; Prabhakar, R.; Mathews, N.; Lam, Y.; Mhaisalkar, S. *Phys. Chem. Chem. Phys.* **2011**, *13*, 19307.
- (65) Gong, F.; Wang, H.; Xu, X.; Zhou, G.; Wang, Z. *J. Am. Chem. Soc.* **2012**, *134*, 10953.
- (66) Chen, X.; Tang, Q.; He, B.; Lin, L.; Yu, L. *Angew. Chem., Int. Ed.* **2014**, *53*, 10799.
- (67) Pichot, F.; Pitts, J.; Gregg, B. *Langmuir* **2000**, *16*, 5626.
- (68) Kuang, D.; Brillet, J.; Chen, P.; Takata, M.; Uchida, S.; Miura, H.; Sumioka, K.; Zakeeruddin, S.; Gratzel, M. *ACS Nano* **2008**, *2*, 1113.
- (69) Weerasinghe, H.; Huang, F.; Cheng, Y. *Nano Energy* **2013**, *2*, 174.
- (70) Nour-Mohammadi, F.; Nguyen, S.; Boschloo, G.; Hagfeldt, A.; Lund, T. *J. Phys. Chem. B* **2005**, *109*, 22413.
- (71) Wang, P.; Wenger, B.; Humphry-Baker, R.; Moser, J.; Teuscher, J.; Kantlehner, W.; Mezger, J.; Stoyanov, E.; Zakeeruddin, S.; Gratzel, M. *J. Am. Chem. Soc.* **2005**, *127*, 6850.
- (72) Winter, M.; Brodd, R. *Chem. Rev.* **2004**, *104*, 4245.
- (73) Xu, K. *Chem. Rev.* **2004**, *104*, 4303.
- (74) Nogueira, A.; Longo, C.; De Paoli, M. *Coord. Chem. Rev.* **2004**, *248*, 1455.
- (75) Yu, Z.; Vlachopoulos, N.; Gorlov, M.; Kloo, L. *Dalton Trans.* **2011**, *40*, 10289.
- (76) Gorlov, M.; Kloo, L. *Dalton Trans.* **2008**, 2655.
- (77) Freitas, J.; Nogueira, A.; De Paoli, M. *J. Mater. Chem.* **2009**, *19*, 5279.
- (78) Zhang, W.; Cheng, Y.; Yin, X.; Liu, B. *Macromol. Chem. Phys.* **2011**, *212*, 15.
- (79) Clifford, J.; Palomares, E.; Nazeeruddin, M.; Gratzel, M.; Durrant, J. *J. Phys. Chem. C* **2007**, *111*, 6561.
- (80) Schiffmann, F.; Vondele, J.; Vande, J.; Urakawa, A.; Wirz, R.; Baiker, A. *Proc. Natl. Acad. Sci. U.S.A.* **2010**, *107*, 4830.
- (81) Rowley, J.; Farnum, B.; Ardo, S.; Meyer, G. *J. Phys. Chem. Lett.* **2010**, *1*, 3132.
- (82) Privalov, G.; Timofei, B.; Hagfeldt, A.; Svensson, P.; Kloo, L. *J. Phys. Chem. C* **2009**, *113*, 783.

- (83) Ferber, J.; Stangl, R.; Luther, J. *Sol. Energy Mater. Sol. Cells* **1998**, *53*, 29.
- (84) Ratner, M.; Shriver, D. *Chem. Rev.* **1988**, *88*, 109.
- (85) Arrhenius, S. *A Z. Phys. Chem.* **1889**, *4*, 226.
- (86) Vogel, H. *Phys. Z.* **1921**, *22*, 645.
- (87) Thammann, G.; Hesse, W. *Z. Anorg. Allg. Chem.* **1926**, *156*, 245.
- (88) Fulcher, G. *S. J. Am. Ceram. Soc.* **1925**, *8*, 339.
- (89) Braja, D.; Ghosh, K.; Lott, J.; Ritchie, E. *Chem. Mater.* **2005**, *17*, 661.
- (90) Ishimaru, N.; Kubo, W.; Kitamura, T.; Yanagida, S.; Tsukahara, Y.; Maitani, M.; Wada, Y. *Mater. Sci. Eng., B* **2011**, *176*, 996.
- (91) Wu, C.; Guo, S.; Jia, L.; Han, S.; Chi, B.; Pu, J.; Jian, L. *RSC Adv.* **2013**, *3*, 13968.
- (92) Aziz, M.; Noor, I.; Sahraoui, B.; Arof, A. *Opt. Quantum Electron.* **2014**, *46*, 133.
- (93) Tu, C.; Liu, K.; Chien, A.; Lee, C.; Ho, K.; Lin, K. *Eur. Polym. J.* **2008**, *44*, 608.
- (94) Jovanovski, V.; Orel, B.; Jese, R.; Vuk, A.; Mali, G.; Hocevar, S.; Grdadolnik, J.; Stathatos, E.; Lianos, P. *J. Phys. Chem. B* **2005**, *109*, 14387.
- (95) Miyamoto, T.; Shibayama, K. *J. Appl. Phys.* **1973**, *44*, 5372.
- (96) Turnbull, D.; Cohen, M. *J. Chem. Phys.* **1961**, *34*, 120.
- (97) Cohen, M.; Turnbull, D. *J. Chem. Phys.* **1959**, *31*, 1164.
- (98) Simpson, J.; Bidstrup, S. *J. Polym. Sci., Part B* **1993**, *31*, 609.
- (99) Koike, T.; Ishizaki, N. *J. Appl. Polym. Sci.* **1999**, *71*, 207.
- (100) Bonhote, P.; Dias, A.; Papageorgiou, N.; Kalyanasundaram, K.; Gratzel, M. *Inorg. Chem.* **1996**, *35*, 1168.
- (101) Papageorgiou, N.; Athanassov, Y.; Armand, M.; Bonhote, P.; Pettersson, H.; Azam, A.; Gratzel, M. *J. Electrochem. Soc.* **1996**, *143*, 3099.
- (102) Kubo, W.; Murakoshi, K.; Kitamura, T.; Yoshida, S.; Haruki, M.; Hanabusa, K.; Shirai, H.; Wada, Y.; Yanagida, S. *J. Phys. Chem. B* **2001**, *105*, 12809.
- (103) Yamanaka, N.; Kawano, R.; Kubo, W.; Masaki, N.; kitamura, T.; Wada, Y.; Watanabe, M.; Yanagida, S. *J. Phys. Chem. B* **2007**, *11*, 4763.
- (104) Ishimaru, N.; Kubo, W.; Kitamura, T.; Yanagida, S.; Tsukahara, Y.; Maitani, M.; Wada, Y. *Mater. Sci. Eng., B* **2011**, *176*, 996.
- (105) Jerman, I.; Jovanovski, V.; SurcaVuk, A.; Hocevar, S.; Gaberscek, M.; Jesih, A.; Orel, B. *Electrochim. Acta* **2008**, *53*, 2281.
- (106) Jovanovski, V.; Orel, B.; Jerman, I.; Hocevar, S.; Ogorevc, B. *Electrochim. Commun.* **2007**, *9*, 2062.
- (107) de Freitas, J.; Goncalves, A.; De Paoli, M.; Durrant, J.; Nogueira, A. *Electrochim. Acta* **2008**, *53*, 7166.
- (108) Zakeeruddin, S.; Gratzel, M. *Adv. Funct. Mater.* **2009**, *19*, 2187.
- (109) Usui, H.; Matsui, H.; Tanabe, N.; Yanagida, S. *J. Photochem. Photobiol., A* **2004**, *164*, 97.
- (110) Kawano, R.; Watanabe, M. *Chem. Commun.* **2003**, 330.
- (111) Dahms, H.; Rock, R.; Seligson, D. *J. Phys. Chem.* **1968**, *72*, 859.
- (112) Ruff, I.; Botor, L. *J. Chem. Phys.* **1985**, *83*, 1292.
- (113) Bach, U.; Tachibana, Y.; Moser, J.; Haque, S.; Durrant, J.; Gratzel, M.; Klug, D. *J. Am. Chem. Soc.* **1999**, *121*, 7445.
- (114) Haque, S. A.; Tachibana, Y.; Willis, R.; Moser, J.; Gratzel, M.; Klug, D.; Durrant, J. *J. Phys. Chem. B* **2000**, *104*, 538.
- (115) Nelson, J.; Haque, S.; Klug, D.; Durrant, J. *J. Phys. Rev. B* **2001**, *63*, 205321.
- (116) O'Regan, B.; Schwartz, D.; Zakeeruddin, S.; Gratzel, M. *Adv. Mater.* **2000**, *12*, 1263.
- (117) Haque, S.; Park, T.; Holmes, A.; Durrant, J. *ChemPhysChem* **2003**, *4*, 89.
- (118) Kroese, J.; Hirata, N.; Schmidt-Mende, L.; Orizu, C.; Ogier, S.; Carr, K.; Gratzel, M.; Durrant, J. *Adv. Funct. Mater.* **2006**, *16*, 1832.
- (119) Schmidt-Mende, L.; Gratzel, M. *Thin Solid Films* **2006**, *500*, 296.
- (120) Dualeh, A.; Moehl, T.; Nazeeruddin, M.; Gratzel, M. *ACS Nano* **2013**, *7*, 2292.
- (121) Hamann, T.; Ondersma, J. *Energy Environ. Sci.* **2011**, *4*, 370.
- (122) Han, L.; Koide, N.; Chiba, Y.; Islam, A.; Komiya, R.; Nobuhiro, F.; Fukui, A.; Yamanaka, R. *Appl. Phys. Lett.* **2005**, *86*, 213501.
- (123) Fischer, A.; Pettersson, H.; Hagfeldt, A.; Boschloo, G.; Kloof, L.; Gorlov, M. *Sol. Energy Mater. Sol. Cells* **2007**, *91*, 1062.
- (124) Campbell, W.; Burrell, A.; Officer, D.; Jolley, K. *Coord. Chem. Rev.* **2004**, *248*, 1363.
- (125) Ito, S.; Nazeeruddin, M.; Liska, P.; Comte, P.; Charvet, R.; Pechy, P.; Jirousek, M.; Kay, A.; Zakeeruddin, M.; Gratzel, M. *Prog. Photovoltaics: Res. Appl.* **2006**, *14*, 589.
- (126) Tsubomura, H.; Matsumura, M.; Nomura, Y.; Amamiya, T. *Nature* **1976**, *261*, 402.
- (127) Desilvestro, J.; Gratzel, M.; Kavan, L.; Moser, J.; Augustynski, J. *J. Am. Chem. Soc.* **1985**, *107*, 2988.
- (128) Kalyanasundaram, K.; Vlachopoulos, N.; Krishnan, V.; Monnier, A.; Gratzel, M. *J. Phys. Chem.* **1987**, *91*, 2342.
- (129) Vlachopoulos, N.; Liska, P.; Augustynski, J.; Gratzel, M. *J. Am. Chem. Soc.* **1988**, *110*, 1216.
- (130) Liska, P.; Vlachopoulos, N.; Nazeeruddin, M.; Comte, P.; Gratzel, M. *J. Am. Chem. Soc.* **1988**, *110*, 3686.
- (131) Liu, Y.; Hagfeldt, A.; Xiao, X.; Lindquist, S. *Sol. Energy Mater. Sol. Cells* **1998**, *55*, 267.
- (132) Law, C.; Pathirana, S.; Li, X.; Anderson, A.; Barnes, P.; Listorti, A.; Ghaddar, T.; O'Regan, B. *Adv. Mater.* **2010**, *22*, 4505.
- (133) Tributsch, H. *Coord. Chem. Rev.* **2004**, *248*, 1511.
- (134) Hauch, A.; Georg, A. *Electrochim. Acta* **2001**, *46*, 3457.
- (135) Gratzel, M. *J. Photochem. Photobiol., C* **2003**, *4*, 145.
- (136) Kato, N.; Takeda, Y.; Higuchi, K.; Takeichi, A.; Sudo, E.; Tanaka, H.; Motohiro, T.; Sano, T.; Toyoda, T. *Sol. Energy Mater. Sol. Cells* **2009**, *93*, 893.
- (137) Kato, N.; Higuchi, K.; Tanaka, H.; Nakajima, J.; Sano, T.; Toyoda, T. *Sol. Energy Mater. Sol. Cells* **2011**, *95*, 301.
- (138) Gutmann, V. *Electrochim. Acta* **1976**, *21*, 661.
- (139) Hara, K.; Horiguchi, T.; Kinoshita, T.; Sayama, K.; Arakawa, H. *Sol. Energy Mater. Sol. Cells* **2001**, *70*, 151.
- (140) Kebede, Z.; Lindquist, S. E. *Sol. Energy Mater. Sol. Cells* **1999**, *57*, 259.
- (141) Fukui, A.; Komiya, R.; Yamanaka, R.; Islam, A.; Han, L. *Sol. Energy Mater. Sol. Cells* **2006**, *90*, 649.
- (142) Lee, K.; Suryanarayanan, V.; Ho, K. *J. Power Sources* **2009**, *188*, 635.
- (143) Stergiopoulos, T.; Kontos, A.; Likodimos, V.; Perganti, D.; Falaras, P. *J. Phys. Chem. C* **2011**, *115*, 10236.
- (144) Wu, J.; Lan, Z.; Lin, J.; Huang, M.; Li, P. *J. Power Sources* **2007**, *173*, 585.
- (145) Wu, J.; Lan, Z.; Lin, J.; Huang, M.; Hao, S.; Fan, L. *Electrochim. Acta* **2007**, *52*, 7128.
- (146) Hong, J.; Joo, M.; Vittal, R.; Kim, K. *J. Electrochem. Soc.* **2002**, *149*, 493.
- (147) Cahen, D.; Hodes, G.; Grazel, M.; Guillemoles, J.; Riess, I. *J. Phys. Chem. B* **2000**, *104*, 2053.
- (148) Rogers, R. D.; Seddon, K. R. *Science* **2003**, *302*, 792.
- (149) Dupont, J.; de Souza, R. F.; Suarez, P. A. Z. *Chem. Rev.* **2002**, *102*, 3667.
- (150) Welton, T. *Coord. Chem. Rev.* **2004**, *248*, 2459.
- (151) Gebbie, M. A.; Valtiner, M.; Banquy, X.; Fox, E. T.; Henderson, W. A.; Israelachvili, J. N. *Proc. Natl. Acad. Sci. U.S.A.* **2013**, *110*, 9674.
- (152) Mecerreyes, D. *Prog. Polym. Sci.* **2011**, *36*, 1629.
- (153) Weingartner, H. *Angew. Chem., Int. Ed.* **2008**, *47*, 654.
- (154) Li, F.; Jennings, J.; Wang, X.; Fan, L.; Koh, Z.; Yu, H.; Yan, L.; Wang, Q. *J. Phys. Chem. C* **2014**, *118*, 17153.
- (155) Wang, P.; Zakeeruddin, S. M.; Humphry-Baker, R.; Gratzel, M. *Chem. Mater.* **2004**, *16*, 2694.
- (156) Wang, P.; Zakeeruddin, S.; Moser, J.; Gratzel, M. *J. Phys. Chem. B* **2003**, *107*, 13280.
- (157) Kuang, D.; Wang, P.; Ito, S.; Zakeeruddin, S.; Gratzel, M. *J. Am. Chem. Soc.* **2006**, *128*, 7732.
- (158) Wang, P.; Klein, C.; Humphry-Baker, R.; Zakeeruddin, S.; Gratzel, M. *Appl. Phys. Lett.* **2005**, *86*, 123508.
- (159) Chen, L.; Xue, B.; Liu, X.; Li, K.; Luo, Y.; Meng, Q.; Wang, R.; Chen, L. *Chin. Phys. Lett.* **2007**, *24*, 555.

- (160) Fei, Z.; Kuang, D.; Zhao, D.; Klein, C.; Ang, W.; Zakeeruddin, S.; Gratzel, M.; Dyson, P. *Inorg. Chem.* **2006**, *45*, 10407.
- (161) Ito, S.; Zakeeruddin, S.; Humphry-Baker, R.; Liska, P.; Charvet, R.; Comte, P.; Nazeeruddin, M.; Pechy, P.; Takata, M.; Miura, H.; Uchida, S.; Gratzel, M. *Adv. Mater.* **2006**, *18*, 1202.
- (162) Fabregat-Santiago, F.; Bisquert, J.; Palomares, E.; Otero, L.; Kuang, D.; Zakeeruddin, S.; Gratzel, M. *J. Phys. Chem. C* **2007**, *111*, 6550.
- (163) Fan, L.; Kang, S.; Wu, J.; Hao, S.; Lan, Z.; Lin, J. *Energy Sources A* **2010**, *32*, 1559.
- (164) Xu, D.; Zhang, H.; Chen, X.; Feng, Y. *J. Mater. Chem. A* **2013**, *1*, 11933.
- (165) Chen, X.; Xu, D.; Qiu, L.; Li, S.; Zhang, W.; Yan, F. *J. Mater. Chem. A* **2013**, *1*, 8759.
- (166) Wang, L.; Zhang, H.; Ge, R.; Wang, C.; Guo, W.; Shi, Y.; Gao, Y.; Ma, T. *RSC Adv.* **2013**, *3*, 12975.
- (167) Shi, D.; Pootrakulchote, N.; Li, R.; Guo, J.; Wang, Y.; Zakeeruddin, S.; Gratzel, M.; Wang, P. *J. Phys. Chem. C* **2008**, *112*, 17046.
- (168) Sauvage, F.; Chhor, S.; Marchioro, A.; Moser, J.; Gratzel, M. *J. Am. Chem. Soc.* **2011**, *133*, 13103.
- (169) Krossing, I.; Reisinger, A. *Coord. Chem. Rev.* **2006**, *250*, 2721.
- (170) Wang, P.; Zakeeruddin, S.; Moser, J.; Baker, R.; Gratzel, M. *J. Am. Chem. Soc.* **2004**, *126*, 7164.
- (171) Bai, Y.; Cao, Y.; Zhang, J.; Wang, M.; Li, R.; Wang, P.; Zakeeruddin, S.; Gratzel, M. *Nat. Mater.* **2008**, *7*, 626.
- (172) Cao, Y.; Zhang, J.; Bai, Y.; Li, R.; Zakeeruddin, S.; Gratzel, M.; Wang, P. *J. Phys. Chem. C* **2008**, *112*, 13775.
- (173) Paulsson, H.; Hagfeldt, A.; Kloo, L. *J. Phys. Chem. B* **2003**, *107*, 13665.
- (174) Paulsson, H.; Kloo, L.; Hagfeldt, A.; Boschloo, G. *J. Electroanal. Chem.* **2006**, *586*, 56.
- (175) Paulsson, H.; Berggrund, M.; Svantesson, E.; Hagfeldt, A.; Kloo, L. *Sol. Energy Mater. Sol. Cells* **2004**, *82*, 345.
- (176) Ramirez, R.; Sanchez, E. *Sol. Energy Mater. Sol. Cells* **2006**, *90*, 2384.
- (177) Ramirez, R.; Torres-Gonzalez, L.; Sanchez, E. *J. Electrochem. Soc.* **2007**, *154*, B229.
- (178) Santa-Nokki, H.; Busi, S.; Kallioinen, J.; Lahtinen, M.; Korppi-Tommola, J. *J. Photochem. Photobiol. A* **2007**, *186*, 29.
- (179) Xi, C.; Cao, Y.; Cheng, Y.; Wang, M.; Jing, X.; Zakeeruddin, S.; Gratzel, M.; Wang, P. *J. Phys. Chem. C* **2008**, *112*, 11063.
- (180) Fredin, K.; Gorlov, M.; Pettersson, H.; Hagfeldt, A.; Kloo, L.; Boschloo, G. *J. Phys. Chem. C* **2007**, *111*, 13261.
- (181) Son, K.; Kang, M.; Vittal, R.; Lee, J.; Kim, K. *J. Appl. Electrochem.* **2008**, *38*, 1647.
- (182) Wachter, P.; Zistler, M.; Schreiner, C.; Berginc, M.; Krasovec, U. O.; Gerhard, D.; Wasserscheid, P.; Hinsch, A.; Gores, H. *J. Photochem. Photobiol. A* **2008**, *197*, 25.
- (183) Zistler, M.; Schreiner, C.; Wachter, P.; Wasserscheid, P.; Gerhard, D.; Gores, H. *J. Int. J. Electrochem. Sci.* **2008**, *3*, 236.
- (184) Yang, S.; Yoon, H.; Lee, S.; Lee, H. *Mater. Lett.* **2009**, *63*, 1465.
- (185) Neo, C.; Ouyang, J. *Electrochim. Acta* **2012**, *85*, 1.
- (186) Matsumoto, H.; Matsuda, T.; Tsuda, T.; Hagiwara, R.; Ito, Y.; Miyazaki, Y. *Chem. Lett.* **2001**, *26*.
- (187) Datta, J.; Bhattacharya, A.; Kundu, K. *Bull. Chem. Soc. Jpn.* **1988**, *61*, 1735.
- (188) Haque, S.; Tachibana, Y.; Klug, D.; Durrant, J. *J. Phys. Chem. B* **1998**, *102*, 1745.
- (189) Cameron, P.; Peter, L. *J. Phys. Chem. B* **2005**, *109*, 7392.
- (190) O'Regan, B.; Durrant, J. *J. Phys. Chem. B* **2006**, *110*, 8544.
- (191) Huang, S.; Schlichthorl, G.; Nozik, A.; Gratzel, M.; Frank, A. *J. Phys. Chem. B* **1997**, *101*, 2576.
- (192) Boschloo, G.; Haggman, L.; Hagfeldt, A. *J. Phys. Chem. B* **2006**, *110*, 13144.
- (193) Kopidakis, N.; Neale, N. R.; Frank, A. *J. Phys. Chem. B* **2006**, *110*, 12485.
- (194) Mori, S.; Kubo, W.; Kanzaki, T.; Masaki, N.; Wada, Y.; Yanagida, S. *J. Phys. Chem. C* **2007**, *111*, 3522.
- (195) O'Regan, B.; Lopez-Duarte, I.; Martinez-Diaz, M.; Forneli, A.; Albero, J.; Morandeira, A.; Palomares, E.; Torres, T.; Durrant, J. *J. Am. Chem. Soc.* **2008**, *130*, 2906.
- (196) Reynal, A.; Forneli, A.; Martinez-Ferrero, E.; Sanchez-Diaz, A.; Vidal-Ferran, A.; O'Regan, B.; Palomares, E. *J. Am. Chem. Soc.* **2008**, *130*, 13558.
- (197) Miyashita, M.; Sunahara, K.; Nishikawa, T.; Uemura, Y.; Koumura, N.; Hara, K.; Mori, A.; Abe, T.; Suzuki, E.; Mori, S. *J. Am. Chem. Soc.* **2008**, *130*, 17874.
- (198) O'Regan, B.; Walley, K.; Juozapavicius, M.; Anderson, A.; Matar, F.; Ghaddar, T.; Zakeeruddin, S.; Klein, C.; Durrant, J. *J. Am. Chem. Soc.* **2009**, *131*, 3541.
- (199) Papageorgiou, N.; Gratzel, M.; Infelta, P. *Sol. Energy Mater. Sol. Cells* **1996**, *44*, 405.
- (200) Zistler, M.; Wachter, P.; Wasserscheid, P.; Gerhard, D.; Hinsch, A.; Sastrawan, R.; Gores, H. *Electrochim. Acta* **2006**, *52*, 161.
- (201) Pelet, S.; Moser, J.; Gratzel, M. *J. Phys. Chem. B* **2000**, *104*, 1791.
- (202) Lagemaat, J.; Park, N.; Frank, A. *J. J. Phys. Chem. B* **2000**, *104*, 2044.
- (203) Kopidakis, N.; Schiff, E.; Park, N.; Frank, A. *J. J. Phys. Chem. B* **2000**, *104*, 3930.
- (204) Solbrand, A.; Lindstrom, H.; Hagfeldt, A.; Lindquist, S. *J. Phys. Chem. B* **1997**, *101*, 2514.
- (205) Nakade, S.; Kambe, S.; Kitamura, T.; Wada, Y.; Yanagida, S. *J. Phys. Chem. B* **2001**, *105*, 9150.
- (206) Nister, D.; Keis, K.; Lindquist, S.; Hagfeldt, A. *Sol. Energy Mater. Sol. Cells* **2002**, *73*, 411.
- (207) Frank, A.; Kopidakis, N.; Lagemaat, J. *Coord. Chem. Rev.* **2004**, *248*, 1165.
- (208) Olson, C. *J. Phys. Chem. B* **2006**, *110*, 9619.
- (209) Shi, Y.; Zhan, C.; Wang, L.; Ma, B.; Gao, R.; Zhu, Y.; Qiu, Y. *Phys. Chem. Chem. Phys.* **2009**, *11*, 4230.
- (210) Benedetti, J.; de Paoli, M.; Nogueira, A. *Chem. Commun.* **2008**, *9*, 1121.
- (211) Watson, D.; Meyer, G. *Coord. Chem. Rev.* **2004**, *248*, 139.
- (212) Wang, H.; Bell, J.; Desilvestro, J.; Bertoz, M.; Evans, G. *J. Phys. Chem. C* **2007**, *111*, 15125.
- (213) Toivola, M.; Ahlskog, F.; Lund, P. *Sol. Energy Mater. Sol. Cells* **2006**, *90*, 2881.
- (214) Marcus, R. *J. Chem. Phys.* **1956**, *24*, 966.
- (215) Cong, J.; Yang, X.; Kloob, L.; Sun, L. *Energy Environ. Sci.* **2012**, *5*, 9180.
- (216) Tian, H.; Sun, L. *J. Mater. Chem.* **2011**, *21*, 10592.
- (217) Li, L.; Yang, X.; Gao, J.; Tian, H.; Zhao, J.; Hagfeldt, A.; Sun, L. *J. Am. Chem. Soc.* **2011**, *133*, 8458.
- (218) Wang, Z.; Sayama, K.; Sugihara, H. *J. Phys. Chem. B* **2005**, *109*, 22449.
- (219) Teng, C.; Yang, X.; Yuan, C.; Li, C.; Chen, R.; Tian, H.; Li, S.; Hagfeldt, A.; Sun, L. *Org. Lett.* **2009**, *11*, 5542.
- (220) Ning, Z.; Zhang, Q.; Wu, J.; Tian, H. *J. Organomet. Chem.* **2009**, *694*, 2705.
- (221) Rani, S.; Suri, P.; Mehra, R. *Prog. Photovoltaics* **2011**, *19*, 180.
- (222) Gorlov, M.; Pettersson, H.; Hagfeldt, A.; Kloo, L. *Inorg. Chem.* **2007**, *46*, 3566.
- (223) Oskam, G.; Bergeron, B.; Meyer, G.; Searson, P. *J. Phys. Chem. B* **2001**, *105*, 6867.
- (224) Bergeron, B.; Marton, A.; Oskam, G.; Meyer, G. *J. Phys. Chem. B* **2004**, *109*, 937.
- (225) Wang, M.; Chamberland, N.; Breau, L.; Moser, J.; Humphry-Baker, R.; Marsan, B.; Zakeeruddin, S.; Gratzel, M. *Nat. Chem.* **2010**, *2*, 385.
- (226) Burschka, J.; Brault, V.; Ahmad, S.; Breau, L.; Nazeeruddin, M.; Marsan, B.; Zakeeruddin, S.; Gratzel, M. *Energy Environ. Sci.* **2012**, *5*, 6089.
- (227) Zhang, Z.; Chen, P.; Murakami, T.; Zakeeruddin, S.; Gratzel, M. *Adv. Funct. Mater.* **2008**, *18*, 341.
- (228) Tian, H.; Jiang, X.; Yu, Z.; Kloo, L.; Hagfeldt, A.; Sun, L. *Angew. Chem., Int. Ed.* **2010**, *49*, 7328.

- (229) Tian, H.; Yang, X.; Cong, J.; Chen, R.; Liu, J.; Hao, Y.; Hagfeldt, A.; Sun, L. *Chem. Commun.* **2009**, 6288.
- (230) Nusbaumer, H.; Moser, J.; Zakeeruddin, S.; Nazeeruddin, M.; Gratzel, M. *J. Phys. Chem. B* **2001**, 105, 10461.
- (231) Nelson, J.; Amick, T.; Elliott, C. *J. Phys. Chem. C* **2008**, 112, 18255.
- (232) Hamann, T.; Brunschwig, B.; Lewis, N. *J. Phys. Chem. B* **2006**, 110, 25514.
- (233) Cameron, P.; Peter, L.; Zakeeruddin, S.; Gratzel, M. *Coord. Chem. Rev.* **2004**, 248, 1447.
- (234) Feldt, S.; Gibson, E.; Gabrielsson, E.; Sun, L.; Boschloo, G.; Hagfeldt, A. *J. Am. Chem. Soc.* **2010**, 132, 16714.
- (235) Zhou, D.; Yu, Q.; Cai, N.; Bai, Y.; Wang, Y.; Wang, P. *Energy Environ. Sci.* **2011**, 4, 2030.
- (236) Bai, Y.; Zhang, J.; Zhou, D.; Wang, Y.; Zhang, M.; Wang, P. *J. Am. Chem. Soc.* **2011**, 133, 11442.
- (237) Liu, J.; Zhang, J.; Xu, M.; Zhou, D.; Jing, X.; Wang, P. *Energy Environ. Sci.* **2011**, 4, 3021.
- (238) Yum, J.; Baranoff, E.; Kessler, F.; Moehl, T.; Ahmad, S.; Bessho, T.; Marchioro, A.; Ghadiri, E.; Moser, J.; Yi, C.; Nazeeruddin, M.; Gratzel, M. *Nat. Commun.* **2012**, 3, 631.
- (239) Hardin, B.; Snaith, H.; McGehee, M. *Nat. Photonics* **2012**, 6, 162.
- (240) Li, T.; Spokoyny, A.; She, C.; Farha, O.; Mirkin, C.; Marks, T.; Hupp, J. *J. Am. Chem. Soc.* **2010**, 132, 4580.
- (241) Hagberg, D.; Jiang, X.; Gabrielsson, E.; Linder, M.; Marinado, T.; Brinck, T.; Hagfeldt, A.; Sun, L. *J. Mater. Chem.* **2009**, 19, 7232.
- (242) Bai, Y.; Yu, Q.; Cai, N.; Wang, Y.; Zhang, M.; Wang, P. *Chem. Commun.* **2011**, 47, 4376.
- (243) Gregg, B.; Pichot, F.; Ferrere, S.; Fields, C. *J. Phys. Chem. B* **2001**, 105, 1422.
- (244) Hamann, T.; Farha, O.; Hupp, J. *J. Phys. Chem. C* **2008**, 112, 19756.
- (245) Feldt, S.; Cappel, U.; Johansson, E.; Boschloo, G.; Hagfeldt, A. *J. Phys. Chem. C* **2010**, 114, 10551.
- (246) Daeneke, T.; Kwon, T.; Holmes, A.; Duffy, N.; Bach, U.; Spiccia, L. *Nat. Chem.* **2011**, 3, 211.
- (247) Kambe, S.; Nakade, S.; Kitamura, T.; Wada, Y.; Yanagida, S. *J. Phys. Chem. B* **2002**, 106, 2967.
- (248) Nakade, S.; Saito, Y.; Kubo, W.; Kanzaki, T.; Kitamura, T.; Wada, Y.; Yanagida, S. *Electrochim. Commun.* **2003**, 5, 804.
- (249) Bella, F.; Sacco, A.; Pugliese, D.; Laurenti, M.; Bianco, S. *J. Power Sources* **2014**, 264, 333.
- (250) Kusama, H.; Konishi, Y.; Sugihara, H.; Arakawa, H. *Sol. Energy Mater. Sol. Cells* **2003**, 80, 167.
- (251) Kusama, H.; Arakawa, H. *Sol. Energy Mater. Sol. Cells* **2004**, 81, 87.
- (252) Kusama, H.; Arakawa, H. *J. Photochem. Photobiol. A* **2004**, 162, 441.
- (253) Huang, S.; Schlichthorl, G.; Nozik, A.; Gratzel, M.; Frank, A. *J. Phys. Chem. B* **1997**, 101, 2576.
- (254) Schlichthorl, G.; Huang, S.; Sprague, J.; Frank, A. *J. Phys. Chem. B* **1997**, 101, 8141.
- (255) Boschloo, G.; Haggman, L.; Hagfeldt, A. *J. Phys. Chem. B* **2006**, 110, 13144.
- (256) Shi, C.; Dai, S.; Wang, K.; Pan, X.; Kong, F.; Hu, L. *Vib. Spectrosc.* **2005**, 39, 99.
- (257) Durr, M.; Yasuda, A.; Nelles, G. *Appl. Phys. Lett.* **2006**, 89, 3.
- (258) Yin, X.; Zhao, H.; Chen, L.; Tan, W.; Zhang, J.; Weng, Y.; Shuai, Z.; Xiao, X.; Zhou, X.; Li, X.; Lin, Y. *Surf. Interface Anal.* **2007**, 39, 809.
- (259) Lan, Z.; Wu, J.; Lin, J.; Huang, M.; Li, P.; Li, Q. *Electrochim. Acta* **2008**, 53, 2296.
- (260) Kelly, C.; Farzad, F.; Thompson, D.; Stipkala, J.; Meyer, G. *J. Langmuir* **1999**, 15, 7047.
- (261) Watson, D.; Meyer, G. *Coord. Chem. Rev.* **2004**, 248, 1391.
- (262) Haque, S.; Palomares, E.; Cho, B.; Green, A.; Hirata, N.; Klug, D.; Durrant, J. *J. Am. Chem. Soc.* **2005**, 127, 3456.
- (263) Koops, S.; O'Regan, B.; Barnes, P.; Durrant, J. *J. Am. Chem. Soc.* **2009**, 131, 4808.
- (264) Jennings, J.; Wang, Q. *J. Phys. Chem. C* **2010**, 114, 1715.
- (265) Kopidakis, N.; Benkstein, K.; Lagemaat, J.; Frank, A. *J. Phys. Chem. B* **2003**, 107, 11307.
- (266) Zhang, C.; Huang, Y.; Huo, Z.; Chen, S.; Dai, S. *J. Phys. Chem. C* **2009**, 113, 21779.
- (267) Gratzel, M. *J. Photochem. Photobiol. A* **2004**, 164, 3.
- (268) Yu, Z.; Gorlov, M.; Boschloo, G.; Kloof, L. *J. Phys. Chem. C* **2010**, 114, 22330.
- (269) Wright, P. *Electrochim. Acta* **1998**, 43, 1137.
- (270) Editorial. *Electrochim. Acta* **2011**, 57, 4.
- (271) Wang, Y. *Sol. Energy Mater. Sol. Cells* **2009**, 93, 1167.
- (272) Wang, P.; Zakeeruddin, S.; Moser, J.; Nazeeruddin, M.; Sekiguchi, T.; Gratzel, M. *Nat. Mater.* **2003**, 2, 402.
- (273) Song, J.; Wang, Y.; Wan, C. *J. Power Sources* **1999**, 77, 183.
- (274) Mohmeyer, N.; Wang, P.; Schmidt, H.; Zakeeruddin, S.; Gratzel, M. *J. Mater. Chem.* **2004**, 14, 1905.
- (275) Wu, J.; Lan, Z.; Wang, D.; Hao, S.; Lin, J.; Huang, Y.; Yin, S.; Sato, T. *Electrochim. Acta* **2006**, 51, 4243.
- (276) Xia, J.; Li, F.; Huang, C.; Zhai, J.; Jiang, L. *Sol. Energy Mater. Sol. Cells* **2006**, 90, 944.
- (277) Lu, S.; Koeppe, R.; Gunes, S.; Sariciftci, N. *Sol. Energy Mater. Sol. Cells* **2007**, 91, 1081.
- (278) Gerbaldi, C.; Nair, J.; Meligrana, G.; Bongiovanni, R.; Bodoardo, S.; Penazzi, N. *Electrochim. Acta* **2010**, 55, 1460.
- (279) Zhou, Y.; Lin, G.; Shih, A.; Hu, S. *J. Power Sources* **2009**, 192, 544.
- (280) Roy, D.; Cambre, J.; Sumerlin, B. *Prog. Polym. Sci.* **2010**, 35, 278.
- (281) Simon, P.; Gogotsi, Y. *Nat. Mater.* **2008**, 7, 845.
- (282) Wu, J.; Hao, S.; Lan, Z.; Lin, J.; Huang, M.; Huang, Y.; Fang, L.; Yin, S.; Sato, T. *Adv. Funct. Mater.* **2007**, 17, 2645.
- (283) Wu, J.; Lan, Z.; Lin, J.; Huang, M.; Hao, S.; Sato, T.; Yin, S. *Adv. Mater.* **2007**, 19, 4006.
- (284) Song, D.; Cho, W.; Lee, J.; Kang, Y. *J. Phys. Chem. Lett.* **2014**, 5, 1249.
- (285) Megahed, S.; Scrosati, B. *Interface* **1995**, 4, 34.
- (286) Cao, F.; Oskam, G.; Pearson, P. *J. Phys. Chem.* **1995**, 99, 17071.
- (287) Wu, J.; Li, P.; Hao, S.; Yang, H.; Lan, Z. *Electrochim. Acta* **2007**, 52, 5334.
- (288) Lan, Z.; Wu, J.; Lin, J.; Huang, M. *Electrochim. Acta* **2012**, 60, 17.
- (289) Lan, Z.; Wu, J.; Lin, J.; Huang, M. *Sci. China Chem.* **2012**, 55, 242.
- (290) Yang, H.; Huang, M.; Wu, J.; Lan, Z.; Hao, S.; Lin. *J. Mater. Chem. Phys.* **2008**, 110, 38.
- (291) Lan, Z.; Wu, J.; Wang, D.; Hao, S.; Lin, J.; Huang, Y. *Sol. Energy* **2006**, 80, 1483.
- (292) Lan, Z.; Wu, J.; Wang, D.; Hao, S.; Lin, J.; Huang, Y. *Sol. Energy* **2007**, 81, 117.
- (293) Huang, M.; Yang, H.; Wu, J.; Lin, J.; Lan, Z.; Li, P.; Hao, S. *J. Sol-Gel. Sci. Technol.* **2007**, 42, 65.
- (294) Li, Q.; Wu, J.; Tang, Q.; Lan, Z.; Li, P.; Zhang, T. *Polym. Compos.* **2009**, 30, 1687.
- (295) Kang, M.; Kim, J.; Won, J.; Kang, Y. *J. Photochem. Photobiol. A* **2006**, 183, 15.
- (296) Stephan, A. *Eur. Polym. J.* **2006**, 42, 21.
- (297) Nogueira, F.; Alonso-Vante, N.; De Paoli, M. *Synth. Met.* **1999**, 105, 23.
- (298) Gazotti, W.; Spinace, M.; Girotto, E.; De Paoli, M. *Solid State Ionics* **2000**, 130, 281.
- (299) Nogueira, A.; Spinace, M.; Gazotti, W.; Girotto, E.; De Paoli, M. *Solid State Ionics* **2001**, 140, 327.
- (300) Silva, G.; Lemes, N.; Fonseca, C.; De Paoli, M. *Solid State Ionics* **1997**, 93, 105.
- (301) Nogueira, A.; De Paoli, M.; Montanari, I.; Monkhouse, R.; Nelson, J.; Durrant, J. *J. Phys. Chem. B* **2001**, 105, 7517.

- (302) Kim, J.; Kang, M.; Kim, Y.; Won, J.; Kang, Y. *Solid State Ionics* **2005**, *176*, 579.
- (303) Ileperuma, O.; Kumara, G.; Yang, H.; Murakami, K. *J. Photochem. Photobiol., A* **2011**, *217A*, 308.
- (304) Ileperuma, O. A. *Mater. Technol.* **2013**, *28*, 65.
- (305) Kang, M. G.; Kim, K. M.; Ryu, K. S.; Chang, S. H.; Park, N. G.; Hong, J. S.; Kim, K. *J. Electrochem. Soc.* **2004**, *151*, E257.
- (306) Lee, K. S.; Jun, Y.; Park, J. H. *Nano Lett.* **2012**, *12*, 2233.
- (307) Seo, S.; Yun, S.; Woo, J.; Park, D.; Kang, M.; Hinsch, A.; Moon, S. *Electrochem. Commun.* **2011**, *13*, 1391.
- (308) Huo, Z.; Zhang, C.; Fang, X.; Cai, M. *J. Power Sources* **2010**, *195*, 4384.
- (309) Yu, Q.; Yu, C.; Guo, F.; Wang, J.; Jiao, S.; Gao, S.; Lia, H.; Zhao, L. *Energy Environ. Sci.* **2012**, *5*, 6151.
- (310) Yang, C.; Ho, W.; Yang, H.; Hsueh, M. *J. Mater. Chem.* **2010**, *20*, 6080.
- (311) Gu, G.; Bouvier, S.; Wu, C.; Laura, R.; Rzeznik, M.; Abraham, K. *Electrochim. Acta* **2000**, *45*, 3127.
- (312) Kim, J. Y.; Kim, S. H. *Solid State Ionics* **1999**, *124*, 91.
- (313) Armand, M. *Adv. Mater.* **1990**, *2*, 278.
- (314) Shen, X. L.; Xu, W. L.; Xu, J.; Liang, G. J.; Yang, H. J.; Yao, M. *Solid State Ionics* **2008**, *179*, 2027.
- (315) Suryanarayanan, V.; Lee, K.; Ho, W.; Chen, H.; Ho, K. *Sol. Energy Mater. Sol. Cells* **2007**, *91*, 1467.
- (316) Kang, M.; Ahn, K.; Lee, J. *J. Power Sources* **2008**, *180*, 896.
- (317) Lan, Z.; Wu, J.; Hao, S.; Lin, J.; Huang, M.; Huang, Y. *Energy Environ. Sci.* **2009**, *2*, 524.
- (318) Murai, S.; Mikoshiba, S.; Sumino, H.; Hayase, S. *J. Photochem. Photobiol., A* **2002**, *148*, 33.
- (319) Kato, T.; Okazaki, A.; Hayase, S. *Chem. Commun.* **2005**, 363.
- (320) Komiya, R.; Han, L.; Yamanaka, R.; Islam, A.; Mitate, T. *J. Photochem. Photobiol., A* **2004**, *164*, 123.
- (321) Yin, X.; Tan, W.; Xiang, W.; Lin, Y.; Zhang, J.; Xiao, X.; Li, X.; Zhou, X.; Fang, S. *Electrochim. Acta* **2010**, *55*, 5803.
- (322) Kato, T.; Okazaki, A.; Hayase, S. *J. Photochem. Photobiol., A* **2006**, *179*, 42.
- (323) Ren, Y.; Zhang, Z.; Fang, S.; Yang, M.; Cai, S. *Sol. Energy Mater. Sol. Cells* **2002**, *71*, 253.
- (324) Wang, L.; Fang, S.; Lin, Y.; Zhou, X.; Li, M. *Chem. Commun.* **2005**, 5687.
- (325) Su, J.; Tsai, C.; Wang, S.; Huang, T.; Wu, C.; Wong, K. *RSC Adv.* **2012**, *2*, 3722.
- (326) Matsumoto, M.; Wada, Y.; Kitamura, T.; Shigaki, K.; Inoue, T.; Ikeda, M.; Yanagida, S. *Bull. Chem. Soc. Jpn.* **2001**, *74*, 387.
- (327) Bella, F.; Bongiovanni, R. *J. Photochem. Photobiol., C* **2013**, *16*, 1.
- (328) Parvez, M.; In, I.; Park, J.; Lee, S.; Kim, S. *Sol. Energy Mater. Sol. Cells* **2011**, *95* (SI), 318.
- (329) Lan, Z.; Wu, J.; Lin, J.; Huang, M. *J. Power Sources* **2007**, *164*, 921.
- (330) Tang, Z.; Wu, J.; Liu, Q.; Zheng, M.; Tang, Q.; Lan, Z.; Lin, J. *J. Power Sources* **2012**, *203*, 282.
- (331) Lan, Z.; Wu, J.; Lin, J.; Huang, M. *Electrochim. Acta* **2007**, *52*, 6673.
- (332) Li, P.; Wu, J.; Huang, M.; Hao, S.; Lan, Z.; Liu, Q.; Kang, S. *Electrochim. Acta* **2007**, *53*, 903.
- (333) Tang, Z.; Wu, J.; Liu, Q.; Lan, Z.; Fan, L.; Lin, J.; Huang, M. *Electrochim. Acta* **2010**, *55*, 4883.
- (334) Tang, Z.; Liu, Q.; Tang, Q.; Wu, J.; Wang, J.; Chen, S.; Cheng, C.; Yu, H.; Lan, Z.; Lin, J.; Huang, M. *Electrochim. Acta* **2011**, *58*, 52.
- (335) Wu, J.; Lan, Z.; Wang, D.; Hao, S.; Lin, J.; Wei, Y.; Yin, S.; Sato, T. *J. Photochem. Photobiol., A* **2006**, *181*, 333.
- (336) Lan, Z.; Wu, J.; Lin, J.; Huang, M. *Polym. Adv. Technol.* **2011**, *22*, 1812.
- (337) Li, P.; Wu, J.; Hao, S.; Lan, Z.; Li, Q.; Huang, Y. *J. Appl. Polym. Sci.* **2011**, *120*, 1752.
- (338) Lan, Z.; Wu, J.; Lin, J.; Huang, M. *C. R. Chim.* **2010**, *13*, 1401.
- (339) Bella, F.; Ozzello, E.; Bianco, S.; Bongiovanni, R. *Chem. Eng. J.* **2013**, *225*, 873.
- (340) Kim, S.; Parvez, M.; In, I.; Lee, H.; Park, J. *Electrochim. Acta* **2009**, *54*, 6306.
- (341) Kal, S. H.; Joseph, J.; Lee, J.; Kim, K. *J. Electrochem. Soc.* **2005**, *152*, A1378.
- (342) Qin, D.; Zhang, Y.; Huang, S.; Luo, Y.; Li, D.; Meng, Q. *Electrochim. Acta* **2011**, *56*, 8680.
- (343) Lee, H.; Han, C.; Sung, Y.; Sekhon, S.; Kim, K. *Curr. Appl. Phys.* **2011**, *11*, S158.
- (344) Bella, F.; Nair, J.; Gerbaldi, C. *RSC Adv.* **2013**, *3*, 15993.
- (345) Bella, F.; Bongiovanni, R.; Kumar, R.; Kulandainathan, M.; Stephan, A. *J. Mater. Chem. A* **2013**, *1*, 9033.
- (346) Hong, S.; Ngoc, U.; Hong, S.; Kang, P. *J. Mater. Chem.* **2012**, *22*, 18854.
- (347) Bella, F.; Pugliese, D.; Nair, J.; Sacco, A.; Bianco, S.; Gerbaldi, C.; Barolo, C.; Bongiovanni, R. *Phys. Chem. Chem. Phys.* **2013**, *15*, 3706.
- (348) Koh, J.; Koh, J.; Park, N.; Kim, J. *Sol. Energy Mater. Sol. Cells* **2010**, *94*, 436.
- (349) Mikoshiba, S.; Murai, S.; Sumino, H.; Hayase, S. *Chem. Lett.* **2002**, *31*, 918.
- (350) Murai, S.; Mikoshiba, S.; Sumino, H.; Kato, T.; Hayase, S. *Chem. Commun.* **2003**, 1534.
- (351) Shibata, Y.; Kado, T.; Shiratuchi, R.; Takashima, W.; Kaneto, K.; Hayase, S. *Chem. Commun.* **2003**, 2730.
- (352) Sakaguchi, S.; Ueki, H.; Kato, T.; Kado, T.; Shiratuchi, R.; Takashima, W.; Kaneto, K.; Hayase, S. *J. Photochem. Photobiol., A* **2004**, *164*, 117.
- (353) Mikoshiba, S.; Murai, S.; Sumino, H.; Kado, T.; Kosugi, D.; Hayase, S. *Curr. Appl. Phys.* **2005**, *5*, 152.
- (354) Ferrere, S.; Gregg, B. A. *J. Phys. Chem. B* **2001**, *105*, 7602.
- (355) Cunningham, M. *Prog. Polym. Sci.* **2008**, *33*, 365.
- (356) Lissi, E.; Aljaro, J. *J. Polym. Sci. C* **1976**, *14*, 499.
- (357) Winther-Jensen, O.; Armel, V.; Forsyth, M.; MacFarlane, D. *Macromol. Rapid Commun.* **2010**, *31*, 479.
- (358) Wu, J.; Lin, J.; Zhou, M. *Macromol. Rapid Commun.* **2000**, *21*, 1032.
- (359) Lin, J.; Wu, J.; Yang, Z.; Pu, M. *Macromol. Rapid Commun.* **2001**, *22*, 422.
- (360) Yang, H.; Ileperuma, O.; Shimomura, M.; Murakami, K. *Sol. Energy Mater. Sol. Cells* **2009**, *93*, 1083.
- (361) Dong, R.; Shen, S.; Chen, H.; Wang, C.; Shih, P.; Liu, C.; Vittal, R.; Lin, J.; Ho, K. *J. Mater. Chem. A* **2013**, *1*, 8471.
- (362) Wang, C.; Wang, L.; Shi, Y.; Zhang, H.; Ma, T. *Electrochim. Acta* **2013**, *91*, 302.
- (363) Park, S.; Lim, J.; Song, I.; Atmakuri, N.; Song, S.; Kwon, Y.; Choi, J.; Park, T. *Adv. Energy Mater.* **2012**, *2*, 219.
- (364) Park, S.; Song, I.; Lim, J.; Kwon, Y.; Choi, J.; Song, S.; Lee, J.; Park, T. *Energy Environ. Sci.* **2013**, *6*, 1559.
- (365) Park, S.; Lim, J.; Kwon, Y.; Song, I.; Choi, J.; Song, S.; Park, T. *Adv. Energy Mater.* **2013**, *3*, 184.
- (366) Chen, J.; Xia, J.; Fan, K.; Peng, T. *Electrochim. Acta* **2011**, *56*, 554.
- (367) Kim, J.; Kang, M.; Kim, Y.; Won, J.; Park, N.; Kang, Y. *Chem. Commun.* **2004**, 1662.
- (368) Wang, H.; Li, H.; Meng, Q. *J. Am. Chem. Soc.* **2005**, *127*, 6394.
- (369) Lee, C.; Chen, P.; Vittal, R.; Ho, K. *J. Mater. Chem.* **2010**, *20*, 2356.
- (370) Chen, J.; Peng, T.; Fan, K.; Xia, J. *J. Mater. Chem.* **2011**, *21*, 16448.
- (371) Chen, C.; Teng, H.; Lee, Y. *Adv. Mater.* **2011**, *23*, 4199.
- (372) Lim, S.; Choi, Y.; Song, K.; Kim, D. *Electrochim. Commun.* **2011**, *13*, 1284.
- (373) Stathatos, E.; Lianos, P.; Zakeeruddin, S.; Liska, P.; Gratzel, M. *Chem. Mater.* **2003**, *15*, 1825.
- (374) Kubo, W.; Kitamura, T.; Hanabusa, K.; Wada, Y.; Yanagida, S. *Chem. Commun.* **2002**, 374.
- (375) Kubo, W.; Kambe, S.; Nakade, S.; Kitamura, T.; Hanabusa, K.; Wada, Y.; Yanagida, S. *J. Phys. Chem. B* **2003**, *107*, 4374.

- (376) Berginc, M.; Hocevar, M.; Krasovec, U.; Hinsch, A.; Sastrawan, R.; Topic, M. *Thin Solid Films* **2008**, *516*, 4645.
- (377) Huo, Z.; Dai, S.; Wang, K.; Kong, F.; Zhang, C.; Pan, X.; Fang, X. *Sol. Energy Mater. Sol. Cells* **2007**, *91*, 1959.
- (378) Yanagida, S. *C. R. Chim.* **2006**, *9*, S97.
- (379) Croce, F.; Appeteccchi, G.; Persi, L.; Scrosati, B. *Nature* **1998**, *394*, 456.
- (380) Croce, F.; Persi, L.; Ronci, F.; Scrosati, B. *Solid State Ionics* **2000**, *135*, 47.
- (381) Clemente, A.; Panero, S.; Spila, E.; Scrosati, B. *Solid State Ionics* **1996**, *85*, 273.
- (382) Katsaros, G.; Stergiopoulos, T.; Arabatzis, I. M.; Papadokostaki, K. G.; Falaras, P. *J. Photochem. Photobiol., A* **2002**, *149*, 191.
- (383) Stergiopoulos, T.; Arabatzis, I. M.; Katsaros, G.; Falaras, P. *Nano Lett.* **2002**, *2*, 1259.
- (384) Han, H.; Liu, W.; Zhang, J.; Zhao, X. *Adv. Funct. Mater.* **2005**, *15*, 1940.
- (385) Zhang, J.; Han, H.; Wu, S.; Xu, S.; Zhou, C.; Yang, Y.; Zhao, X. *Nanotechnology* **2007**, *18*, 295606.
- (386) Akhtar, M.; Chun, J.; Yang, O. *Electrochem. Commun.* **2007**, *9*, 2833.
- (387) Wang, P.; Zakeeruddin, S.; Comte, P.; Exnar, I.; Gratzel, M. *J. Am. Chem. Soc.* **2003**, *125*, 1166.
- (388) Yang, H.; Yu, C.; Song, Q.; Xia, Y.; Li, F.; Chen, Z.; Li, X.; Yi, T.; Huang, C. *Chem. Mater.* **2006**, *18*, 5173.
- (389) Kim, J.; Kim, T.; Kim, D.; Park, N.; Ahn, K. *J. Power Sources* **2008**, *175*, 692.
- (390) Yoon, I.; Song, H.; Won, J.; Kang, Y. *J. Phys. Chem. C* **2014**, *118*, 3918.
- (391) Xue, B.; Wang, H.; Hu, Y.; Li, H.; Wang, Z.; Meng, Q.; Huang, X.; Sato, O.; Chen, L.; Fujishima, A. *Photochem. Photobiol. Sci.* **2004**, *3*, 918.
- (392) Li, D.; Qin, D.; Deng, M.; Luo, Y.; Meng, Q. *Energy Environ. Sci.* **2009**, *2*, 283.
- (393) An, H.; Xue, B.; Li, D.; Li, H.; Meng, Q.; Guo, L.; Chen, L. *Electrochem. Commun.* **2006**, *8*, 170.
- (394) Chi, W.; Roh, D.; Kim, S.; Heo, S.; Kim, J. *Nanoscale* **2013**, *5*, 5341.
- (395) Namutdinova, G.; Sensfuss, S.; Schrodner, M.; Hinsch, A.; Sastrawan, R.; Gerhard, D.; Himmler, S.; Wasserscheid, P. *Solid State Ionics* **2006**, *177*, 3141.
- (396) Zhang, X.; Yang, H.; Xiong, H.; Li, F.; Xia, Y. *J. Power Sources* **2006**, *160*, 1451.
- (397) Xia, J.; Li, F.; Yang, H.; Li, X.; Huang, C. *J. Mater. Sci.* **2007**, *42*, 6412.
- (398) Geng, Y.; Sun, X.; Cai, Q.; Shi, Y.; Li, H. *Rare Metals* **2006**, *25*, 201.
- (399) Ito, B.; de Freitas, J.; De Paoli, M.; Nogueira, A. *J. Braz. Chem. Soc.* **2008**, *19*, 688.
- (400) Tu, C.; Liu, K.; Chien, A.; Yen, M.; Weng, T.; Ho, K.; Lin, K. *J. Polym. Sci., Part A* **2008**, *46*, 47.
- (401) Park, J.; Kim, B.; Moon, J. *Electrochim. Solid State Lett.* **2008**, *11*, B171.
- (402) Lai, Y.; Chiu, C.; Chen, J.; Wang, C.; Lin, J.; Lin, K.; Ho, K. *Sol. Energy Mater. Sol. Cells* **2009**, *93*, 1860.
- (403) Jin, L.; Chen, D. *Electrochim. Acta* **2012**, *72*, 40.
- (404) Wang, X.; Deng, R.; Kulkarni, S.; Wang, X.; Pramana, S.; Wong, C.; Gratzel, M.; Uchida, S.; Mhaisalkar, S. *J. Mater. Chem. A* **2013**, *1*, 4345.
- (405) Wang, X.; Kulkarni, S.; Ito, B.; Batabyal, S.; Nonomura, K.; Wong, C.; Gratzel, M.; Mhaisalkar, S.; Uchida, S. *ACS Appl. Mater. Interfaces* **2013**, *5*, 444.
- (406) Suzuki, K.; Yamaguchi, M.; Kumagai, M.; Yanagida, S. *Chem. Lett.* **2003**, *32*, 28.
- (407) Chen, P.; Lee, C.; Vittal, R.; Ho, K. *J. Power Sources* **2010**, *195*, 3933.
- (408) Fukushima, T.; Kosaka, A.; Ishimura, Y.; Yamamoto, T.; Takigawa, T.; Ishii, N.; Aida, T. *Science* **2003**, *300*, 2072.
- (409) Saito, Y.; Kubo, W.; Kitamura, T.; Wada, Y.; Yanagida, S. *J. Photochem. Photobiol., C* **2004**, *164*, 153.
- (410) Ikeda, N.; Teshima, K.; Miyasaka, T. *Chem. Commun.* **2006**, *16*, 1733.
- (411) Zhang, J.; Han, H.; Wu, S.; Xu, S.; Yang, Y.; Zhou, C.; Zhao, X. *Solid State Ionics* **2007**, *178*, 29.
- (412) Kawano, R.; Katakabe, T.; Shimosawa, H.; Nazeeruddin, M.; Graetzel, M.; Matsui, H.; Kitamura, T.; Tanabe, N.; Watanabe, M. *Phys. Chem. Chem. Phys.* **2010**, *12*, 1916.
- (413) Akhtar, M.; Li, Z.; Park, D.; Oh, D.; Kwak, D.; Yang, O. *Electrochim. Acta* **2011**, *56*, 9973.
- (414) Benedetti, J.; Correa, A.; Carmello, M.; Almeida, L.; Goncalves, A.; Nogueira, A. *J. Power Sources* **2012**, *208*, 263.
- (415) Wang, Y.; Huang, K.; Dong, R.; Liu, C.; Wang, C.; Ho, K.; Lin, J. *J. Mater. Chem.* **2012**, *22*, 6982.
- (416) Akhtar, M.; Kwon, S.; Stadler, F.; Yang, O. *Nanoscale* **2013**, *5*, 5403.
- (417) Gun, J.; Kulkarni, S.; Xiu, W.; Batabyal, S.; Sladkevich, S.; Prikhodchenko, P.; Gutkin, V.; Lev, O. *Electrochim. Commun.* **2012**, *19*, 108.
- (418) Mohan, V.; Murakami, K.; Kono, A.; Shimomura, M. *J. Mater. Chem. A* **2013**, *1*, 7399.
- (419) Costa, R.; Lodermeier, F.; Casillas, R.; Guldi, D. *Energy Environ. Sci.* **2014**, *7*, 1281.
- (420) Mohmeyer, N.; Kuang, D.; Wang, P.; Schmidt, H.; Zakeeruddin, S.; Gratzel, M. *J. Mater. Chem.* **2006**, *16*, 2978.
- (421) Wang, P.; Zakeeruddin, S.; Exnar, I.; Gratzel, M. *Chem. Commun.* **2002**, 2972.
- (422) Zhao, Y.; Zhai, J.; Tan, S.; Wang, L.; Jiang, L.; Zhu, D. *Nanotechnology* **2006**, *17*, 2090.
- (423) Chen, X.; Zhao, J.; Zhang, J.; Qiu, L.; Xu, D.; Zhang, H.; Han, X.; Sun, B.; Fu, G.; Zhang, F.; Yan, Y. *J. Mater. Chem.* **2012**, *22*, 18018.
- (424) Lee, H.; Kim, W.; Park, S.; Shin, W.; Jin, S.; Lee, J.; Han, S.; Jung, K.; Kim, M. *Macromol. Symp.* **2006**, *235*, 230.
- (425) Jeon, N.; Hwang, D.; Kang, Y.; Im, S.; Kim, D. *Electrochim. Commun.* **2013**, *34*, 1.
- (426) Rong, Y.; Li, X.; Liu, G.; Wang, H.; Ku, Z.; Xu, M.; Liu, L.; Hu, M.; Yang, Y.; Zhang, M.; Liu, T.; Han, H. *J. Power Sources* **2013**, *235*, 243.
- (427) Huang, X.; Qin, D.; Zhang, X.; Luo, Y.; Huang, S.; Li, D.; Meng, Q. *RSC Adv.* **2013**, *3*, 6922.
- (428) Wang, M.; Yin, X.; Xiao, X.; Zhou, X.; Yang, Z.; Li, X.; Lin, Y. *J. Photochem. Photobiol., A* **2008**, *194*, 20.
- (429) Wang, G.; Wang, L.; Zhuo, S.; Fang, S.; Lin, Y. *Chem. Commun.* **2011**, *47*, 2700.
- (430) Chi, W.; Koh, J.; Ahn, S.; Shin, J.; Ahn, H.; Ryu, D.; Kim, J. *Electrochim. Commun.* **2011**, *13*, 1349.
- (431) Li, Q.; Tang, Q.; Du, N.; Qin, Y.; Xiao, J.; He, B.; Chen, H.; Chu, L. *J. Power Sources* **2014**, *248*, 816.
- (432) Li, Q.; Tang, Q.; Lin, L.; Chen, X.; Chen, H.; Chu, L.; Xu, H.; Li, M.; Qin, Y.; He, B. *J. Power Sources* **2014**, *245*, 468.
- (433) Li, Q.; Chen, H.; Lin, L.; Li, P.; Qin, Y.; Li, M.; He, B.; Chu, L.; Tang, Q. *J. Mater. Chem. A* **2013**, *1*, 5326.
- (434) Hanabusa, K.; Tange, J.; Taguchi, Y.; Koyama, T.; Shirai, H. *J. Chem. Soc., Chem. Commun.* **1993**, 390.
- (435) Stathatos, E.; Lianos, P.; Lavrencic-Stangar, U.; Orel, B. *Adv. Mater.* **2002**, *14*, 354.
- (436) Nogueira, A. F.; Durrant, J. R.; DePaoli, M. A. *Adv. Mater.* **2001**, *13*, 826.
- (437) Wu, J.; Hao, S.; Lan, Z.; Lin, J.; Huang, M.; Huang, Y.; Li, P.; Yin, S.; Sato, T. *J. Am. Chem. Soc.* **2008**, *130*, 11568.
- (438) Lowman, G.; Hammond, P. *Small* **2005**, *1*, 1070.
- (439) Meng, Q.; Takahashi, K.; Zhang, X.; Sutanto, I.; Rao, T.; Satom, O.; Fujishima, A. *Langmuir* **2003**, *19*, 3572.
- (440) Saito, Y.; Azechi, T.; Kitamura, T.; Hasegawa, Y.; Wada, Y.; Yanagida, S. *Coord. Chem. Rev.* **2004**, *248*, 1469.
- (441) Chung, I.; Lee, B.; He, J.; Chang, R.; Kanatzidis, M. *Nature* **2012**, *485*, 486.

- (442) Bach, U.; Lupo, D.; Comte, P.; Moser, J. E.; Weissortel, F.; Salbeck, J.; Spreitzer, H.; Gratzel, M. *Nature* **1998**, *395*, 583.
- (443) Snaith, H.; Moule, A.; Klein, C.; Meerholz, K.; Friend, R.; Gratzel, M. *Nano Lett.* **2007**, *7*, 3372.
- (444) Nogueira, A.; De Paoli, M. *Sol. Energy Mater. Sol. Cells* **2000**, *61*, 135.
- (445) Wang, G.; Zhuo, S.; Wang, L.; Fang, S.; Lin, Y. *Sol. Energy* **2012**, *86*, 1546.
- (446) Midya, A.; Xie, Z.; Yang, J.; Chen, Z.; Blackwood, D.; Wang, J.; Adams, S.; Loh, K. *Chem. Commun.* **2010**, *46*, 2091.
- (447) Wang, H.; Zhang, X.; Gong, F.; Zhou, G.; Wang, Z. *Adv. Mater.* **2012**, *24*, 121.
- (448) Wang, H.; Li, J.; Gong, F.; Zhou, G.; Wang, Z. *J. Am. Chem. Soc.* **2013**, *135*, 12627.
- (449) Li, J.; Lv, K.; Sun, H.; Wang, Z. *Nano* **2014**, 1440006.
- (450) He, J.; Mosurkal, R.; Samuelson, L.; Li, L.; Kumar, J. *Langmuir* **2003**, *19*, 2169.
- (451) Handa, S.; Haque, S. A.; Durrant, J. R. *Adv. Funct. Mater.* **2007**, *17*, 2878.
- (452) Patrocinio, A.; Paterno, L.; Murakami, I. *J. Phys. Chem. C* **2010**, *114*, 17954.
- (453) Kim, K.; Moon, J.; Kim, E.; Kim, H.; Jang, S.; Lee, W. *J. Mater. Chem.* **2012**, *22*, 11179.
- (454) Kitamura, K.; Shiratori, S. *Nanotechnology* **2011**, *22*, 195703.
- (455) MacFarlane, D.; Huang, J.; Forsyth, M. *Nature* **1999**, *402*, 792.
- (456) Howlett, P.; Shekibi, Y.; MacFarlane, D.; Forsyth, M. *Adv. Eng. Mater.* **2009**, *11*, 1044.
- (457) Pringle, J.; Howlett, P.; MacFarlane, D.; Forsyth, M. *J. Mater. Chem.* **2010**, *20*, 2056.
- (458) Adebahr, J.; Aaron, J.; MacFarlane, D.; Forsyth, M. *J. Phys. Chem. B* **2005**, *109*, 20087.
- (459) MacFarlane, D.; Meakin, P.; Amini, N.; Forsyth, M. *J. Phys.: Condens. Matter* **2001**, *13*, 8257.
- (460) Chen, Z.; Yang, H.; Li, X.; Li, F.; Yi, T.; Huang, C. *J. Mater. Chem.* **2007**, *17*, 1602.
- (461) Armel, V.; Pringle, J.; Wagner, P.; Forsyth, M.; Officer, D.; MacFarlane, D. *Chem. Commun.* **2011**, *47*, 9327.
- (462) Armel, V.; Forsyth, M.; MacFarlane, D.; Pringle, J. *Energy Environ. Sci.* **2011**, *4*, 2234.
- (463) Dai, Q.; MacFarlane, D.; Howlett, P.; Forsyth, M. *Angew. Chem., Int. Ed.* **2004**, *44*, 313.
- (464) Wang, P.; Dai, Q.; Zakeeruddin, S.; Forsyth, M.; MacFarlane, D.; Graetzel, M. *J. Am. Chem. Soc.* **2004**, *126*, 13590.
- (465) Wang, H.; Wang, Z.; Xue, B.; Meng, Q.; Huang, X.; Chen, L. *Chem. Commun.* **2004**, 2186.
- (466) Rutkowska, I.; Andreczyk, A.; Zoladek, S.; Goral, M.; Darowicki, K.; Kulesza, P. *J. Solid State Electrochem.* **2011**, *15*, 2545.
- (467) Yanagida, S.; Yu, Y.; Manseki, K. *Acc. Chem. Res.* **2009**, *42*, 1827.
- (468) Smestad, G.; Spiekermann, S.; Kowalik, J.; Grant, C.; Schwartzberg, A.; Zhang, J.; Tolbert, L.; Moons, E. *Sol. Energy Mater. Sol. Cells* **2003**, *76*, 85.
- (469) Bach, U.; Daeneke, T. *Angew. Chem., Int. Ed.* **2012**, *51*, 10451.
- (470) Tennakone, K.; Kumara, G.; Kumarasinghe, A.; Wijayantha, K.; Sirimanne, P. M. *Semicond. Sci. Technol.* **1995**, *10*, 1689.
- (471) Kumara, G.; Konno, A.; Senadeera, G.; Jayaweera, P.; De Silva, D.; Tennakone, K. *Sol. Energy Mater. Sol. Cells* **2001**, *69*, 195.
- (472) Tennakone, K.; Senadeera, G.; De Silva, D.; Kottekoda, I. *Appl. Phys. Lett.* **2000**, *77*, 2367.
- (473) O'Regan, B.; Schwartz, D. *Chem. Mater.* **1998**, *10*, 1501.
- (474) Tennakone, K.; Kumara, G.; Kottekoda, I.; Wijayantha, K.; Perrera, V. *J. Phys. D: Appl. Phys.* **1998**, *31*, 1492.
- (475) Tennakone, K.; Perera, V.; Kottekoda, I.; Kumara, G. *J. Phys. D* **1999**, *32*, 374.
- (476) Kumara, G.; Kaneko, S.; Okuya, M.; Tennakone, K. *Langmuir* **2002**, *18*, 10493.
- (477) Kumara, G.; Konno, A.; Shiratsuchi, K.; Tsukahara, J.; Tennakone, K. *Chem. Mater.* **2002**, *14*, 954.
- (478) Tennakone, K.; Perera, V.; Kottekoda, I.; De Silva, L.; Kumara, G.; Konno, A. *J. Electron. Mater.* **2001**, *30*, 992.
- (479) Zhang, X.; Liu, H.; Taguchi, T.; Meng, Q.; Sato, O.; Fujishima, A. *Sol. Energy Mater. Sol. Cells* **2004**, *81*, 197.
- (480) Perera, V.; Tennakone, K. *Sol. Energy Mater. Sol. Cells* **2003**, *79*, 249.
- (481) Sirimanne, P. M.; Jeranko, T.; Bogdanoff, P.; Fiechter, S.; Tributsch, H. *Semicond. Sci. Technol.* **2003**, *18*, 708.
- (482) Taguchi, T.; Zhang, X.; Sutanto, I.; Tokuhiro, K.; Rao, T.; Watanabe, H.; Nakamori, T.; Uragami, M.; Fujishima, A. *Chem. Commun.* **2003**, *19*, 2480.
- (483) Kumara, G.; Okuya, M.; Murakami, K.; Kaneko, S.; Jayaweera, V.; Tennakone, K. *J. Photochem. Photobiol. A* **2004**, *164*, 183.
- (484) Mahrov, B.; Boschloo, G.; Hagfeldt, A.; Siegbahn, H.; Rensmo, H. *J. Phys. Chem. B* **2004**, *108*, 11604.
- (485) Karlsson, P.; Bolik, S.; Richter, J. *J. Chem. Phys.* **2004**, *120*, 11224.
- (486) Sakamoto, H.; Igarashi, S.; Niume, K.; Nagai, M. *Org. Electron.* **2011**, *12*, 1247.
- (487) Sakamoto, H.; Igarashi, S.; Uchida, M.; Niume, K.; Nagai, M. *Org. Electron.* **2012**, *13*, 514.
- (488) Hehl, R.; Thiele, G. *Z. Anorg. Allg. Chem.* **2000**, *626*, 2167.
- (489) Premalal, E.; Dematage, N.; Kumara, G.; Rajapakse, R.; Shimomura, M.; Murakami, K.; Konno, A. *J. Power Sources* **2012**, *203*, 288.
- (490) O'Regan, B.; Schwartz, D. *J. Appl. Phys.* **1996**, *80*, 4749.
- (491) Mahrov, B.; Hagfeldt, A.; Lenzmann, F.; Boschloo, G. *Sol. Energy Mater. Sol. Cells* **2005**, *88*, 351.
- (492) O'Regan, B.; Lenzmann, F.; Muis, R.; Wienke, J. *Chem. Mater.* **2002**, *14*, 5023.
- (493) Perera, V.; Senevirathna, M.; Pitigala, P.; Tennakone, K. *Sol. Energy Mater. Sol. Cells* **2005**, *86*, 443.
- (494) O'Regan, B.; Scully, S.; Mayer, A. *J. Phys. Chem. B* **2005**, *109*, 4616.
- (495) O'Regan, B. C.; Lenzmann, F. *J. Phys. Chem. B* **2004**, *108*, 4342.
- (496) Kim, S.; Park, K.; Yum, J.; Sung, Y. *Sol. Energy Mater. Sol. Cells* **2006**, *90*, 283.
- (497) Wong, K.; Ananthanarayanan, K.; Gajjela, S.; Balaya, P. *Mater. Chem. Phys.* **2011**, *125*, 553.
- (498) Kawazoe, H.; Yasukawa, M.; Hyodo, H.; Kurita, M.; Yanagi, H.; Hosono, H. *Nature* **1973**, *89*, 939.
- (499) He, J.; Lindstrom, H.; Hagfeldt, A.; Lindquist, S. *J. Phys. Chem. B* **1999**, *103*, 8940.
- (500) Yamada, K.; Funabiki, S.; Horimoto, H.; Matsui, T.; Okuda, T.; Ichiba, S. *Chem. Lett.* **1991**, *5*, 801.
- (501) Chung, I.; Song, J.; Im, J.; Androulakis, J.; Malliakas, C.; Li, H.; Freeman, A.; Kenney, J.; Kanatzidis, M. *J. Am. Chem. Soc.* **2012**, *134*, 8579.
- (502) Mallouk, T. *Nature* **2012**, *485*, 450.
- (503) Chen, Z.; Wang, J.; Ren, Y.; Yu, C.; Shum, K. *Appl. Phys. Lett.* **2012**, *101*, 093901.
- (504) Shum, K.; Chen, Z.; Qureshi, J.; Yu, C.; Wang, J.; Pfenninger, W.; Vockic, N.; Midgley, J.; John, T. *Appl. Phys. Lett.* **2010**, *96*, 221903.
- (505) Yu, C.; Chen, X.; Wang, J.; Pfenninger, W.; Vockic, N.; Kenney, J.; Shum, K. *J. Appl. Phys.* **2011**, *110*, 063526.
- (506) Chen, Z.; Yu, C.; Shum, K.; Wang, J.; Pfenninger, W.; Vockic, N.; Midgley, J.; John, T. *J. Lumin.* **2012**, *132*, 345.
- (507) Zhou, Y.; Garces, H.; Senturk, B.; Ortiz, A.; Padture, N. *Mater. Lett.* **2013**, *110*, 127.
- (508) Lee, B.; Stoumpos, C.; Zhou, N.; Hao, F.; Malliakas, C.; Yeh, C.; Marks, T.; Kanatzidis, M.; Chang, R. *J. Am. Chem. Soc.* **2014**, *136*, 15379.
- (509) Schon, J.; Kloc, C.; Bucher, E.; Batiogg, B. *Nature* **2000**, *403*, 408.
- (510) Shaheen, S.; Brabec, C.; Sariciftci, N.; Padinger, F.; Fromherz, T.; Hummelen, J. *Appl. Phys. Lett.* **2001**, *78*, 841.

- (511) Sirringhaus, H.; Brown, P.; Friend, R.; Nielsen, M.; Bechgaard, K.; Langeveld-Voss, B.; Spiering, A.; Janssen, R.; Meijer, E.; Herwig, P.; de Leeuw, D. *Nature* **1999**, *401*, 685.
- (512) Katz, H.; Laquindanum, J.; Lovinger, A. *Chem. Mater.* **1998**, *10*, 633.
- (513) VanSlyke, S.; Chen, C.; Tang, C. *Appl. Phys. Lett.* **1996**, *69*, 2160.
- (514) Hung, L.; Tang, C.; Mason, M. *Appl. Phys. Lett.* **1997**, *70*, 152.
- (515) Murakoshi, K.; Kogure, R.; Wada, Y.; Yanagida, S. *Chem. Lett.* **1997**, *471*.
- (516) Murakoshi, K.; Kogure, R.; Wada, Y.; Yanagida, S. *Sol. Energy Mater. Sol. Cells* **1998**, *55*, 113.
- (517) Kitamura, T.; Maitani, M.; Matsuda, M.; Wada, Y.; Yanagida, S. *Chem. Lett.* **2001**, *1054*.
- (518) Tan, S.; Zhai, J.; Wan, M.; Jiang, L.; Zhu, D. *Synth. Met.* **2003**, *137*, 1511.
- (519) Tan, S.; Zhai, J.; Xue, B.; Wan, M.; Meng, Q.; Li, Y.; Jiang, L.; Zhu, D. *Langmuir* **2004**, *20*, 2934.
- (520) Tan, S.; Zhai, J.; Wan, M.; Meng, Q.; Li, Y.; Jiang, L.; Zhu, D. *J. Phys. Chem. B* **2004**, *108*, 18693.
- (521) Kudo, N.; Honda, S.; Shimazaki, Y.; Ohkita, H.; Ito, S. *Appl. Phys. Lett.* **2007**, *90*, 183513.
- (522) Zafer, C.; Karapire, C.; Sariciftci, N. S.; Icli, S. *Sol. Energy Mater. Sol. Cells* **2005**, *88*, 11.
- (523) Lancelle-Beltran, E.; Prene, P.; Boscher, C.; Belleville, P.; Buvat, P.; Lambert, S.; Guillet, F.; Marcel, C.; Sanchez, C. *Eur. J. Inorg. Chem.* **2008**, *903*.
- (524) Coakley, K. M.; Liu, Y. X.; McGehee, M. D.; Frindell, K. L. *Adv. Funct. Mater.* **2003**, *13*, 301.
- (525) Coakley, K. M.; McGehee, M. D. *Appl. Phys. Lett.* **2003**, *83*, 3380.
- (526) Lancelle-Beltran, E.; Prene, P.; Boscher, C.; Belleville, P.; Buvat, P.; Sanchez, C. *Adv. Mater.* **2006**, *18*, 2579.
- (527) Zhu, R.; Jiang, C. Y.; Liu, B.; Ramakrishna, S. *Adv. Mater.* **2009**, *21*, 994.
- (528) Jiang, K.; Manseki, K.; Yu, Y.; Masaki, N.; Suzuki, K.; Song, Y.; Yanagida, S. *Adv. Funct. Mater.* **2009**, *19*, 2481.
- (529) Mor, G.; Kim, S.; Paulose, M.; Varghese, O.; Shankar, K.; Basham, J.; Grimes, C. *Nano Lett.* **2009**, *9*, 4250.
- (530) Giacomo, F.; Razza, S.; Matteocci, F.; Epifanio, A.; Licoccia, S.; Brown, T.; Carlo, A. *J. Power Sources* **2014**, *251*, 152.
- (531) Wu, J.; Yue, G.; Xiao, Y.; Ye, H.; Lin, J.; Huang, M. *Electrochim. Acta* **2010**, *55*, 5798.
- (532) Peng, F.; Wu, J.; Li, Q.; Wang, Y.; Yue, G.; Xiao, Y.; Li, Q.; Lan, Z.; Fan, L.; Lin, J.; Huang, M. *Electrochim. Acta* **2011**, *56*, 5184.
- (533) Yue, G.; Wu, J.; Xiao, Y.; Lin, J.; Huang, M.; Lan, Z.; Fan, L. *Electrochim. Acta* **2012**, *85*, 182.
- (534) Yue, G.; Wu, J.; Xiao, Y.; Ye, H.; Lin, J.; Huang, M. *Chin. Sci. Bull.* **2011**, *56*, 325.
- (535) Yue, G.; Wu, J.; Huang, Y.; Xiao, Y.; Lan, Z. *Funct. Mater. Lett.* **2012**, *5*, 1260004.
- (536) Yue, G.; Wu, J.; Xiao, Y.; Lin, J.; Huang, M. *Front. Optoelectron. China* **2011**, *4*, 108.
- (537) Yue, G.; Wu, J.; Lin, J.; Huang, M.; Yao, Y.; Fan, L.; Xiao, Y. *Front. Optoelectron. China* **2011**, *4*, 369.
- (538) Wu, J.; Yue, G.; Xiao, Y.; Lin, J.; Huang, M.; Lan, Z.; Tang, Q.; Huang, Y.; Fan, L.; Yin, S.; Sato, T. *Sci. Rep.* **2013**, *3*, 1283.
- (539) Saito, Y.; Kitamura, T.; Wada, Y.; Yanagida, S. *Synth. Met.* **2002**, *131*, 185.
- (540) Saito, Y.; Fukuri, N.; Senadeera, R.; Kitamura, T.; Wada, Y.; Yanagida, S. *Electrochim. Commun.* **2004**, *6*, 71.
- (541) Fukuri, N.; Saito, Y.; Kubo, W.; Senadeera, G.; Kitamura, T.; Wada, Y.; Yanagida, S. *J. Electrochem. Soc.* **2004**, *151*, A1745.
- (542) Senadeera, R.; Fukuri, N.; Saito, Y.; Kitamura, T.; Wada, Y.; Yanagida, S. *Chem. Commun.* **2005**, 2259.
- (543) Senadeera, G.; Kitamura, T.; Wada, Y.; Yanagida, S. *J. Photochem. Photobiol. A* **2006**, *184*, 234.
- (544) Mozer, A.; Jiang, K.; Wada, Y.; Masaki, N.; Mori, S.; Yanagida, S. *Appl. Phys. Lett.* **2006**, *89*, 043509.
- (545) Kim, Y.; Sung, Y.; Xia, J.; Lira-Cantu, M.; Masaki, N.; Yanagida, S. *J. Photochem. Photobiol. A* **2008**, *193*, 77.
- (546) Xia, J.; Masaki, N.; Jiang, K.; Yanagida, S. *J. Mater. Chem.* **2007**, *17*, 2845.
- (547) Xia, J.; Masaki, N.; Lira-Cantu, M.; Kim, Y.; Jiang, K.; Yanagida, S. *J. Am. Chem. Soc.* **2008**, *130*, 1258.
- (548) Liu, X.; Zhang, W.; Uchida, S.; Cai, L.; Liu, B.; Ramakrishna, S. *Adv. Mater.* **2010**, *22*, E150.
- (549) Kim, J.; Koh, B.; Kim, S.; Ahn, H.; Ahn, D.; Jong, H.; Kim, E. *Adv. Funct. Mater.* **2011**, *21*, 4633.
- (550) Wagner, J.; Pielichowski, J.; Hinsch, A.; Pielichowski, K.; Bogdal, D.; Pajda, M.; Kurek, S.; Burczyk, A. *Synth. Met.* **2004**, *146*, 159.
- (551) Chang, J.; Rhee, J.; Im, S.; Lee, Y.; Kim, H.; Seok, S.; Nazeeruddin, M.; Gratzel, M. *Nano Lett.* **2010**, *10*, 2609.
- (552) Im, S.; Lim, C.; Chang, J.; Lee, Y.; Maiti, N.; Kim, H.; Nazeeruddin, M.; Gratzel, M.; Seok, S. *Nano Lett.* **2011**, *11*, 4789.
- (553) Chang, J.; Im, S.; Lee, Y.; Kim, H.; Lim, C.; Heo, J.; Seok, S. *Nano Lett.* **2012**, *12*, 1863.
- (554) Pattantyus-Abraham, A.; Kramer, I.; Barkhouse, A.; Wang, X.; Konstantatos, G.; Debnath, R.; Levina, L.; Raabe, I.; Nazeeruddin, M.; Gratzel, M.; Sargent, E. *ACS Nano* **2011**, *4*, 3374.
- (555) Semonin, O.; Luther, J.; Choi, S.; Chen, H.; Gao, J.; Nozik, A.; Beard, M. *Science* **2011**, *334*, 1530.
- (556) Etgar, L.; Zhang, W.; Gabriel, S.; Hickey, S.; Nazeeruddin, M.; Eychmüller, A.; Liu, B.; Gratzel, M. *Adv. Mater.* **2012**, *24*, 2202.
- (557) Haridas, K.; Ostrauskaite, J.; Thelakkat, M.; Heim, M.; Bilke, R.; Haarer, D. *Synth. Met.* **2001**, *121*, 1573.
- (558) Peter, K.; Wietasch, H.; Peng, B.; Thelakkat, M. *Appl. Phys. A: Mater. Sci. Process.* **2004**, *79*, 65.
- (559) Gebeyehu, D.; Brabec, C.; Sariciftci, N. S. *Thin Solid Films* **2002**, *403*, 271.
- (560) Spiekermann, S.; Smestad, G.; Kowalik, J.; Tolbert, L.; Gratzel, M. *Synth. Met.* **2001**, *121*, 1603.
- (561) Li, J.; Osasa, T.; Hirayama, Y.; Sano, T.; Wakisaka, K.; Matsumura, M. *Jpn. J. Appl. Phys.* **2006**, *45*, 8728.
- (562) Fukuri, N.; Masaki, N.; Kitamura, T.; Wada, Y.; Yanagida, S. *J. Phys. Chem. B* **2006**, *110*, 25251.
- (563) Yuan, S.; Tang, Q.; He, B.; Yang, P. *J. Power Sources* **2014**, *254*, 98.
- (564) Li, Q.; Chen, X.; Tang, Q.; Cai, H.; Qin, Y.; He, B.; Li, M.; Jin, S.; Liu, Z. *J. Power Sources* **2014**, *248*, 923.
- (565) Li, Q.; Chen, X.; Tang, Q.; Xu, H.; He, B.; Qin, Y. *J. Mater. Chem. A* **2013**, *1*, 8055.
- (566) Li, Q.; Wu, J.; Tang, Z.; Xiao, Y.; Lin, J.; Huang, M. *Electrochim. Acta* **2010**, *55*, 2777.
- (567) Lee, J.; Kim, W.; Lee, H.; Shin, W. S.; Jin, S.; Lee, W.; Kim, M. *J. Polym. Adv. Technol.* **2006**, *17*, 709.
- (568) Warnan, J.; Pellegrin, Y.; Blart, E.; Odobel, F.; Zhang, W.; Liu, B.; Babu, V.; Ramakrishna, S. *Macromol. Rapid Commun.* **2011**, *32*, 1190.
- (569) Kruger, J.; Plass, R.; Cevey, L.; Piccirelli, M.; Gratzel, M.; Bach, U. *Appl. Phys. Lett.* **2001**, *79*, 2085.
- (570) Kruger, J.; Plass, R.; Gratzel, M.; Matthieu, H. *J. Appl. Phys. Lett.* **2002**, *81*, 367.
- (571) Schmidt-Mende, L.; Zakeeruddin, S.; Gratzel, M. *Appl. Phys. Lett.* **2005**, *86*, 013504.
- (572) Schmidt-Mende, L.; Bach, U.; Humphry-Baker, R.; Horiuchi, T.; Miura, H.; Ito, S.; Uchida, S.; Gratzel, M. *Adv. Mater.* **2005**, *17*, 813.
- (573) Wang, M.; Moon, S.; Xu, M.; Chittibabu, K.; Wang, P.; Cevey, N.; Humphry-Baker, R.; Zakeeruddin, S.; Gratzel, M. *Small* **2010**, *6*, 319.
- (574) Cai, N.; Moon, S.; Cevey, L.; Moehl, T.; Humphry-Baker, R.; Wang, P.; Zakeeruddin, S. M.; Gratzel, M. *Nano Lett.* **2011**, *11*, 1452.
- (575) Snaith, H. J.; Gratzel, M. *Appl. Phys. Lett.* **2006**, *89*, 262114.
- (576) Snaith, H. J.; Schmidt-Mende, L. *Adv. Mater.* **2007**, *19*, 3187.
- (577) Burschka, J.; Dualeh, A.; Kessler, F.; Baranoff, E.; Cevey, N.; Yi, C.; Nazeeruddin, M.; Gratzel, M. *J. Am. Chem. Soc.* **2011**, *133*, 18042.

- (578) Kazim, S.; Nazeeruddin, M. K.; Gratzel, M.; Ahmad, S. *Angew. Chem., Int. Ed.* **2014**, *53*, 2812.
- (579) Im, J.; Lee, C.; Lee, J.; Park, S.; Park, N. *Nanoscale* **2011**, *3*, 4088.
- (580) Kim, H.; Lee, C.; Im, J.; Lee, K.; Moehl, T.; Marchioro, A.; Moon, S.; Humphry-Baker, R.; Yum, J.; Moser, J.; Gratzel, M.; Park, N. *Sci. Rep.* **2012**, *2*, 591.
- (581) Lee, M.; Teuscher, J.; Miyasaka, T.; Murakami, T.; Snaith, H. *Science* **2012**, *338*, 643.
- (582) Stranks, S.; Eperon, G.; Grancini, G.; Menelaou, C.; Alcocer, M.; Leijtens, T.; Herz, L.; Petrozza, A.; Snaith, H. *Science* **2013**, *342*, 341.
- (583) Heo, J.; Im, S.; Noh, J.; Mandal, T.; Lim, C.; Chang, J.; Lee, Y.; Kim, H.; Sarkar, A.; Nazeeruddin, M.; Graetzel, M.; Seok, S. *Nat. Photonics* **2013**, *7*, 486.
- (584) Noh, J.; Im, S.; Heo, J.; Mandal, T.; Seok, S. *Nano Lett.* **2013**, *13*, 1764.
- (585) Burschka, J.; Pellet, N.; Moon, S.; Humphry-Baker, R.; Gao, P.; Nazeeruddin, M.; Gratzel, M. *Nature* **2013**, *499*, 316.
- (586) Liu, M.; Johnston, M.; Snaith, H. *Nature* **2013**, *501*, 395.
- (587) Green, M.; Anita, H.; Snaith, H. *Nat. Photonics* **2014**, *8*, 506.
- (588) Zhou, H.; Chen, Q.; Li, G.; Luo, S.; Song, T.; Duan, H.; Hong, Z.; You, J.; Liu, Y.; Yang, Y. *Science* **2014**, *345*, 6196.
- (589) Science News *Science* **2013**, *342*, 1438.
- (590) Bednorz, J.; Muller, K. *Z. Phys. B* **1986**, *64*, 189.
- (591) Kojima, A.; Ikegami, M.; Teshima, K.; Miyasaka, T. *Chem. Lett.* **2012**, *41*, 397.
- (592) Kagan, C.; Mitzi, D.; Dimitrakopoulos, C. *Science* **1999**, *286*, 945.
- (593) Billing, D.; Llemerer, A. *CrystEngComm* **2006**, *8*, 686.
- (594) Heo, J.; Im, S.; Noh, J.; Mandal, T.; Lim, C.; Chang, J.; Lee, Y.; Kim, H.; Sarkar, A.; Nazeeruddin, M.; Gratzel, M.; Seok, S. *Nat. Photonics* **2013**, *7*, 487.
- (595) Chen, Q.; Zhou, H.; Hong, Z.; Luo, S.; Duan, H.; Wang, H.; Liu, Y.; Li, G.; Yang, Y. *J. Am. Chem. Soc.* **2013**, *136*, 622.
- (596) Xu, T.; Qiao, Q. *Energy Environ. Sci.* **2011**, *4*, 2700.
- (597) Pellet, N.; Gao, P.; Gregori, G.; Yang, T.; Nazeeruddin, M.; Maier, J.; Gratzel, M. *Angew. Chem., Int. Ed.* **2014**, *53*, 3151.
- (598) Eperon, G.; Stranks, S.; Menelaou, C.; Johnston, M.; Herz, L.; Snaith, H. *Energy Environ. Sci.* **2014**, *7*, 982.
- (599) Ogomi, Y.; Morita, A.; Tsukamoto, S.; Saitho, T.; Fujikawa, N.; Shen, Q.; Toyoda, T.; Yoshino, K.; Pandey, S.; Ma, T.; Hayase, S. *J. Phys. Chem. Lett.* **2014**, *5*, 1004.
- (600) Knutson, J.; Martin, J.; Mitzi, D. *Inorg. Chem.* **2005**, *44*, 469.
- (601) Hodes, G. *Science* **2013**, *342*, 317.
- (602) Etgar, L.; Gao, P.; Xue, Z.; Peng, Q.; Chandiran, A.; Liu, B.; Nazeeruddin, M.; Graetzel, M. *J. Am. Chem. Soc.* **2012**, *134*, 17396.
- (603) Xiao, Y.; Han, G.; Li, Y.; Li, M.; Chang, Y.; Wu, J. *J. Mater. Chem. A* **2014**, *2*, 16531.
- (604) Xiao, Y.; Han, G.; Li, Y.; Li, M.; Wu, J. *J. Mater. Chem. A* **2014**, *2*, 16856.
- (605) Xing, G.; Mathews, N.; Sun, S.; Lim, S.; Lam, Y.; Gratzel, M.; Mhaisalkar, S.; Sum, T. *Science* **2013**, *342*, 344.
- (606) Giorgi, G.; Fujisawa, J.; Segawa, H.; Yamashita, K. *J. Phys. Chem. Lett.* **2013**, *4*, 4213.
- (607) Wehrenfennig, C.; Eperon, G.; Johnston, M.; Snaith, H.; Herz, L. *Adv. Mater.* **2013**, *26*, 1584.
- (608) Edri, E.; Kirmayer, S.; Kulbak, M.; Hodes, G.; Cahen, D. *J. Phys. Chem. Lett.* **2014**, *5*, 429.
- (609) Yuan, Y.; Xiao, Z.; Yang, B.; Huang, J. *J. Mater. Chem. A* **2014**, *2*, 6027.
- (610) Ye, H.; Zhang, Y.; Fu, D.; Xiong, R. *Angew. Chem., Int. Ed.* **2014**, *53*, 11242.
- (611) Stoumpos, C.; Malliakas, C.; Kanatzidis, M. *Inorg. Chem.* **2013**, *52*, 9019.